ESD-TR-66-516

ADVANCED DIGITAL FM-PM DEMODULATOR ADD-15

(Final Report)

September 1966

William H. Casson

DIRECTOR OF AEROSPACE INSTRUMENTATION
ELECTRONIC SYSTEMS DIVISION
AIR FORCE SYSTEMS COMMAND
United States Air Force
L.G. Hanscom Field, Bedford, Massachusetts

(Prepared under Contract No. AF19(628)-5667 by Defense Electronics, Inc., Rockville, Maryland.)

LEGAL NOTICE

When U. S. Government drawings, specifications or other data are used for any purpose other than a definitely related government procurement operation, the government thereby incurs no responsibility nor any obligation whatsoever; and the fact that the government may have formulated, furnished, or in any way supplied the said drawings, specifications, or other data is not to be regarded by implication or otherwise as in any manner licensing the holder or any other person or conveying any rights or permission to manufacture, use, or sell any patented invention that may in any way be related thereto.

OTHER NOTICES

Do not return this copy. Retain or destroy.

ESD-TR-66-516

ADVANCED DIGITAL FM-PM DEMODULATOR ADD-15

(Final Report)

September 1966

William H. Casson

DIRECTOR OF AEROSPACE INSTRUMENTATION
ELECTRONIC SYSTEMS DIVISION
AIR FORCE SYSTEMS COMMAND
United States Air Force
L.G. Hanscom Field, Bedford, Massachusetts

(Prepared under Contract No. AF19(628)-5667 by Defense Electronics, Inc., Rockville, Maryland.)

FOREWORD

This final report has been prepared by Defense Electronics, Inc., Rockville, Maryland under Contract AF 19(628)-5667. Mr. G. Maccarone, Deputy for Engineering & Technology (ESRIT), Electronic Systems Division was the Project Engineer for this contract.

Work under this report covers the period of 1 November 1965 through 30 September 1966.

REVIEW AND APPROVAL

Publication of this technical report does not constitute Air Force approval of the report's findings or conclusions. It is published only for the exchange and stimulation of ideas.

OTIS R. HILL
Colonel, USAF
Director of Aerospace Instrumentation

ABSTRACT

The objective of this program is to design, fabricate, and evaluate an advanced FM-PM demodulator for telemetry applications. This unit will utilize new circuit techniques which show definite promise of providing improved performance, particularly in the areas of threshold and linearity. The compromises and limitations involved in the new techniques will be thoroughly investigated and the program includes a comprehensive series of tests.

TABLE OF CONTENTS

SECTION I

INTRODUCTION AND SUMMARY

1.1 PROGRAM OBJECTIVE

The overall program objectives are set forth in the contract statement of work which is reproduced for reference as follows:

EXHIBIT B

ADVANCED DEMODULATOR DEVELOPMENT

1. INTRODUCTION

In recent years a number of new demodulator techniques, which show definite promise of improving the sensitivity, linearity, and signal acquisition characteristics of radio receiving systems, have been evolved. In view of the continuing demand for improvement of these parameters in telemetry receivers, it becomes important to determine the applicability of these techniques to the demodulation of telemetry signals. It is therefore, essential that the trade-offs and limitations involved in these techniques be thoroughly investigated and understood before consideration is given to their system application.

2. OBJECTIVE

The objective of this program is to provide for the development and evaluation of advanced demodulators utilizing techniques which show promise of providing improved performance for demodulation of predetection recorded telemetry signals. These demodulators shall result in lower threshold and better linearity.

EXHIBIT "A" (Revised)

STATEMENT OF WORK

The Contractor shall, unless otherwise specified, supply the necessary personnel, facilities, and services to accomplish the following:

Item 1 - Design, fabricate, and test an engineering model of a demodulator using the Contractor's proposed technique. All work shall be compatible with the IRIG 106-60 Telemetry Standards as revised to date, incorporated herein by reference.

a. The design, fabrication, and test program shall include, but not be limited to the following:

(1) The model shall operate with the telemetry receiver employed in the TRKI-12 Receiver/Recorder Group now on the Air Force Eastern Test Range (AFETR). The specifications for this receiver are set forth in Technical Exhibit SE/3516-1105A dated 14 January 1963, as amended by Special Amendment A and Amendments 1 through 10, attached hereto and made a part hereof.

(2) In addition to normal laboratory testing, the Contractor will be responsible for conducting tests at the AFETR with the receiver mentioned in (1) above. The laboratory tests will be conducted using simulated telemetry signals. Range testing will be for the purpose of determining the operational suitability of the model when used with the specified receiver. At the AFETR, the demodulator will be tested using Government

furnished predetection tapes, and will also be evaluated during an actual missile launch. Performance will be stated both quantitatively and qualitatively and in addition, will be compared to that achieved with existing demodulators.

(3) The Contractor shall also make analytical calculations of achievable performance and compare this with actual performance achieved. The test program shall also result in use criteria and indications of performance as related to various trade-off factors.

Item 2 - Data in accordance with the Contractor Data Requirements List, DD Form 1423, attached hereto and made a part hereof.

GENERAL STATEMENT OF WORK

The Contractor shall, unless otherwise indicated herein, supply the necessary personnel, facilities, services and materials to accomplish the work set forth in Exhibits A and B dated 6 August 1965, and made a part hereof and in accordance with the parts of the following documents which are hereby incorporated by reference: Sections II, III, IV (excepting the next to last paragraph), VI (excepting the last sentence of the first paragraph, and the third paragraph entitled "Alternate 2") of the Contractor's Technical Proposal NED/3-65-108, dated 9 April 1965, entitled "Electronics Systems Division Advanced Demodulation Development"; Paragraphs 1 and 4 on pages 1 and 2 and Paragraphs 1 through 4 on pages 2 and 3 (excluding the last three unnumbered paragraphs) of the Contractor's Proposal Supplement NED/3-65-108 undated. In the event of an inconsistency between the aforesaid Contractor's documents, the Proposal Supplement shall govern, and in the event of inconsistency between Exhibits A and B and the Contractor's proposal or proposal supplement, Exhibits A and B shall govern.

CONTRACTOR'S SUMMARY

The Advanced Demodulator is completely compatible with the Model TMR-15 Telemetry Receiver which is part of the TRKI-12 Receiver/Recorder Group now in use at AFETR. The TMR-15 Receiver presently includes three front panel plug-in demodulators, a wide bandwidth, an intermediate bandwidth, and a narrow bandwidth unit, designated as the FMD-C15, FMD-B15, and FMD-A15, respectively. The new demodulator, designated the ADD-15 (Advanced Digital Demodulator) is designed so that it can be both electrically and mechanically substituted for the existing FMD demodulators.

The test program included both laboratory measurements to determine the more basic demodulator characteristics, and also an operational evaluation utilizing simulated complex modulation formats and real-time data obtained from predetection tape recordings. The test program was conducted at the Air Force Eastern Test Range (AFETR) of Patrick Air Force Base and Cape Kennedy, Florida.

The final evaluation includes an extensive analysis of the performance data and a detailed comparison between the new demodulator, and the FMD series of demodulators.

The program end-items include a working engineering model of the demodulator and this Technical Report.

Table 1 is a summary of performance data measured during the test program and provides a performance comparison between the standard FMD series of TMR-15 demodulators and the corresponding modes of the ADD-15 demodulator.

Tests	Reference Section	TMR-15 DEMODULATORS			ADD-15 DEMODULATOR (MODES)			
		FMD-C15	FMD-B15	PMD-A15	WBFM	IBFM	ØLFM	ØLPM
Range of IF BW Accommodated	2	500 kc to 3.3 mc (1)	50 kc to 750 kc (1)		500 kc to 3.3 mc	50 kc to 750 kc	50 kc to 750 kc	50 kc to 3.3 mc
Peak Separation	5.1.1	approximately 5 mc (1)	approximately 1 mc (1)	180° maximum (1)	greater than 18 mc	greater than 1.8 mc	greater than 1 mc	greater than 320°
Static Linearity	4.1 5.1.1	less than 0.5% over ±250 kc (1) less than 1% over ±500 kc (1) less than 2% over ±750 kc (1) less than 5% over ±1.5 mc (1) less than 2% over ±1.5 mc	less than 1% over ±150 kc (1) less than 1% over ±150 kc less than 4% over ±250 kc		less than 2.5% over ±500 kc less than 3.5% over ±1.5 mc less than 5% over ±9 mc	less than 2% over ±150 kc less than 3% over ±250 kc less than 7% over ±900 kc	less than 1% over ±150 kc less than 3% over ±250 kc	less than 2% over ±30° (2) less than 5% over ±90° (2)
Deviation for Rated Video Output	2 3.9	150 kc maximum	15 kc maximum	25° maximum (1)	150 kc maximum	15 kc maximum	15 kc maximum	25° maximum
Video Frequency Response	5.1.3	3 cps to approximately 1 mc (1)	3 cps to approximately 250 kc (1)	50 kc (1)	4 cps to 1.5 mc	4.3 cps to 800 kc (250 kc for high capture)	4.3 cps to 93 kc	500 cps to greater than 1.2 mc
Deviation Meter Ranges	2 3.9	150 kc, 250 kc, 750 kc and 1.5 mc	15 kc, 25 kc, 75 kc, 150 kc and 250 kc	25°, 75° (1) and 150°	150 kc, 250 kc, 750 kc and 1.5 mc	15 kc, 25 kc, 75 kc, 150 kc and 250 kc	15 kc, 25 kc, 75 kc, 150 kc and 250 kc	150°
Pulse Response	5.1.3	Rise Time 0.7 us Decay Time 0.7 us Overshoot and Ringing 35%	Rise Time 2 us Decay Time 3 us Overshoot 2%	Not specified	Rise Time 0.5 us Decay Time 0.5 us Overshoot 20%	Rise Time 1.0 us Decay Time 1.0 us Overshoot 5%	Rise Time 6 us Decay Time 6 us Overshoot 5%	Not measured
Total Harmonic Distortion	5.1.4	0.78% for ±300 kc deviation at 100 kc rate	3.0% for ±125 kc deviation at 100 kc rate	Not specified	1.28% for ±300 kc deviation at 100 kc rate	0.35% for ±125 kc deviation at 100 kc rate	0.36% for ±125 kc deviation at 100 kc rate	Not measured
Intermodulation Distortion	5.1.4	Not measured	Worst case 41 dB below 62.5 kc deviation	Not specified	Not measured	Worst case 40.5 dB below 62.5 kc deviation	Not measured	Not measured
AM Rejection	4.3 5.1.5	Not measured	53 dB at 10 kc, 500 kc IF BW 20 dB at 200 kc, 500 kc IF BW	Not specified	Not measured	29 dB at 10 kc, 500 kc IF BW 38 dB at 200 kc, 500 kc IF BW	64 dB at 10 kc, 500 kc IF BW 48 dB at 200 kc, 500 kc IF BW	Not measured
Capture Ratio	4.2 5.1.7	2.5 dB	4.4 dB	Not specified	2.4 dB	1.0 dB	1.3 dB	Not measured
Threshold and Signal-to-Noise Ratio	5.1.6	6 uv at 3.3 mc IF BW Video SNR = 6 dB at 5.7 uv	2.4 uv at 500 kc IF BW Video SNR = 15 dB at 2.4 uv	Not specified	7.5 uv at 3.3 mc IF BW Video SNR = 3 dB at 5.7 uv	2.4 uv at 500 kc IF BW Video SNR = 15 dB at 2.4 uv	2.4 uv at 500 kc IF BW Video SNR = 19 dB at 2.4 uv	Not applicable Not measured
Fine Tuning Acquisition Range	3.10	Not applicable	Not applicable	±0.0071% min. of rec'd freq. (1)	Not applicable	Not applicable	±100 kc minimum (short loop)	±100 kc minimum (short loop)
Tracking Range	3.10	Not applicable	Not applicable	±0.0071% min. of rec'd freq. (1)	Not applicable	Not applicable	±300 kc minimum	±300 kc minimum
Phase Tracking Loop Bandwidth (3 dB)	4.4.1 4.4.2	Not applicable	Not applicable	continuously adjustable from 20 to 500 cps. (1)	Not applicable	Not applicable	100 kc	470 cps
Lock Threshold	4.4.1 4.4.2	Not applicable	Not applicable	-130 dBm (1)	Not applicable	Not applicable	less than zero dB IF SNR	less than zero dB (2) IF SNR
Phase Jitter	6	Not applicable	Not applicable	1.5° RMS (1)	Not applicable	Not applicable	Not applicable	less than 1.5° RMS
Phase II FM/FM Simulation	5.2.1	See Reference Section						
Phase II PCM/FM Simulation - Threshold	5.2.2	282 bit errors per 3 mega bits at 20 uv	411 bit errors per 1 mega bits at 2.5 uv	Not measured	187 bit errors per 3 mega bits at 20 uv	218 bit errors per 1 mega bits at 2.5 uv	84 bit errors per 1 mega bits at 2.5 uv	Not measured
Phase III PCM Playback Tests	5.3.1	See Reference Section						
Phase III PDM Playback Tests	5.3.2	See Reference Section						

NOTES: (1) Specified Performance - given for reference or when small difference between specified and measured performance.
All ADD-15 data measured. No tests on PMD-A15.

(2) Not measured directly - performance based on indirect measurements and/or calculations.

TABLE 1. PERFORMANCE SUMMARY

SECTION II

INITIAL STUDY

A number of new design approaches for an advanced FM demodulator were given consideration during the initial phases of this program. Part of this study included an evaluation of the presently available FMD series of demodulators which are part of the TMR-15 receiving system, the object being to provide new capability in those areas where the existing demodulator lacks performance for present and particularly for future applications. This was not too easy a task since the TMR-15 receiving system was originally designed to exacting specifications which reflected most of the forseeable future requirements at the time of writing.

However, possible areas for improvement do exist, and include linearity over wider bandwidths for future application, improved threshold characteristics, high capture ratio and solid state higher reliability design. In particular, high capture ratio has recently been recognized to be a major factor in receiver performance under severe multipath conditions, such as caused by the high reflection coefficient and large signal delays associated with ship and airborne telemetry reception over the oceans. Possible new demodulator approaches included phase lock FM discriminators, frequency feedback, and Tan-Lock demodulators. These circuits provide an improved threshold characteristic but have the disadvantage of having to be carefully optimized for a particular modulation format to realize this improvement, and also present problems in achieving high VCO linearity over wide bandwidths. Also these circuits do not represent a particularly new approach.

An initial effort was started on a pulse-averaging type of discriminator incorporating the design principles utilized by demodulators presently used to demodulate FM subcarriers and predetection record carriers. Essentially this circuit generates constant area pulses at the instantaneous input frequency rate, and then integrates the pulses to generate a voltage analog of the input frequency. Presently available pulse-averaging discriminators for lower frequency applications provide excellent linearity over wide deviation bandwidth and this approach appeared to have merit for 10 mc applications.

As the design progressed, it became apparent that the high input frequency demanded very fast switching times in the digital circuitry and although achievable, required rather sophisticated digital techniques. To reduce the requirement on circuit speed, the input signal was down-converted to a lower frequency of approximately 1 mc. However, the combinations of mixer products and the harmonics produced in the digital circuitry generated a cacophony of miscellaneous "birdies" and spurious products. These problems could eventually be eliminated, but because of the bandwidth restrictions at the lower frequency, this approach was discarded.

The demodulator approach finally pursued consists essentially of a phase comparator circuit which includes a constant time delay in series with one input. The delay line produces an odd multiple of 180 degrees phase shift at the input center frequency. The 10 mc input signal is applied to both the direct and delayed input to the phase comparator, with the result that the phase difference appearing at the input to the phase comparator varies linearly over very wide range of input frequency deviation. The output of the phase detector is thus a voltage analog of the input frequency and the circuit constitutes a wideband FM demodulator. A digital type phase detector circuit was utilized to obtain linear operation over a wide range of phase and consequently frequency deviation. This approach does require very fast digital circuitry, but in this case, there is no need for precise monostable timing circuits and the requirements could be realized with fairly conventional and reliable circuitry. The fact that the demodulators incorporate a phase detector as a basic element also suggests the possibility of adding a voltage controlled oscillator to the circuit and providing the demodulator with phase-lock modes. Both a phase-lock FM and a phase-lock PM mode were included in the final design with little increase in complexity.

The overall design objectives were finalized upon completion of this initial study and are summarized as follows:

The new demodulator will provide a significant improvement in linearity over wide deviation bandwidths, as compared with the standard FMD series of demodulators. The unit will also include a phase-lock FM discriminator which will demonstrate an improved threshold characteristic compared to the standard demodulators. A "short-loop" phase-lock PM mode will also be provided primarily to demonstrate the feasibility of this approach and to enhance the flexibility of the package. The new demodulator will be completely compatible both electrically and mechanically, with an unmodified TMR-15 receiving system. In particular, the deviation sensitivity, video output levels, and bandwidths, metering and control functions, and other electrical-mechanical characteristics will be the same as the corresponding FMD demodulators, the object being to be able to switch between the new and a standard demodulator without requiring additional readjustment of the receiver or terminal equipment.

The final questions remaining then, is can these design objectives be realized and most important, will some other demodulator parameter, such as signal-to-noise ratio, be compromised in the new design? This topic is covered in Section VI.

SECTION III

DEMODULATOR DESIGN ANALYSIS

Refer to functional block diagram, figure 1 and the schematic diagram, figure 2.

3.1 INPUT BUFFER

The 10 mc (unlimited) output from the receiver IF amplifier is applied to the demodulator signal input P1 and is AC coupled to an emitter follower Q2. This circuit functions as an input isolation buffer. A 91 ohm resistor in shunt with the high input impedance of the emitter follower provides the proper coaxial input termination, and thus eliminating reflections and frequency/phase response problems. The emitter follower also provides a low output impedance to drive the undelayed and delayed channels.

The output from the buffer is simultaneously applied to two separate signal paths, that is, the input to the undelayed limiter and the input to the switch selected delay lines.

3.2 UNDELAYED CHANNEL

A two-stage limiter is used ahead of each input to the phase comparator. The first (input) limiter stage in the undelayed channel consists of an emitter coupled pair Q5 and Q6, and provides approximately 25 dB gain ahead of the second limiter. The second limiter stage is also an emitter coupled pair Q12 and Q13, with a gain of approximately 15 dB, and the combination of both stages provides more than 50 dB of limiting below the normal input level. AC coupling is used between emitters, and between the first and second stage to obtain stable and highly symmetrical clipping without the need for balance adjustments. The coupling time constants were experimentally determined to optimize the AM rejection capabilities of the limiter. Limiter symmetry was also found to have a significant effect on the demodulator deviation linearity and capture ratio.

The output of the limiter is applied to a differentiating circuit, the purpose of which is to generate very short pulses at the zero crossing of the square wave output of the limiter. The circuit consists of tunnel diode CR5, germanium transistor Q16 and inductor L5. The tunnel diode is a negative resistance device with the characteristic that the junction voltage "jumps" from approximately 65 mv to approximately 500 mv as the diode current is increased to 1 ma. The voltage transition occurs in less than two nanoseconds and is essentially independent of the rise time of the square (current) wave output of the limiter. The tunnel diode voltage rise causes the transistor Q16 to conduct and the rapid change in collector current generates a large amplitude voltage pulse across inductor L5. This pulse is coupled through C41 to R66 and the base of Q18. Resistor R66 provides the proper damping across L5 to prevent ringing, and the LR combination was experimentally optimized to produce trigger pulses with less than five nanoseconds rise time. Zener diode CR8 limits the collector voltage of Q16. A variable resistor (R50) is provided as part of the total common emitter resistance in the second limiter stage. This adjustment varies the current which is being cyclically transferred between Q12 and Q13 during the limiting process, and consequently also varies the current coupled through the tunnel diode (CR5). The purpose of the adjustment is to set the current at which the tunnel diode triggers to correspond to the exact zero crossing of the 10 mc input to the demodulator. This insures optimum AM rejection, capture ratio and deviation linearity.

3.3 DELAYED CHANNEL

The front panel mounted MODE control (S1) is a five (5) position, eleven pole switch which provides four selectable functional modes and a fifth "spare" position for future applications. The

four presently available modes are:

(1) Wide band FM (WBFM)

(2) Intermediate band FM (IBFM)

(3) Phase-lock FM (ØLFM)

(4) Phase-lock PM (ØLPM)

As indicated above, the output signal from the buffer emitter follower is also applied, through the MODE switch, to the input of the delay lines. In the WBFM mode, the 10 mc carrier is applied through a 0.05 microsecond linear delay line (DL3), to the input of an isolation emitter follower (Q3). The 0.05 microsecond delay results in a 180 degree phase shift between the delayed and undelayed channels at exactly 10 mc, and a phase variation from zero to 360 degrees over the frequency range from zero to 20 mc. The parallel combination of L15, C81 and R10 provides the source impedance for DL3 and the network was optimized for phase linearity over an input frequency range of 10 mc ±5 mc. Resistor R12 is in shunt with the high input impedance of emitter follower Q3 which provides the proper termination impedance for the delay line. The emitter follower (Q3) supplies an input signal to the delayed channel limiter, and is designed to have the same output impedance as emitter follower Q2 in order to insure that the delayed and undelayed channels have the same bandwidth and phase characteristics, except for the contribution of the delay line. In the IBFM mode, the 10 mc carrier is applied through two 0.25 microsecond delay lines connected in series, to the input of amplifier Q1. Instead of providing the required 0.5 microsecond delay in a single unit, improved phase linearity and lower overall insertion loss was obtained by utilizing the series combination of two delay lines of half the required delay each. Resistor R4 provides the proper source impedance for the delay line DL1. Resistors R1, R2, R3 and inductor L14 constitute a matching and isolating network between DL1 and DL2. Inductor L1 and resistor R5 in parallel with the input of Q1 form the terminating impedance for the delay line, and were optimized for phase linearity over an input frequency range of 10 mc ±1 mc. The prime function of isolation amplifier Q1 is to provide an additional half cycle phase shift in the IBFM delayed channel. This phase reversal combined with the 0.5 microsecond delay, results in a 180 degree phase shift between the delayed and undelayed channels at exactly 10 mc, and a phase variation from zero to 360 degrees over the frequency range from 9 mc to 11 mc. Amplifier Q1 also compensates for the higher delay line insertion loss in the IBFM mode.

The two-stage limiter consisting of Q7, Q8, and Q14, Q15, and the tunnel diode differentiating circuit consisting of CR6, Q17, and L6, are identical in function and performance with the corresponding circuits in the undelayed channel.

3.4 PHASE COMPARATOR, FLIP-FLOP CIRCUIT

The undelayed and delayed channels each deliver a continuous sequence of fast, positive and negative pulses to the corresponding input drivers of the flip-flop circuit, Q18 and Q19. These pulses occur at the zero crossings of the signals applied to the input of the respective channel limiters, and have a repetition rate equal to the instantaneous (IF) input frequency. As indicated above, the relative phase between the pulses from the undelayed and the delayed channels will be 180 degrees at exactly 10 mc and will range from zero degrees to 360 degrees as the input frequency is varied over a range determined by the selected delay line.

The flip-flop circuit consists of the flip-flop driver Q18 and Q19 and the DC coupled regenerative pair, Q20 and Q21. The flip-flop drivers are designed to conduct only when the base voltage is driven positive. When one of the drivers, Q18 for example, is driven into conduction, the voltage at the base of Q20 is driven negative cutting off Q20. Simultaneously, the collector of Q20 and the base of Q21 (coupled through zener diode CR11) become more positive causing Q21 to conduct. With Q21 conducting the collector of Q21 and the base of Q20 (coupled through zener diode CR10) is held negative with respect to the directly coupled emitters, and Q20 remains cut off after the input pulse has decayed and Q18 has ceased to conduct. Thus, the circuit will

remain in a steady state until a positive pulse is applied to the opposite driver Q19, and the circuit conditions reverse from that indicated above; that is, Q20 is then conducting and Q21 is cut off. The circuit is designed to be nonsaturating and the high degree of regeneration and low circuit impedance result in very fast (approximately five nanoseconds) transitions between the two steady states. Because the drivers conduct only on positive pulses, the negative derivatives are effectively eliminated and the circuit "flips" and "flops" on only the positive going, zero crossings of the input signal to the two limiter channels.

The flip-flop output is taken from the base of Q20 and consists of one or the other of two constant voltage levels depending on which of the two possible steady states the circuit is in. The time the output voltage remains at one level will be equal to the time between a positive trigger pulse applied to one input and the next following positive trigger pulse applied to the other input. The flip-flop output thus consists of a rectangular wave form with a repetition rate equal to the instantaneous (IF) input frequency. The duty cycle of the rectangular signal is proportional to the relative phase between the pulse trains from the delayed and undelayed channels, and varies from zero to 100 percent corresponding to a phase difference ranging from zero to 360 degrees. At 10 mc input frequency the output of the flip-flop is a square wave corresponding to 180 degrees phase difference.

3.5 CONSTANT CURRENT CLIPPER

The output of the flip-flop is applied to a constant current clipping circuit. The purpose of the circuit is to regenerate the rectangular output of the flip-flop, accurately reproducing the duty cycle but maintaining the output pulse amplitude (current) constant within very close limits. This is done to insure that the total charge-per-time, that is current, delivered to the integration circuit (discussed below) is dependent only on duty cycle and is independent of repetition rate, trigger amplitude, drift in the flip-flop and other sources of amplitude variation. This in turn will allow the overall demodulator deviation linearity to be essentially independent of all circuit elements except the delay lines (and switching times at very wide deviations).

The clipping circuit consists of an emitter coupled pair, Q23 and Q24, with a constant current common emitter source Q4. The flip-flop output signal is applied to the base of Q23. The "reference" voltage applied to the base of Q24 is derived from a summation of the voltages appearing at the base of Q20 and Q21. The voltage at these two points, opposite outputs of the flip-flop, consists of an equal DC bias plus rectangular waveforms with reversed duty cycle; that is, when the signal on one base has 90% duty cycle, the signal on the opposite base has a 10% duty cycle, etc.. Thus, the sum of these two voltages will produce a constant DC level at the base of Q24 independent of duty cycle and the relative input phase relationship. This reference voltage is always equal to a voltage midway between the "ON" and "OFF" output level of the flip-flop, which thus results in symmetrical clipping of the rectangular waveform regardless of duty cycle. A large capacitor C63, eliminates any residual signal components on the base of Q24.

When the signal on the base of Q23 is more positive (by 0.2 volts or more) than the reference voltage on the base of Q24, Q24, will be cut off. When the signal on the base of Q23 is more negative than the reference voltage, Q23 will be cut off and Q24 will be fully conducting. The current through Q24 is determined by the current through Q4 and is essentially independent of the base voltage of Q23. Q4 is provided with a high degree of emitter degeneration and is biased from the regulated B- supply, resulting in a constant current through Q4; and a very high current source impedance (collector of Q4). Circuit stability is improved by the small value emitter coupling resistor R94. Resistors R95 and R96 provide some additional balance between the emitter coupled pair and, more important, isolate the signal path from the collector capacity of Q4.

The output of Q24 consists of constant current rectangular pulses with a rise and decay time of less than five nanoseconds.

The complex load impedance in the collector of Q23 is the same as in the collector of Q24. Consequently, the DC voltage drop and the waveform produced at the collector of Q23 is essentially the same as that at the collector of Q24, except that the duty cycle is reversed. Similar to the approach used in the flip-flop to derive a clipping reference voltage, a summation of the two collector voltages is made through the equal resistors R89 and R99.

Since the waveforms on the two collectors are equal in amplitude but 180 degrees out-of-phase, the signal components will cancel in the summation,and the DC voltage at the junction of R89 and R99 will equal the average (DC) value of the DC output,which is constant. The residual signal voltage in the DC output which is due to slight circuit unbalance and waveform difference is more than 40 dB below the collector signal and consists mostly of high frequency "transient" components which are further reduced by capacitor C59. The "average voltage" is utilized as a reference voltage in the DC amplifier discussed in more detail below. Zener diode CR12 provides additional stabilization and filtering to the positive supply voltage for the clipper.

3.6 INTEGRATOR

The constant current rectangular pulse output of the clipper is applied to an integration circuit consisting of collector load resistor R100 and capacitor C65. The time constant of the combination is 0.047 microsecond or approximately one half period of the 10 mc repetition rate. The "average" voltage developed across capacitor C65 is proportional to the current delivered from the collector of Q24 (which is constant amplitude) and the current pulse duration per cycle, that is the duty cycle of the flip-flop output. The circuit constants are such that the "average" voltage across C65 can vary at a rate exceeding 1.5 mc. The integration network is followed by a two section passive filter, L8, R117, C66 and L9, R118, C67, which effectively eliminates the carrier ripple remaining across C65. The filter is carefully designed to contribute a minimum of overshoot, ringing, and other distortion to fast rise (0.25 microseconds) pulses, while also suppressing carrier components as low as 5 mc. The overall frequency response of the composite integrator-filter network is shown in figure 3.

The output of the integrator-filter appearing at the base of Q29, consists of a voltage which is linearly proportional to the phase difference between the signals (pulse trains) applied to the flip-flop drivers Q18 and Q19, that is, the flip-flop-clipper-integrator combination comprises a linear digital phase comparator and is referred to as the "phase detector" in the discussion which follows. The linear phase vs. output voltage relationship extends over an approximate range from 30 degrees to 330 degrees. The "flattening" of the phase response beyond this range (to zero and 360 degrees) is due to the finite switching time of the flip-flop and clipper circuitry. For example, a five nanosecond rise time in the clipper output would correspond to 5 NS/100NS = 5% of the 10 mc period, and would produce 0.05 x 360 = 18 degrees of nonlinearity at the extreme of the phase detector response. The phase response of the digital phase detector circuit is shown in figure 5.

In the WBFM and IBFM mode the normal signal appearing at the base of Q29 consists of a DC component proportional to the input carrier frequency and superimposed demodulated FM video. In the ØLPM mode this signal consists of a DC voltage required to maintain phase lock and the demodulated PM video. In the ØLFM mode, the base voltage will equal the instantaneous phase error voltage required to maintain phase lock. This voltage is the analog of the instantaneous input frequency and will therefore also contain the demodulated FM video. The phase-lock circuit will be discussed in more detail below.

3.7 DARLINGTON CIRCUIT

The output of the phase detector is applied to a Darlington emitter follower consisting of the complementary pair of transistors Q29 and Q30. This circuit provides a number of functions in the demodulator depending on the particular operating mode selected. In all modes the circuit exhibits a high input impedance necessary for proper termination of the integrator-filter

combination. Transistor Q30 provides the low output impedance and high current necessary to drive the DC amplifier , the video amplifier, and particularly the video filter in the IBFM mode. In the ØLFM mode, the phase tracking loop filter is connected between the output of Q29 and the input of Q30. This proved to be a fortunate location for this filter because the low output impedance of Q30 allowed the passive filter characteristic to be easily calculated and also be relatively independent of the active circuit elements. A complementary (PNP transistor followed by a NPN transistor) configuration is used to avoid any DC offset due to the transistors and because circuit drift due to temperature changes tends to cancel in the output. In the WBFM and IBFM modes, a small positive or negative DC offset voltage is introduced at the base of Q30. This voltage compensates for tolerances in the delay lines which result in small deviation from the required 180 degree phase shift at exactly 10 mc input frequency. This "phase error" produces a DC offset at the modes at center frequency. The offset voltage is adjusted by two front panel mounted screwdriver potentiometers, labeled ZERO WBFM and ZERO IBFM respectively, which are selected by the MODE switch. These controls are adjusted for "ZERO" on the receiver tuning meters when tuned for input center frequency. The high value series resistor R161 prevents any significant signal attenuation by the offset network.

3.8 VIDEO OUTPUT

In the WBFM mode the video output from the Darlington circuit is AC coupled to the video output amplifier. This circuit consists of amplifier Q33 and output emitter follower Q34 which is AC coupled to the video output connector. The overall gain of the circuit is approximately 18 dB. The circuit is biased to sharply clip on the negative voltage swing at an output of approximately 4 volts peak-to-peak. This clipping is purposely introduced to prevent degradation of the capture ratio because of an overload which can occur elsewhere in the receiver. This subject is discussed in more detail in the report section on performance. Inductor L16 is a peaking coil which extends the high frequency range of the video amplifier compensating for a small video roll-off introduced by the Darlington circuit and phase detector filter. The peaking coil is optimized for fast pulse reproduction.

In the IBFM mode, the video signal is coupled through a low pass post detection filter which is switched in ahead of the video output amplifier. This filter is a six pole linear phase design with a 36 dB asymptotic roll-off. The function of the filter is to attenuate the high frequency components of the transients produced by interfering in-channel signals and thereby improves the demodulator capture ratio. A more detailed discussion of the filter and capture ratio is given below. The input network of the video amplifier is carefully designed to exhibit the correct (600 ohm resistive) terminating impedance for the filter, thus insuring the correct cut-off frequency and phase linearity for pulse reproduction. The filter assembly A1 is identical to the video filter boards included in the Video Amplifier Unit, model VAU-15 which is part of the TMR-15 receiver group. The video filter assembly is plugged-in to the demodulator chassis and a variety of video bandwidths are available for different applications. The bandwidth presently installed in the unit is 250 kc which is chosen as the best compromise for capture ratio in the IBFM mode. In the ØLFM mode, the video signal is AC coupled directly to the video amplifier. However, in this mode, the phase correction network which must be provided in a phase lock FM discriminator, is connected to the collector of Q33 by the mode switch. This network consists of R150, C89 and R165, and is designed for an overall video high frequency response which is 3 dB down at 100 kc, with no overshoot.

In the ØLPM mode the video signal is coupled through a resistive attenuator network consisting of R148 and the parallel combination of R155 and R149. This network reduces the demodulated PM video approximately 10 dB which is a compromise between PM sensitivity and maximum phase deviation before the receiver overloads. The present circuit allows phase deviation in excess of ±90 degrees without clipping either in the demodulator output amplifier or in the receiver circuitry.

3.9 DC AMPLIFIER

The output of the emitter follower (Q30) is also direct coupled to the input of the DC amplifier. This circuit consists of an emitter coupled differential amplifier stage Q31 and Q32, a direct coupled common emitter amplifier Q28, and an emitter follower output stage Q27. The emitter coupled differential amplifier exhibits excellent temperature stability and linearity, and these characteristics are further improved by the emitter degeneration provided by resistors R136 and R142. The high value common emitter resistor R137 gives the differential amplifier a high "common mode" rejection for equal voltage variations occurring simultaneously on the base of Q31 and Q32. As indicated above, the differential amplifier reference voltage applied to the base of Q31 is derived from a summation of the voltage at the collectors of the constant current clipper, Q23 and Q24. This voltage is equal to the average of the two collector voltages for all duty cycles or, stated somewhat differently, the constant reference voltage is equal to the DC voltage at the collector of Q24 at a 50 percent duty cycle. Any changes in supply voltage or long term current drift will produce the same change in both collectors of the clipper circuit, and thus the same change in the reference voltage. Since there is approximately unity DC gain between the collector of Q24 and the input to the DC amplifier, these voltage variations will be cancelled in the differential stage, and will not produce an output from the DC amplifier. Thus, the DC amplifier is responsive only to the flip-flop duty cycle and therefore the relative phase of the input signals, and is essentially non-responsive to any common mode variation in the phase detector. The output emitter follower is designed to provide an output voltage greater than 20V peak-to-peak into a load of less than 1000 ohms. The large output voltage capabilities of the DC amplifier are required to insure reliable acquisition and phase tracking by the phase lock loop, under conditions of large carrier frequency deviation and center frequency error.

The DC amplifier provides different functions in the demodulator depending on the particular operating mode selected. In the WBFM, IBFM, and ØLFM modes, negative feedback is applied around the DC amplifier by means of the resistive network R144 and R145. In this configuration, the amplifier exhibits a highly stable, closed loop DC gain of approximately 18 dB, which is roughly equal to the ratio of R144 to R145. Phase compensation capacitor C84 is optimized for frequency stability and good pulse reproduction with an overall 3 dB high frequency of about 1.8 mc.

In the WBFM and IBFM and ØLFM modes, the DC amplifier supplies a DC coupled video signal to the DC-FM output of the receiver, the AFC and tuning meter circuits, and the deviation meter circuit. The demodulator includes a voltage divider and a front panel deviation meter range switch S2, which is connected to the output of the DC amplifier. This switch provides five (5) calibrated peak frequency deviation ranges which are listed in the table below. A X10 multiplication factor applies in the WBFM mode. A sixth switch position is also provided for measuring peak phase deviation in the ØLPM mode. However, in the ØLPM mode the video amplifier frequency response is cut off below the modulating frequency range, so the video sample for monitoring phase deviation is taken from a voltage divider connected to the output of the video amplifier.

TABLE 2. DEVIATION METER RANGE SWITCH

(Peak Full Scale Deviation)

Switch Position	WBFM	IBFM/ØLFM	ØLPM
1	150 kc	15 kc	-
2	250 kc	25 kc	-
3	750 kc	75 kc	-
4	1500 kc	150 kc	-
5	-	250 kc	-
6	-	-	150 degrees

In the ØLFM and ØLPM modes the DC amplifier increases the loop phase error voltage and supplies the frequency control function to the voltage controlled oscillator (VCO). In the ØLFM mode the amplifier produces a control voltage which is proportional to the instantaneous frequency deviation of the carrier up to the highest modulating frequency component. In the ØLPM mode, however, the DC amplifier is utilized as an operational amplifier integration circuit in the phase lock loop. This is accomplished by incorporating capacitive feedback around the DC amplifier which results in the following transfer function:

$$\frac{1}{RC}\int e_{\Delta\phi}\,dt$$

where: R = R145
C = series combination of C70 and C83
$e_{\Delta\phi}$ = the phase error voltage.

Resistor R143 provides loop damping and is optimized for an input signal-to-noise ratio of 0 dB.

3.10 VCO

The voltage controlled oscillator consists of an L-C Butler oscillator circuit Q25 and Q26, and an emitter follower isolation buffer Q22. The Butler circuit utilizes a series tuned circuit which couples energy between the emitters of Q25 and Q26. The tuned circuit consists of inductor L7 and the series combination of C62 and the voltage variable capacitor CR16. L7 and CR16 are contained in a shielded assembly which includes a ferrite slug in L7 to adjust the oscillator center frequency. Regenerative feedback is provided by coupling the signal at the collector of Q26 through C61 to the base of Q25. Approximately 9 volts negative reverse bias is applied to the varicap through decoupling network R90, C58, and R91. This voltage is obtained by a highly stable temperature compensated zener diode CR13. A front panel potentiometer R109, is included in the circuit to vary the varicap bias and the VCO center frequency over a small "vernier" range of approximately ±100 kc.

The frequency control voltage is applied through decoupling network L11, R98, C78. A VCO sensitivity adjustment R105, and a control voltage shaping network is provided between the output of the DC amplifier and the VCO control input. The shaping network consists of germanium diodes CR14, CR15 and resistors R116, R111, R113, R146, R107, and R147. The function of this circuit is to compensate for the non-linear capacity-vs-voltage characteristics of the varicap, to obtain a linear frequency vs control voltage response in the VCO.

The shaping circuit consists essentially of a variable slope attenuator which approximates the ideal "correction curve" with three different straight line attentuation slopes. The slope "break points" are fixed by the diode bias. The diode bias and series resistors were determined experimentally for best VCO linearity over ±300 kc pulling range. The time constants in the frequency control circuits are carefully controlled to allow the VCO to be deviated at modulation rates up to 1.5 mc. This insures that the overall loop performance is determined entirely by the loop filter components which, in the present ØLFM mode, were optimized for a modulation response cut off frequency of 100 kc. The VCO sensitivity is adjusted so the video output in the ØLFM mode is the same as in the IBFM mode with the same carrier deviation.

In the WBFM and IBFM mode, the negative supply voltage to the VCO is removed by mode switch wafer S1D, and the VCO is disabled. Resistor R112 supplies a small positive reverse voltage to the oscillator transistors to prevent conduction and possible spurious output signals when the VCO is off.

3.11 PHASE LOCK LOOP

In the ØLFM and ØLPM modes, the 10 mc output of the VCO is connected through a coaxial cable from the emitter of Q22 to the input of the "delayed" channel limiter. A 50 ohm resistor R16 properly terminates the coaxial lead at mode switch wafer S1B. The phase detector generates an error voltage which is proportional to the phase difference between the 10 mc input signal and the output of the VCO. This error voltage is amplifier in the DC amplifier and applied to the

VCO in the correct phase to drive the instantaneous VCO frequency in a direction which tends to maintain a constant 180 degree phase difference at the input of the phase detector. In the ØLFM mode the VCO frequency must equal the instantaneous input frequency during modulation. Therefore, the VCO control voltage, which is linearly proportional to VCO frequency, is a linear analog of the instantaneous input frequency, and thus represents the demodulated FM video signal.

In the ØLPM mode, the response of the DC amplifier is restricted so the VCO can only "track" slow variations in the carrier frequency. For modulation rates above the loop cut-off frequency, the phase detector will generate an error voltage proportional to the instantaneous phase deviation and the voltage will represent the demodulated PM video signal which is applied to the video amplifier. Reliable PM demodulation requires that the peak phase deviation, which also equals the modulation index, does not continuously exceed $\pm\pi$ radians or equal any modulation index resulting in a carrier null, otherwise the phase tracking loop will lose lock.

3.12 POWER SUPPLY

An electronically regulated power supply is included as a separate assembly within the demodulator unit. Since the standard FMD series of demodulators which the ADD-15 is designed to replace, are vacuum tube designs, it was possible to utilize the AC filament supply for part of the power input to the solid state unit. A 2:1 step up transformer is powered from the unregulated 12.6 volt RMS filament input to the demodulator. The output of the transformer is applied to a full wave silicon diode rectifier, and the resulting positive DC voltage is filtered with capacitor C15, C16 and C82 connected in parallel. An electronic series regulator Q9, Q10 and Q11 provides additional filtering and maintains the positive supply voltage constant at approximately 15 volts. Q10 functions as the regulating series element. Q11 is an emitter follower which effectively multiplies the current gain of Q10. The output voltage is sampled by a resistive divider connected between the positive 15 volt supply and the negative 28 volt regulated supply. The divider ratio is designed to produce approximately +0.7 volts at the junction of R42 and R43, and this "error" voltage is applied to the feedback amplifier Q11. Transistor Q11 provides the necessary phase reversal and loop gain and, by controlling base voltage of Q9, acts to maintain its base voltage and thus the output voltage constant. Silicon diode CR3 compensates for the temperature variation in the base emitter voltage of Q11. Capacitor C34 bypasses R42 allowing maximum loop gain for AC components, thus reducing the output ripple to a minimum. The parallel combination of C35 and C36 further reduces the supply output impedance, particularily at high frequencies.

The regulated negative 28 volt supply is obtained from the ADU-15 chassis. The parallel combination of C8 and C9 reduces the supply impedance and provides additional filtering.

Considerable precautions were taken to prevent the high energy signals generated within the demodulator from getting into the receiver or other equipment and causing spurious disturbance. The coaxial input cable is carefully grounded. The VCO output lead is shielded to prevent unnecessary radiation. All unshielded leads, particularily the interlock jumpers, are kept as short as possible, and wherever possible external connections are filtered with ferrite "beads", chokes, and high frequency bypass capacitors. The demodulator chassis is completely enclosed by tightly fitting screwed down covers.

No interference problems were observed during the extensive demodulator tests.

SECTION IV

PERFORMANCE CALCULATION AND ANALYSIS

4.1 DEMODULATOR DEVIATION BANDWIDTH AND LINEARITY

The digital demodulator deviation bandwidth in the WBFM and IBFM modes is determined by the linear range of the digital phase detector and the value of linear time delay provided in the "delayed" input to the phase detector.

The digital phase detector provides a voltage output which is linearly proportional to the input differential phase over a range exceeding 320 degrees or 180 ±160 degrees.

In the WBFM mode, a constant time delay of 0.05 microseconds is switched into the "delayed" channel input to the phase detector. This delay produces a differential phase shift at the 10 mc input center frequency of:

$$\frac{\tau}{T} = \frac{.05}{0.1} = 0.5 \text{ cycle or } 180 \text{ degrees}$$

where: τ = time delay in microseconds
T = period of input signal = $\frac{1}{10 \text{ mc}}$ = 0.1 microsecond

With the differential phase equal to 180 degrees, the phase detector flip-flop generates a 50 percent duty cycle pulse train, and the resulting integrated DC level corresponds to the demodulator center frequency output voltage.

The linear frequency deviation range corresponding to ±160 degrees and 0.05 microsecond delay is given as follows:

$$\Delta f = \frac{1}{\tau} \cdot \Delta\phi = \frac{1}{\tau} \left(\pm\frac{160}{360}\right), \qquad \text{where: } \Delta\phi = \text{phase shift in cycles.}$$

$$\Delta f = \frac{1}{0.05 \cdot 10^{-6}} (\pm.445) = \pm 9 \text{ mc}$$

that is, the demodulator will provide a linear deviation bandwidth of 18 mc peak-to-peak.

For the IBFM mode, a lumped delay of 0.5 microsecond is switched into the delayed channel. This delay results in five complete cycles of differential phase shift, so in order to obtain 180 degrees phase difference at center frequency, it was necessary to also provide in the delayed channel an additional common emitter stage which effects the extra half cycle shift. In this case:

$$\Delta f = \frac{1}{\tau} \quad \Delta\phi = \frac{1}{0.5 \cdot 10^{-6}} (\pm .445) = \pm 0.9 \text{ mc}$$

providing a linear deviation bandwidth of 1.8 mc peak-to-peak. With frequency deviation beyond ±1 mc, the demodulator response is repeated at 2 mc increments resulting in a "sawtooth" response for very wide deviations. For example, the demodulator output voltage is the same for instantaneous input frequency of 10 mc, +0.5 mc, +2.5 mc, +4.5 mc, etc., with a similar effect occurring below center frequency. This phenomenon causes no problems since the IBFM mode would never be used with IF bandwidth greater than 2 mc and in most applications would be used with IF bandwidth of 750 kc or less.

As indicated later in this report, the measured linear range of both demodulators exceeds that predicted above, indicating that the phase detector is linear over a wider angular range than was assumed.

The demodulator linearity critically depends on the linear relationship of phase variation vs frequency provided by the delay line, that is, the constancy of time delay with frequency. Some difficulty was encountered during the design of the demodulator in eliminating small variations in delay over the frequency range of interest. In the WBFM mode, a 50 ohm coaxial cable was originally tried to provide the required 0.05 microsecond delay. However, it was found that the demodulator linearity was quite sensitive to the cable termination and the final design utilized a lumped constant delay line. The delay line terminations were experimentally optimized for best linearity over the deviation bandwidth calculated above. However, it was not possible to compensate for small delay fluctuations which result in approximately 1 percent "wiggles" in the demodulator response curves. This problem is more noticeable in the IBFM mode in which the input frequency is much closer to the delay line cutoff frequency (approximately 12 mc). It is reasonable to assume that these nonlinearities can be eliminated with improved delay lines which are designed specifically for this application with special attention given to these problem areas.

4.2 CAPTURE RATIO

Capture ratio is a measure of the ability of an FM demodulator to suppress undesired signals which are sufficiently close to the desired (tuned) frequency to pass through the receiver IF amplifier. Capture is defined as the ratio of undesired to desired signal amplitude for a specified degree of undesired signal suppression in the demodulated output. (The reciprocal ratio expressed in dB is also commonly specified.)

An interfering FM signal produces very large "Pulses" of frequency deviation at a repetition rate equal to the instantaneous difference frequency between the desired and undesired signals. The maximum peak-to-peak resultant deviation is given by:

$$\Delta f = \frac{1 + r}{1 - r} D$$

r = ratio of undesired to desired signal amplitude.
D = peak-to-peak deviation of desired and undesired signals.

For example, for a design goal of r = 0.9 (.92 dB) and D = 250 kc, the resultant deviation could be as high as 4.75 mc peak-to-peak. Suppression of interference due to the undesired signal requires that the voltage output of the demodulator be proportional to the "average" value of the desired signal. This can be accomplished by designing the discriminator and the following video circuits with sufficient bandwidth and dynamic range to linearly accommodate the large deviation, fast rise time, and large amplitude pulses produced by the interference. Additional requirements for high capture ratio include uniformity of predetection passband response and wideband, highly saturated limiters. An interfering signal also produces large carrier amplitude variations given by:

$$A = \frac{1 + r}{1 - r} = \frac{1 + 0.9}{0.1} = 19/1$$

or almost 26 dB in the above example. These amplitude variations must be effectively removed by the limiters.

The above discussion is based on an analysis by Arguimbau [1-3] who suggests wideband discriminator to achieve high capture ratio for FM broadcast applications. However, because of the much wider bandwidths required for telemetry applications recent designs for high capture ratio receivers are based on a suggestion by Baghdady [4-6]. This approach utilizes as many as three cascoded sections of limiter-IF filter combinations, with the IF bandwidth of each section progressively reduced (tapered) towards the discriminator. Although practical and providing capture ratios of 0.9 and higher, this approach is somewhat complicated and expensive and the design must be optimized for particular modulation formats.

---

[1] L. B. Arguimbau and J. Granlund, "Interference in Frequency Modulation Reception", Tech. Rep. No. 42, Res. Lab. Elec. M. I. T., Cambridge, Mass.

[2] L. B. Arguimbau and J. Granlund, "Transatlantic Communication by Frequency Modulation", Proc. NEC, Vol. 3, P-644; Nov. 1947.

[3] L. B. Arguimbau and J. Granlund, "Sky-Wave FM Receiver", Electronics, Vol. 22, P-101-103; Dec. 1949.

[4] E. J. Baghdady, "Frequency-Modulation Interference Rejection with Narrow-Band Limiters", PROC. IRE, Vol. 43, P-51-61; Jan. 1955.

[5] E. J. Baghdady, "FM-Demodulator Time-Constant Requirements for Interference Rejection", PROC. IRE, Vol. 46, P-432-440, Feb. 1958.

[6] E. J. Baghdady, "Theory of Stronger-Signal Capture in FM Rejection", PROC. IRE, Vol. 46, P-728-738; Apr. 1958.

The very wide deviation bandwidth capabilities of the digital demodulator suggest the possibility of utilizing the Arguimbau approach to achieve high capture ratio.

The digital demodulator provides a peak-to-peak bandwidth of 2 mc in the IBFM mode and almost 20 mc in the WBFM mode. Although 2 mc does not equal the theoretical bandwidth requirement illustrated in the example above, the digital demodulator is considerably wider than the standard FMD-B15 demodulator. Furthermore, instead of the "S" curve response of typical discriminator circuits, the digital demodulator provides additional linear 2 mc "cycles" above and below ±1 mc from center frequency. The video circuits following the digital integrator were designed to have sufficient dynamic range to accommodate the maximum deviation capability of the demodulator without overloading. Because the TMR-15 receiver overloads with the deviation peak generated by interfering signals, a linear passive low pass filter is included in the demodulator video output circuit in the IBFM mode. This filter removes the large interference pulses without affecting the demodulator response to the "average" desired carrier frequency.

The limiters included in the demodulator package were also carefully designed for a high degree of symmetrical clipping and wide bandwidth. The capture ratio test is described in detail in Section V, where the test data shows the digital demodulator providing a capture ratio of 1.0 dB in the IBFM mode. By carefully optimizing the tunnel diode current in the differentiating circuit, a capture ratio of less than 0.6 dB has been consistently obtained with the digital demodulator under the same test conditions.

4.3 AM REJECTION

AM rejection is the ability of an FM demodulator to suppress the effects of amplitude variations of the FM carrier, on the demodulated FM output signal. For the purpose of this report, AM rejection is defined as the ratio in dB, of demodulator output produced by a frequency deviation of ±125 kc, to the demodulator output produced by 50 percent amplitude modulation, at various modulation frequencies.

The demodulator includes a two-stage limiter in the delayed and undelayed input channels to the phase detector. The tunnel diode differentiating circuit in each channel also functions as an excellent "third" limiter, since the diode switching time and consequently the trigger pulse amplitude is virtually independent of the diode current rise time. The demodulator capture ratio was found to be degraded by asymmetrical clipping in the limiters, and both the linear stages preceding the limiters, and the limiter circuits were carefully designed for stable symmetrical clipping.

The overall limiter threshold, which is defined as the input level corresponding to a 30 percent reduction of the phase detector trigger pulse amplitude, is at least 50 dB below the normal input level to the demodulator, and the limiters are well saturated on receiver noise. Because the limiter performs well in those areas indicated above, it was expected that the demodulator would exhibit a high AM rejection. However, experimental results failed to substantiate this assumption, and the initial measurements indicated a rather poor AM rejection capability. Particularly surprising was the fact that the AM rejection was degraded at the low modulation frequencies, with a measured value of only 20 dB at a 1 kc modulation rate.

Preliminary investigation showed a very low residual envelope variation at the limiter outputs as was indeed predicted. A more thorough investigation revealed information on the basic mechanism producing the output distortion, and provided more insight into the demodulator characteristics. The more standard types of FM demodulators, such as the Foster-Seeley or phase lock circuits, are true frequency discriminators in that the output voltage is proportional to actual frequency deviation. The (undesired) output of such a discriminator produced by an amplitude modulated carrier is due to at least three sources. The first is the sensitivity of the discriminator circuit to AM. This problem is substantially eliminated by properly designed, saturated limiters. A second source of AM modulating components in the FM output, is the incidental FM or PM produced in the modulation process at the signal source. This problem is difficult to isolate and cannot be completely eliminated. However, it can be reduced by proper

modulator design and particularly by amplitude modulating at the lowest possible frequency, for example at the receiver second intermediate frequency. The third source of degraded AM rejection performance, and the source which usually limits performance after the first two have been reduced, is the incidental phase modulation produced in the limiters preceding the discriminators.

Since for phase modulation $\Delta\phi = \frac{\Delta F}{F_m}$ = modulation index which equals a constant, the resulting incidental frequency deviation is proportional to modulating frequency. Again, since the "typical" discriminator output is proportional to frequency deviation, this source of AM interference is recognized by an AM rejection plot which degrades at approximately 6 dB per octave of modulating frequency. A possible complication which may result in erroneous conclusions is the phase shifting of the AM sidebands in the receiver IF amplifier, with a resulting incidental FM that generally increases as the modulating frequency is increased, and the sidebands move closer to the skirts of the IF filters. However, this problem is easily isolated by operating the receiver with a much wider than normal IF bandwidth; 3.3 mc was used for these tests. The receiver AM rejection is not normally a simple 6 dB per octave plot, but a composite due to the different interference mechanism predominating as the modulating frequency is varied. A typical receiver will produce an approximately constant AM rejection figure of between 50 and 40 dB up to modulating frequencies of 10 kc. Beyond this frequency, the AM rejection degrades at a more or less uniform rate until other factors (such as modulator and video amplifier response) alter the trend.

The digital demodulator, although providing the full capabilities of an FM demodulator, is essentially a phase sensitive device; that is the demodulated output is a function of the instantaneous phase difference at the phase detector input.

If a typically "good" limiter can produce a 46 dB AM rejection (±125 kc reference deviation) at a modulating frequency of 10 kc, and if we assume that at least one-half the disturbance is due to incidental PM in the limiter, then the following relations hold.

$$\text{Modulation index (incidental FM)} = \frac{\Delta F}{F_m} = \frac{1.25}{10} = .125 = \pm\Delta\phi$$

where: ΔF = 40 dB below ±125 kc = ±1.25 kc
F_m = 10 kc
$\Delta\phi$ = incidental PM (radians)

For the IBFM mode of the digital demodulator, maximum output occurs for ±180 degree phase difference into the phase detector, which corresponds to ±1 mc frequency deviation. ±125 kc deviation corresponds to ±22 degrees phase difference and 40 dB below ±125 kc reference corresponds to ±0.22 degrees phase error or 0.0038 radians.

Again assuming that the limiters preceding the demodulator phase detector provide about the same performance as the "typical" limiter above, it is seen that the required phase error into the phase detector must be $\frac{125}{0.0038}$ = 33 times, or greater than 30 dB below the incidental PM produced in the limiter. The actual phase error produced at the phase detector will be equal to the difference in the incidental PM between the two inputs and will be critically dependent on the degree of "phase tracking" between the delayed and undelayed limiter channels. Thus, the AM rejection capability of the digital demodulator is a function not only of the absolute amount of incidental PM, but is critically dependent on the limiters to produce the same $\Delta\phi$ corresponding to the same amplitude variations, over a wide range of modulating frequencies and input level.

Some conclusions can be made concerning the demodulator performance based on the above analysis. Since the digital demodulator is sensitive to phase and not frequency deviation, and since the incidental PM produced in the limiters is constant with modulating frequency, the AM rejection should remain constant with modulating frequency. This characteristic is in contrast to the "typical" frequency discriminator which has an AM rejection roughly inversely

proportional to modulating frequency. The experimental results in Section V support these predicted results for both types of FM demodulators.

Some effort was expended in the digital demodulator, to equalize the incidental phase shift between the delayed and undelayed limiter channels. This was done by "trimming" the stray capacitance in different parts of the circuit with small value fixed and variable capacitors. The final value of AM rejection was approximately constant at 30 dB with modulating frequencies beyond 100 kc.

Additional experiments support the assumed interference mechanism. A crude limiter was temporarily connected ahead of the digital demodulator, and although no effort was made to reduce the incidental PM produced in this limiter, it did reduce the envelope variations at the demodulator input. The digital demodulator acts as a true frequency discriminator to signals applied to the input (ahead of the delay lines) and the additional limiter greatly improved the AM rejection. On the other hand, when the limiter was placed ahead of only one limiter channel, the AM rejection was highly degraded indicating a large incidental PM unbalance at the phase detector.

Also the test data indicates that the AM rejection in the ØLFM mode is very good, actually exceeding the performance of the FMD-B15. The same limiter channel is used in both the IBFM and ØLFM mode but in the latter case, the demodulator functions as a true FM sensitive device.

Thus, the AM rejection of the digital demodulator compares quite unfavorably with the standard demodulators at the lower modulating frequencies, but actually provides better performance at the higher frequencies. The low frequency performance could be somewhat improved with additional "phase tracking" between limiter channels, but this characteristic of the demodulator probably represents a fundamental limitation in performance.

4.4 PHASE LOCK LOOP CALCULATIONS

The phase lock calculations are based on a summary analysis of coherent phase tracking loops given in JPL Technical Report No. 32-215, The Pioneer IV Lunar Probe: A Minimum-Power FM/FM Systems Designs.

4.4.1 PHASE LOCK PM DEMODULATOR

The phase lock loop 3 dB bandwidth for the PM mode was chosen to be 400 cps, optimized for an IF input S/N of zero dB. This selection was a compromise between low frequency response on the one hand, and incidental 60 and 120 cps jitter, microphonics, and loop capture range on the other hand. Loop damping was optimized at the fairly high input S/N of zero dB because it was felt that this demodulator would be primarily used for wideband PM demodulation rather than for a tracking function at low levels, and this approach insured a minimum variation of loop bandwidth due to the limiter suppression effect. The open loop constants were measured experimentally.

G_o = loop gain at threshold = $2\pi K_m K_{vco} K_a A_o$

K_m = phase detector sensitivity = 0.8 volts/radian

K_{vco} - Vco sensitivity = 7.10^4 Cy/sec/volt

K_a - DC loop gain = 1

A_o - limiter suppression at zero dB S/N = 0.7

$f_o = \frac{B_o}{2\pi}$ - loop bandwidth at threshold (Zero dB S/N) = 400 cps

$B_o = 2.5 \cdot 10^3$ radians/sec

$$G_o = 2\pi \times 0.8 \times 7 \times 10^4 \times 1 \times 0.7 = 2.5 \times 10^5$$

$$T_1 = R_1C = \frac{G_o}{B_o^2} = \frac{2.5 \times 10^5}{6.25 \times 10^6} = 4.0 \times 10^{-2}; \; R_1 = 2.2\text{K ohms}$$

$$C = \frac{T_1}{R_1} = \frac{4.0 \times 10^{-2}}{2.2 \times 10^3} = 18.2 \times 10^{-6} = 18.2 \text{ microfarads}$$

C was optimized experimentally at a value of 25 microfarads. The reason for the discrepancy between calculated and final value is due to the fact that the DC "operational" amplifier has insufficient gain (x 34) to be considered a perfect integrator.

$$T_2 = R_2C = \frac{2\mu}{B_o} = \frac{1.4}{2.5 \times 10^3} = 5.6{:}10^{-4} \qquad \mu = \text{damping factor} = 0.7$$

$$R_2 = \frac{T_2}{C} = \frac{5.6 \times 10^{-4}}{2.5 \times 10^{-5}} = 22.4 \text{ ohms}$$

R_2 was optimized experimentally at a value of 24 ohms.

The loop single sided noise bandwidth $B_{LO} = 3.33\, f_o = 1332$ cps

At strong signal levels the loop bandwidth will increase to f_N as follows:

$$f_N = \sqrt{\frac{1}{A_o}}\, f_o = \sqrt{\frac{1}{.7}}\, f_o = 1.2\, f_o$$

$$f_N = 1.2 \times 400 = 480 \text{ cps}$$

The overall frequency response of the PM demodulator is shown in figure 4. F_N which equals 3 dB low frequency response measures 470 cps.

4.4.2 PHASE LOCK FM DEMODULATOR

The phase lock FM discriminator was optimized for the standard IRIG FM/FM format with a high frequency cutoff of 100 kc including the phase correction network. As seen from the loop response curves, Figure 14 of JPL Report 32-215, B_o corresponds to the 3 dB cutoff frequency when the phase correction network has been optimized for no overshoot. The loop was designed for threshold conditions, approximately 8 dB IF S/N, and the limiter suppression factor is 1.

G_o - loop gain = $2\pi K_m K_{vco} K_a$

K_m - phase detector sensitivity = 0.8 volts/radian

K_{vco} - VCO sensitivity = 7×10^4 cy/sec/volt

K_a - DC loop gain = 7

B_o - loop bandwidth = 100 kc = 6.28×10^5 radians/sec

$$G_o = 2\pi \times 0.8 \times 7{\cdot}10^4 \times 7 = 2.46 \times 10^6$$

$$T_1 = R_1C = \frac{G_o}{B_o^2} = \frac{2.46 \times 10^6}{.397 \times 10^{12}} = 6.24 \times 10^{-6}$$

$$R_1 = 3.3K$$

$$C = \frac{T_1}{R_1} = \frac{6.24 \times 10^{-6}}{3.3 \times 10^{3}} = 1890 \times 10^{-12}$$

$$= 1890 \text{ picofarads}$$

C was optimized experimentally at 1600 picofarads.

$$T_2 = R_2 C = \frac{2\mu}{B_o} = \frac{1.4}{6.24 \times 10^{5}} = 2.25 \times 10^{-6} \qquad \mu = \text{damping factor} = 0.7$$

$$R_2 = \frac{T_2}{C} = \frac{2.25 \times 10^{-6}}{1.6 \times 10^{-9}} = 1.41 \times 10^{3} = 1.4K \text{ ohms}$$

R_2 was optimized experimentally at 1.3K ohms.

The phase correction network was designed for a cutoff frequency equal to $\omega_{co} = \frac{\sqrt{2}}{2} B_o = \frac{1}{RC}$

$$R = 1.5K$$

$$C = \frac{\sqrt{2}}{R B_o} = \frac{\sqrt{2}}{1.5 \times 10^{3} \times 6.28 \times 10^{5}}$$

C = 1500 picofarads, the value used

4.5 SIGNAL-TO-NOISE RATIO CALCULATIONS

The signal-to-noise ratio of the demodulated output for each demodulator tested is given below. For these calculations, the following assumptions are made:

(1) Input noise spectral density is a constant over the IF Bandwidth, equal to the white noise output of a 50 ohm source resistor at standard conditions.

$$4KTR = -174 \text{ dbm/cycle bandwidth}$$

(2) Receiver Noise figure equals 9 dB.

(3) Predetection noise bandwidth equal to the nominal 3 dB IF Bandwidth.

(4) Post-detection equivalent rectangular low pass bandwidth equal to the nominal 3 dB video filter bandwidth.

(5) FM threshold, defined as a 1 dB deviation from asymptote of plotted curve, is assumed to occur as predicted in Figure 9 of [7] corresponding to the ratio of predetection to post-detection bandwidth.

(3) and (4) are valid assumptions because of the high shape factor and because correction factors would be much less than the tolerance on the nominal bandwidth.

4.5.1 WIDEBAND DEMODULATORS

3.3 mc IF Bandwidth (B)

750 kc Video Bandwidth (f_m)

Predetection to post-detection bandwidth ratio (B/f_m) = 4.4

---

[7] L. H. Enloe "Decreasing the Threshold in FM by Frequency Feedback". PROC. IRE., Jan. 1962.

±300 kc Deviations (ΔF)

FM threshold [7] approximately 8 dB.

Input noise level = -174 dbm + 10 log 3.3×10^6 + NF

= -174 + 65.2 + 9 = -99.8 dbm

Threshold input level = -99.8 + 8 = -91.8 dbm (5.7 microvolts)

$\left(\frac{S}{N}\right)_{AM}$ in equivalent AM Bandwidth (2 fm) at threshold =

$-(-174 + 10 \log 1.5 \times 10^6 + NF) - 92 = 11.2$ dB

$\left(\frac{S}{N}\right)_o = 3\beta^2 \left(\frac{S}{N}\right)_{AM}$ (Power Ratios); $\beta = \frac{\Delta F}{f_m}$

$\left(\frac{S}{N}\right)_o$ dB = 10 log $3\beta^2$ + $\left(\frac{S}{N}\right)_{AM}$ dB

$\beta = \frac{\Delta F}{f_m} = \frac{300}{750} = 0.4$ $\qquad 3\beta^2 = .48$

$\beta^2 = 0.16$ $\qquad 10 \log 3\beta^2 = -3.2$ dB

$\left(\frac{S}{N}\right)_o = 11.2 - 3.2 - 1 = 7$ dB at threshold

4.5.2 INTERMEDIATE BANDWIDTH DEMODULATORS

500 kc IF Bandwidth (B)

100 kc Video Bandwidth (f_m)

Predetection to post-detection bandwidth ratio $B/f_m = 5$

FM threshold [7] approximately 8.5 dB

Input noise level = -174 dbm + 10 log 5×10^5 + NF

= -174 + 57 + 9 = -108 dbm

Threshold input level = -108 dbm + 8.5 = -99.5 dbm (2.4 microvolts)

$\left(\frac{S}{N}\right)_{AM}$ in equivalent AM bandwidth (2 fm) at threshold =

$-(-174 + 10 \log 2.10^5 + NF) - 99.5 = 12.5$ dB

$\left(\frac{S}{N}\right)_o$ dB = 10 log $3\beta^2$ + $\left(\frac{S}{N}\right)_{AM}$ dB

$\beta = \frac{\Delta F}{f_m} = \frac{125}{100} = 1.25$ $\qquad 3\beta^2 = 4.7$

$\beta^2 = 1.56$ $\qquad 10 \log 3\beta^2 = +6.7$ dB

$\left(\frac{S}{N}\right)_o = 12.5 + 6.7 - 1 = 18.2$ dB

---

[7] L. H. Enloe "Decreasing the Threshold in FM by Frequency Feedback". PROC. IRE., Jan. 1962.

The threshold level of the phase lock FM demodulator should be improved (reduced) approximately by the ratio of the IF bandwidth to the equivalent noise bandwidth of the tracking loop filter. The noise bandwidth =

$$3.33\ f_o = 333 \text{ kc for 100 kc loop bandwidth threshold}$$

$$\text{improvement} = 10 \log \frac{500}{333} = 1.8 \text{ dB}$$

4.6 EXTENSION OF PHASE-LOCK ACQUISITION RANGE

The transfer function of the digital phase detector is linear over approximately 320 degrees. When the phase-lock loop is out-of-lock, the phase detector output consists of a sawtooth waveform at a repetition rate equal to the difference between the input and the VCO frequency. This waveform is shown diagrammatically in figure 5. A significant feature of this waveform is that the sawtooth slope at "high beat" is reversed from the slope at "low beat". If the output of the phase detector was a true sawtooth, the effective DC component of the waveform would be midway between the peaks, and would remain constant at all high and low beat frequencies.

However, by adjusting the flip-flop circuit constants, the sawtooth will appear truncated as shown in figure 5. This truncation produces a DC "offset" voltage, and because of the reversal of the slope, and thus the polarity of the truncation, this DC voltage reverses polarity as the input and VCO frequency pass through "zero" beat.

This offset voltage will appear at the input of the loop operational amplifier, and the amplitude and polarity can be adjusted so that the voltage drives the VCO frequency toward the input signal. As indicated above, this offset voltage reverses polarity at zero beat and secondary effects cause the absolute value of the voltage to increase with increasing beat frequency.

The result is that with proper design and optimization, this offset voltage can be utilized to greatly increase the range of reliable phase-lock loop acquisition and decrease the acquisition time.

In order to acquire lock with a given difference between the input and VCO frequency, the offset polarity must be correct and the voltage amplitude must be adjusted to equal or exceed that voltage required to pull the VCO by the given frequency error. If the error voltage is insufficient to pull the VCO by at least the difference frequency, the loop will not lock and the VCO may be driven away from the input signal.

The acquisition range is a function of the degree of truncation and therefore is limited by the linearity degradation which can be compromised in the design.

In the ADD-15-ØLPM mode, this approach was utilized to obtain a reliable acquisition range of ±300 kc with respect to the 10 mc input frequency with a loop 3 dB bandwidth of 470 cps. This acquisition range required approximately 10 percent truncation in the phase detector transfer function.

The actual circuit adjustments required to produce this effect were somewhat critical and sensitive to temperature variations. Since this approach can greatly increase the acquisition performance of phase-lock loops without the need for sophisticated sweep and lock circuits, the circuit should be further analyzed and developed.

SECTION V

TEST DATA ANALYSIS

The Digital Demodulator was thoroughly evaluated in a test program conducted at the Air Force Eastern Test Range (AFETR). The test program was conducted in general accordance with a test plan submitted by DEI as required by the contract. This original test plan is included for reference as an appendix in this report. Minor deviations from the original test plan were made in some instances, but the intent of the program to evaluate the demodulator under a variety of laboratory and field conditions was fully satisfied.

The program was divided into three phases. The first test phase consisted of laboratory measurements of the more basic demodulator parameters of both the new digital demodulator and the FMD series of demodulators which are included as part of the original TMR-15 Telemetry Receiver Group. A direct performance comparison between the different operating modes of the ADD-15 and the most closely corresponding FMD demodulators is made for most of the tests. The first phase of the tests was conducted at the AF Technical Laboratory at Patrick AFB.

5.1 PHASE I TESTS - LABORATORY MEASUREMENTS

5.1.1 STATIC (DC) LINEARITY

This test consisted of measuring the FM demodulator output voltage (DC) as a function of the IF input frequency. The test setup is shown in figures 6a and 6b. Because an overload occurs in a video amplifier of the main chassis of the ADU-15 with output voltage corresponding to very wide frequency deviation, the DC output of the ADD-15 was measured at the output of the demodulator, at the emitter of emitter follower Q30. The output of the standard FMD discriminator was obtained at the FM/DC output at J11 on the ADU-15 rear panel. The ADU-15 does not overload with frequency deviation corresponding to the standard FMD discriminator peaks and the frequency deviation vs. voltage curves taken at J11 represent the FMD discriminator characteristics.

The measured and normalized numerical data taken with the various demodulators is shown in tables 3 through 7. In order to graphically compare the characteristics of the demodulator, it was necessary to normalize the FMD numerical data so the FMD units and the equivalent modes of the ADD-15 have the same average frequency sensitivity (slope). Also, since all demodulators are adjusted to produce the same output voltage at center frequency, the curves are slightly offset along the voltage axis in order to be more easily analyzed. Figure 7 is a plot of the discriminator DC output voltage vs. IF input frequency for the FMD-C15 demodulator and the ADD-15 demodulator in the WBFM mode. The FMD-C15 exhibits a linear frequency range of approximately ±1.8 mc with a peak-to-peak separation of approximately 4.5 mc. The deviation from best straight line is less than 2% over a frequency range of ±1.5 mc. [8] As seen from the numerical data table 4 and figure 7, the ADD-15, WBFM exhibits a linear frequency range in excess of ±9 mc. The deviation from best straight line is less than 2.5% over a frequency range of ±500 kc, less than 3.5% over a frequency range of ±1.5 mc and less than 5% over a frequency range of ±9 mc.

Figure 8 is a plot of the discriminator DC output vs. IF input frequency for the FMD-B15 demodulator and of both the IBFM and ØLFM modes of the ADD-15 demodulator. The FMD-B15 exhibits a linear range of approximately ±400 kc with a peak-to-peak separation of approximately 1 mc. The DC output voltage is clipped in the ADU-15 chassis at approximately -300 kc but this effect is accounted for by extrapolation, assuming a symmetrical discriminator response. (This response was later verified by the discriminator design data.) The deviation from best straight line is less than 1% over a frequency range of ±150 kc, and less than 4% over a frequency range of ±250 kc.

---

[8] Calculated by dividing the difference between the measured voltage and the best straight line drawn through the plotted curve at center frequency, by the ordinate of the best straight line at the frequency corresponding to the measured deviation (X100). The slope of the best straight line was calculated from the measured data in most cases, and deviations were calculated at points where the plotted curve and the best straight line appeared (graphically) to have the greatest percentage difference over a frequency deviation range from ±20% to ±100% of the specified range.

The ADD-15, IBFM exhibits a linear frequency range from +850 kc to -1050 kc. The asymmetrical deviation range is due to the small tolerance error in the IBFM delay line which is providing 0.5 microsecond delay at approximately 9.50 mc. The deviation from best straight line is less than 2% over a frequency range of ±150 kc, less than 3% over the range of ±250 kc, and less than 7% over the range of ±900 kc, with respect to 9.50 mc.

The Digital Demodulator in both the WBFM and IBFM modes exhibits a much wider linear frequency range than the corresponding FMD units. However, over a smaller frequency range equal to the linear range of the standard FMD demodulators, the ADD-15 exhibits small "wiggles" in the response curve. These nonlinearities vary with different delay lines and are due to small variations in time delay with frequency. This is particularly noticeable when the devices are operated near cut-off frequency as is the case with the 0.5 microsecond unit. The result is that the ADD-15 provides equal or slightly degraded performance compared to the standard demodulator when evaluated over the smaller deviation ranges. This effect is discussed in more detail in Section VI of this report.

The ADD-15, ØLFM exhibits a linear frequency range of approximately ±500 kc. The actual oscillator pulling range is somewhat greater than this at strong signal levels. The deviation from best straight line is less than 1% over the frequency range of ±150 kc and less than 3% over the range ±250 kc.

The VCO shaping network is optimized for a pulling range of ±300 kc with "corners" at approximately 9.95 mc, 10.1 mc, and 10.2 mc. The shaping network was experimentally optimized utilizing sweep oscillator with less than ideal linearity. It appears from the curves that further optimization is required for static linearity and, although rather tedious, this can be accomplished by adjusting the shaping network constants. It is also apparent from the curves that the deviation sensitivity in the ØLFM mode does not quite equal the sensitivity in the IBFM mode, as it should. This is easily corrected by a slight adjustment of the VCO sensitivity control, R105.

5.1.2 SWEPT RESPONSE AND OSCILLOSCOPE REPRODUCTION

The response of the demodulators to a periodically varying (swept) input frequency was displayed on a synchronized oscilloscope. Both the Standard FMD demodulators and the Digital demodulator were evaluated with various ranges of sweep deviation (width), and the resulting response curves were recorded with a Polaroid oscilloscope camera. These photographs are shown in figures 9 through 21. Unfortunately, the linearity of available sweep generators operated with wide sweep width is inadequate for quantitative linearity measurements. The slope discontinuities and "wiggles" apparent in the photographs were carefully analyzed. It can be seen that many of the more pronounced non-linearities occur at the same instantaneous sweep frequency in different demodulators and with different sweep widths, indicating that the source of the non-linearities is independent of the demodulators and is probably in the generator. This deduction is further supported by the static linearity plots which show a much better linearity than the photographs.

Because of the overload problem in the ADU-15 main chassis, the demodulator response was measured both at the FM/DC output J11 and at the emitter of Q30, as was also done for the static linearity tests.

The oscilloscope pattern was adjusted so the response curves cross the center of the scope graticule as the instantaneous input frequency equals 10 MC (center frequency).

Figure 9. Response of FMD-C15 measured at FM/DC output, J11 of ADU-15. Sweep width equals ±2.4 mc. Photo shows peaks of discriminator response at approximately ±2.25 mc. Horizontal line corresponds to discriminator output during sweep generator blanking (input signal off) and has no particular significance.

Figure 10. Response of ADD-15, WBFM measured at J11. Sweep width equals ±2.4 mc. Retrace level corresponds to steady state of flip-flop during the blanking interval. Discontinuity

in slope is apparently produced in sweep generator since it appears at same frequency in figure 9 through figure 12, although the effect is somewhat marked by the rounding of the FMD-C15 response.

Figure 11. Response of FMD-C15 measured at J11. Sweep width equals ±2.0 mc. Photo shows maximum linear range of discriminator.

Figure 12. Response of ADD-15, WBFM measured at J11. Sweep width equals ±2.0 mc.

Figure 13. Response of ADD-15 WBFM measured at emitter of Q30. Sweep width equals ±2.4 mc. Photo shows same response as figure 10 except that slope is reversed because of amplifiers between Q30 and J11.

Figure 14. Response of ADD-15 WBFM measured at emitter of Q30. Sweep width equals generator maximum ±4.5 mc. Photo shows wide deviation range of discriminator. Fuzziness of upper part of curve is due to insufficient filtering of 5.5 mc carrier at emitter of Q30. Additional filtering in receiver video circuits effectively eliminates residual carrier components.

Figure 15. Response of ADD-15 WBFM measured at emitter of Q30. Sweep width equals 1 mc. Photo shows response with narrow sweep width. Slope discontinuity apparently produced in sweep generator since it appears at the same frequency in figures 15 through 20 (taking account of the different sweep width).

Figure 16. Response of FMD-B15 measured at J11. Sweep width equals ±320 kc. Photo shows linear range of discriminator and start of clipping in ADU-15 at +5v corresponding to approximately +300 kc.

Figure 17. Response of ADD-15, IBFM measured at J11. Sweep width equals ±300 kc. Photo shows linear range of discriminator and start of clipping (barely noticeable in top right of curve). Note that slope discontinuities are the same for the two different discriminators shown in figures 16 and 17.

Figure 18. Response of ADD-15, IBFM measured at the emitter of Q30. Sweep width in excess of ±1 mc. Photo shows entire linear range of the demodulator which is slightly less than ±1 mc. The photo also shows the finish of the next lower "cycle" and the start of the next higher "cycle" produced as the sweep deviates beyond the frequencies corresponding to zero and 360 degrees phase shift respectively, in IBFM delay line. The flattening of the response at the ends is due to switching time limitations in the flip-flop circuits of the demodulator.

Figure 19. Response of ADD-15, IBFM measured at the emitter of Q30. Sweep width equals ±250 kc.

Figure 20. Response of ADD-15, ØLFM measured at the emitter of Q30. Sweep width is approximately ±800 kc. Photo shows full deviation capability of demodulator. The fuzzy trace on each side of the response curve is the beat frequency produced when the VCO is out of lock with the IF input signal. The phase tracking loop loses lock when the input frequency is deviated beyond the VCO pulling range, which in this case is from -550 kc to +600 kc.

Figure 21. Response of ADD-15, ØLFM measured at the emitter of Q30. Sweep width is equal to ±150 kc.

5.1.3 VIDEO FREQUENCY AND PULSE RESPONSE

The demodulator sinewave frequency response and pulse response was measured by modulating the RF/FM generator (Boonton Model 202J) and observing the video output of the Video Amplifier Unit VAU-15, on a calibrated oscilloscope. The FM deviation, IF bandwidth, and video bandwidth were chosen to both simulate typical operating conditions and also to demonstrate the full capabilities of the demodulator within the limitations of the test instruments. The results of the tests are summarized as follows:

Frequency Response:

FMD-C15	±300 KC Deviation 3.3 MC IF Bandwidth Video Filter in DIRECT (bypass) position Video Response less than 2 dB down at 5 cps, 3 dB down at 3 cps, 2.5 dB down at 1 mc.
ADD-15, WBFM	±300 KC Deviation 3.3 MC IF Bandwidth Video Filter in DIRECT position Video Response 3 dB down at 4 cps, 3 dB down at 900 kc.

Additional measurements determined that the video generator (Wavetek Model 104) used to modulate the RF/FM generator was 1.8 dB down at 800 kc and 2 dB down at 900 kc. The specifications on the RF/FM generator also indicate a roll-off of modulation response at 1 mc. Thus the video high frequency response figures for the FMD-C15 and ADD-15, WBFM are limited by the test instruments.

The overall frequency response from the input of the digital demodulator integrator circuit through the video output is plotted in figure 3. The high frequency response is 3 dB down at approximately 1.5 mc and this curve represents the full capabilities of the demodulator. The somewhat wider response of the FMD-C15 indicated in the above data was found to be the result of a small high frequency boost produced by a peaking coil in the demodulator.

FMD-B15	±125 KC Deviation 3.3 MC IF Bandwidth Video Filter in DIRECT position Video Response 3 dB down at 3 cps, 3 dB down at 200 kc.
ADD-15, IBFM	±125 KC Deviation 3.3 MC IF Bandwidth Video Filter in DIRECT position

In order to fully evaluate the digital demodulator in the IBFM mode, frequency response was measured with three different post-detection filter assemblies (A1) sequentially plugged into the demodulator module. A BY-PASS filter card provided a straight through connection with no bandwidth restrictions. The other cards had a nominal cut-off frequency of 750 kc and 250 kc, the latter being the bandwidth required for high capture ratio.

	Video low frequency response less than 3 dB down at 4.3 cps
	High frequency response with BY-PASS 3 dB down at 800 kc
	High frequency response with 750 KC filter 3 dB down at 600 kc
	High frequency response with 250 KC filter 3 dB down at 250 kc
ADD-15, ØLFM	±125 KC Deviation 3.3 MC IF Bandwidth Video Filter in DIRECT position Video response 3 dB down at 4.3 cps, 3 dB down at 93 kc, 0.2 dB overshoot at 20 kc

The phase lock FM mode was designed for optimum performance with the standard IRIG FM/FM format. The experimental results indicate an adequate high frequency response for the high frequency limit of Channel E which is 80.5 kc. Higher frequency subcarriers can be easily accommodated by minor changes in the component values of the phase lock loop filter R133, C92, R163 and phase correction network C89, R165.

Pulse Response:

FMD-C15	±300 KC Deviation 3.3 MC IF Bandwidth Video Filter in DIRECT position Rise Time 0.7 microsecond Decay Time 0.7 microsecond Overshoot and Ringing 35%
ADD-15, WBFM	±300 KC Deviation 3.3 MC IF Bandwidth Video Filter in DIRECT position Rise Time 0.5 microsecond Decay Time 0.5 microsecond Ringing Negligible Overshoot 20%
FMD-B15	±125 KC Deviation 3.3 MC IF Bandwidth Video Filter in DIRECT position Rise Time 2 microseconds Decay Time 3 microseconds Overshoot 2%
ADD-15, IBFM	±125 KC Deviation 3.3 MC IF Bandwidth Video Filter in DIRECT position Rise Time 1.0 microsecond Decay Time 1.0 microsecond Overshoot 5%
ADD-15, ØLFM	±125 KC Deviation 3.3 MC IF Bandwidth Video Filter in DIRECT position Rise Time 6 microseconds Decay Time 6 microseconds Overshoot less than 5%

5.1.4 TOTAL HARMONIC AND INTERMODULATION DISTORTION

Harmonic Distortion: The overall receiver total harmonic distortion (THD) was measured with a Hewlett-Packard Distortion Analyzer Model 331A, which was connected to the video output of the VAU-15. The RF/FM generator was modulated with an HP Model 200 CD sinewave generator which had a measured THD of less than 0.2% over the modulating frequency range. A 3.3 MC IF bandwidth was used for all THD tests in order to minimize the effect of the IF amplifier on the measurements. The ADD-15 contained the 750 kc post-detection filter assembly for the IBFM mode.

THD Test Conditions for all Demodulators:

3.3 MC IF Bandwidth
400 KC Video Bandwidth
Video output level 4 volts peak-to-peak into 75 ohm
RF Input Level 100 millivolts

FMD-C15

±300 KC Deviation
0.4% THD at 1 kc, mostly second and third harmonics
0.75% THD at 100 kc, mostly second and third harmonics

ADD-15, WBFM

±300 KC Deviation
0.66% THD at 1 kc, mostly second harmonic
1.28% THD at 100 kc, mostly second and third harmonics

FMD-B15

±125 KC Deviation
0.2% THD at 1 kc, mostly hum and noise
3.0% THD at 100 kc, mostly second and third harmonics

ADD-15, IBFM

±125 KC Deviation
0.35% THD at 1 kc, mostly hum and noise
0.35% THD at 100 kc, mostly hum and noise

ADD-15, ØLFM

±125 KC Deviation
0.68% THD at 1 kc, mostly third harmonic
0.36% THD at 100 kc, mostly hum and noise

The ADD-15, WBFM is not quite as good as the FMD-C15 but both units provide high performance. The ADD-15 IBFM provides considerably better performance than the FMD-B15 at the higher modulation frequencies. This is probably due to the much improved phase linearity of the digital demodulator and its effect on the sidebands of the FM spectrum. The low distortion in the ADD-15, ØLFM at the 100 kc modulating frequency is due in part to the bandwidth limitations in this mode.

Intermodulation Distortion: Intermodulation was measured with the test setup shown in figure 22. The two simulated subcarriers at 11 kc and 30 kc were adjusted to produce equal FM deviation and the generator was adjusted for a composite peak deviation of ±125 kc. First and higher order products were calculated and measured with the selective voltmeter. Changing the IF bandwidth had only a minor effect on the distortion products.

FMD-B15

±125 KC Peak Deviation
3.3 MC IF Bandwidth
100 KC Video Bandwidth

FREQUENCY	Relative Amplitude with Respect to Individual Subcarriers
11 KC	0 dB
30 KC	0 dB
8 KC	-60 dB
19 KC	-45 dB
41 KC	-41 dB
49 KC	-55 dB
52 KC	-60 dB
71 KC	-55 dB

FMD-B15

±125 KC Peak Deviation
500 KC IF Bandwidth
100 KC Video Bandwidth

FREQUENCY	Relative Amplitude
11 KC	0 dB
30 KC	0 dB
8 KC	-58 dB
19 KC	-49 dB
41 KC	-51 dB
49 KC	-44 dB
52 KC	-43 dB
71 KC	-41 dB

ADD-15, IBFM

±125 KC Peak Deviation
500 KC IF Bandwidth
100 KC Video Bandwidth

FREQUENCY	Relative Amplitude
11 KC	0 dB
30 KC	0 dB
8 KC	-55 dB
19 KC	-54 dB
41 KC	-62 dB
49 KC	-43 dB
52 KC	-42 dB
71 KC	-40.5 dB

5.1.5 AM REJECTION

AM Rejection was discussed in some detail in Section IV of this report. This discussion includes a prediction of performance based on an analysis of the mechanism producing AM interference in an FM system. Since the digital demodulator was modified to improve AM rejection after the AFETR test program, the data obtained during these tests is given only for reference. The final demodulator performance is shown in figures 24 through 29.

The test setup for measuring AM rejection is shown in figure 23. AM rejection figures are the ratio in dB of the demodulator output with a 50 percent amplitude modulated carrier to the demodulator output with ±125 kc FM deviation. The RF carrier input level is 50 millivolts, the AGC response is set at 1000 milliseconds and the video filter is set in the DIRECT position for all tests. The ADD-15 contained 250 kc post-detection filter assembly for the IBFM mode.

The following data includes two sets of AM rejection figures. Column 1 is the data taken during the test program conducted at AFETR. Column 2 is data taken at the DEI laboratory facility after the digital demodulator was modified to improve AM rejection. The design of the FMD demodulator was not modified and the difference in the two sets of data on the standard demodulator is evidently due to difference among demodulators of the same type and AM generators. The general trend in the data is the same for both sets of data on the FMD.

FMD-B15 3.3 MC IF Bandwidth

FREQUENCY	AM Rejection (1)	AM Rejection (2) Figure 24
1 KC	46 dB	58 dB
10 KC	47 dB	52 dB
30 KC	46 dB	44 dB

continued

FMD-B15, cont'd

FREQUENCY	AM Rejection (1)	AM Rejection (2) Figure 24
50 KC	43.5 dB	39 dB
80 KC	41 dB	33 dB
100 KC	40 dB	30 dB
200 KC		21 dB
300 KC		18 dB
400 KC		17 dB
500 KC		17 dB

ADD-15, IBFM 3.3 MC IF Bandwidth

FREQUENCY	AM Rejection (1)	AM Rejection (2) Figure 25
1 KC	19.5 dB	29 dB
10 KC	20.8 dB	30 dB
30 KC	25 dB	31 dB
50 KC	28 dB	30 dB
80 KC	30 dB	29 dB
100 KC	30 dB	29 dB
200 KC		25 dB
300 KC		20 dB
400 KC		18 dB
500 KC		20 dB

FMD-B15 500 KC IF Bandwidth

FREQUENCY	AM Rejection (1)	AM Rejection (2) Figure 26
1 KC	46 dB	58 dB
10 KC	46 dB	53 dB
30 KC	45.5 dB	43 dB
50 KC	41.5 dB	37 dB
80 KC	36 dB	30 dB
100 KC	33.5 dB	27 dB
200 KC		20 dB
400 KC		20 dB
500 KC		40 dB

ADD-15, IBFM 500 KC IF Bandwidth

FREQUENCY	AM Rejection (2) Figure 27
1 KC	29 dB
10 KC	29 dB
30 KC	30 dB
50 KC	32 dB
80 KC	34 dB
100 KC	35 dB
200 KC	38 dB
400 KC	37 dB
500 KC	48 dB

ADD-15, ØLFM 3.3 MC IF Bandwidth

FREQUENCY	AM Rejection (2) Figure 28
1 KC	69 dB
10 KC	54 dB
30 KC	44 dB
50 KC	39 dB
80 KC	35 dB
100 KC	33 dB
200 KC	35 dB
400 KC	40 dB
500 KC	43 dB

ADD-15, ØLFM 500 KC IF Bandwidth

FREQUENCY	AM Rejection (2) Figure 29
1 KC	67 dB
10 KC	64 dB
30 KC	55 dB
50 KC	48 dB
80 KC	41 dB
100 KC	40 dB
200 KC	48 dB
400 KC	54 dB
500 KC	65 dB

The experimental results fairly closely substantiate the performance predictions made in Section IV. In particular the AM rejection of the true frequency discriminators, FMD-B15 and ADD-15 ØLFM, degrades at approximately 6 dB per octave between 10 kc and 100 kc modulating frequency. Beyond 100 kc the curves are modified by the IF and post-detection bandwidths.

In figure 24 the curve begins to "round-off" at approximately 200 kc which is the measured FMD-B15 high frequency cut-off. In figure 26 the curve turns sharply downward at 250 kc which equals 1/2 IF bandwidth. In figures 28 and 29 the curves peak at the phase lock demodulator high frequency cut-off at 100 kc with the rate of drop off increased by the narrower IF bandwidth in figure 29. In contrast to "typical" curves indicated above, the AM rejection of the digital demodulator remains essentially constant between 30 dB and 35 dB from 1 kc to above 100 kc. Figures 25 and 27 show a pronounced peaking at approximately 400 kc which is possibly due to significant differential phase shift between the delayed and undelayed channels at this frequency. The peak in figure 27 is reduced because of the attenuation of the AM sidebands in the narrower IF bandwidth.

5.1.6 SIGNAL-TO-NOISE RATIO AND THRESHOLD

The video output signal-to-noise ratio was measured as a function of RF input level to the receiver. The test setup is shown in figure 30. In order to measure true S/N (rather than S + N/N) down to very low RF levels, the signal (video) component was measured with a narrow bandwidth selective voltmeter. This method allows a determination of the limiter suppression of signal component as the IF S/N drops below 0 dB. The noise components are measured with modulation removed.

The measured numerical data is shown in tables 8 through 12. The plotted test data and a comparison of the different demodulators is shown in figures 31 and 32.

Figure 31 is a plot of the video S/N vs. RF input level for the FMD-C15 and the ADD-15 WBFM. Both demodulators were tested under the same operating conditions listed as follows:

3.3 MC IF Bandwidth
750 KC Video Bandwidth
±300 KC Deviation

A 2.8 dB error in the noise reference level was found in the recorded data for the ADD-15, WBFM. The dashed curve reflects the uncorrected data.

Theoretical calculations predict the FM threshold (8 dB IF S/N) to occur at approximately 5.7 microvolts RF input with a corresponding video S/N of 7 dB. The curves indicate a video S/N of 3 dB for the ADD-15 WBFM and 5 dB for the FMD-B15 at the 5.7 microvolt level. The 1 dB threshold break of the ADD-15 WBFM occurs at 7.5 microvolts; threshold of the FMD-C15 occurs at 6 microvolts. Figure 32 is a plot of the video S/N vs. input level for the FMD-B15, ADD-15 IBFM, and ADD-15 ØLFM. All three demodulators were tested under the same operating conditions listed as follows:

500 KC IF Bandwidth
100 KC Video Bandwidth
±125 KC Deviation

Theoretical calculations predict the FM threshold (8 dB IF S/N) to occur at approximately 2.4 microvolts with a corresponding video S/N of 18.2 dB for the FMD-B15 and ADD-15 IBFM. The threshold for the ADD-15 ØLFM should occur approximately 1.8 dB below the threshold level of the ADD-15 IBFM. Also, because of the slight video bandwidth compression associated with the phase lock demodulator, the ADD-15 ØLFM should provide a S/N approximately 1 dB higher than the ADD-15 IBFM range. The curves indicate a S/N of 15 dB for the FMD-B15 and ADD-15 IBFM and a S/N of 19 dB for the ADD-15 ØLFM, at the 2.4 microvolt level. The 1 dB threshold "break" occurs at approximately 2.4 microvolts for all three demodulator modes.

5.1.7 CAPTURE RATIO

Capture ratio is one of the more complicated measurements performed on the demodulator and the test procedure will be described in detail. The test setup is shown in figure 33. Two RF generators are connected to the RF input of the receiver through isolation pads and a power divider. One generator (designated desired signal) is modulated at a 10.5 kc rate, the other generator (designated undesired signal) is modulated at a 30 kc rate.

Each generator is individually connected and tuned to the receiver and the deviation of each signal is carefully adjusted to produce the same video output level as indicated by a selective voltmeter tuned to the modulating frequency. The two generators are then simultaneously connected and adjusted for the same input level into the receiver. In order to precisely equalize the RF input level, the modulation is momentarily turned off and the generators are adjusted for 100% effective amplitude modulation of the receiver IF signal, which is monitored on an oscilloscope. The amplitude modulation "frequency" is equal to the slight difference in the RF input frequency and after the amplitudes have been adjusted, the generators are tuned for "zero beat."

With both generators connected and modulated, the selective voltmeter is tuned to the undesired modulating frequency, 30 kc. The output level of the undesired signal generator, which is being monitored with an RF voltmeter, is slowly reduced until the 30 kc video output is reduced 30 dB below the reference level established with the generators connected individually.

The reduction in the undesired signal level (in dB) required to reduce the undesired video signal by 30 dB is defined as the capture ratio of the receiver.

Test Results: Because the capture ratio measurement requires a number of critical adjustments, the procedure was repeated on each demodulator a few times as indicated in the data.

FMD-C15

3.3 MC IF Bandwidth
1500 KC Video Bandwidth
±300 KC Deviation

Capture Ratio 2.4 dB, 2.5 dB

ADD-15, WBFM	3.3 MC IF Bandwidth 1500 KC Video Bandwidth ±300 KC Deviation
	Capture Ratio 2.4 dB 2.3 dB
FMD-B15	500 KC IF Bandwidth 100 KC Video Bandwidth ±125 KC Deviation
	Capture Ratio 4.5 dB 4.3 dB 4.4 dB 4.3 dB
ADD-15, IBFM	500 KC IF Bandwidth 100 KC Video Bandwidth ±125 KC Deviation
	Capture Ratio 1.0 dB 0.9 dB 1.0 dB 1.0 dB
ADD-15, ØLFM	500 KC IF Bandwidth 100 KC Video Bandwidth ±125 KC Deviation
	Capture Ratio 1.3 dB 1.1 dB

5.2 PHASE II TESTS - PERFORMANCE WITH SIMULATED DATA FORMATS

The Phase II and Phase III Tests were conducted at the Air Force TEL IV Telemetry Station on Merritt Island, Florida. These experiments consisted of an evaluation of both the standard FMD series of demodulators and the new digital demodulator with various complex modulation formats which are representative of present and future telemetry requirements.

The actual test setup was quite complicated and utilized much of the TEL IV facility including the automatic cross-bar signal distribution system. However, the essentials of the various tests are straightforward and simply described. An RF/FM signal generator, Boonton Model 202J, was modulated with different signal formats obtained from modulation simulators. A TMR-15 receiver group was tuned to the RF output of the generator, and the video output of the receiver was fed to the appropriate terminal equipment such as FM/FM subcarrier demodulators, PDM and PCM processors and digital-to-analog converters. The output of the data processing equipment was applied to various display devices such as oscillographs and numerical readouts. Each demodulator was plugged into the same receiver group while being tested to eliminate variations in test conditions due to differences in receivers and ancillary equipment. The RF input to the receiver was varied in steps over a range determined by the test conditions and the corresponding demodulator threshold.

5.2.1 FM/FM SIMULATION

For this test the modulation format is a signal composite of 15 FM/FM subcarriers, corresponding to IRIG standard channels 4 through 18. In order to evaluate the effects of intermodulation between channels, a special modulation scheme was devised. Channels 5, 7, 8, 9, 11, 14, 16 and 18 were left unmodulated. Channels 6, 12, and 17 were modulated with a 5 cps

triangle wave. Channels 4, 10, and 15 were modulated with a 5 cps square wave. The modulating signals were non-coherent and the frequency was kept low to conserve oscillograph paper. The individual channel deviation was adjusted in accordance with the standard used for the MINUTEMAN missile, which is 12 dB per octave from 10.5 kc through 70 kc.

The demodulated output of the receiver was fed to the subcarrier demodulator system EMR Model 210. The data output of representative subcarrier demodulator was recorded on a photo oscillograph (Honeywell Model 1612 Visicorder). The RF input level to the receiver was varied in steps corresponding to a data quality ranging from essentially noise-free to complete obliteration in noise, with the absolute input level depending on the particular demodulator and test conditions.

A comparison between the FMD-C15 and the ADD-15 WBFM is shown in figure 34. This illustration is a composite of two oscillographs, sequentially run for each of the two demodulators, and shows recordings of the data output from both modulated and unmodulated subcarriers. (The undisturbed horizontal lines are unused oscillograph channels.)

Test Conditions:
- 3.3 MC IF Bandwidth
- 100 KC Video Bandwidth
- ±300 KC Deviation
- RF Input Level indicated on figure 34

A subjective analysis of figure 34 indicates that the performance of both demodulators is essentially equal over the entire RF level range. (The actual analysis was made on the original oscillographs which show more detail than some of the photographs.) For example, at the 1.4 microvolt level, which is the approximate threshold of the system, the noise in the corresponding data channels appears to be the same for both demodulators. Intermodulation products produced between the modulated channels were not severe enough to produce spurious outputs in unmodulated channels which are "clean" at strong signal levels. The results of this test would be expected on the basis of the signal-to-noise ratio measurements shown in figure 31.

A comparison between the FMD-B15, the ADD-15 IBFM, and the ADD-15 ØLFM is shown in figure 35. Figure 35 is a composite of three oscillographs, sequentially run for each of the three demodulators, and shows recordings of the data output from both modulated and unmodulated subcarriers.

Test Conditions:
- 300 KC IF Bandwidth
- 100 KC Video Bandwidth
- ±125 KC Deviation
- RF Input Level indicated on figure 35

A subjective analysis of figure 35 again indicates that the three demodulators perform equally well over the entire RF level range. Referring to the third unmodulated trace from the top of each oscillograph, the number of dropouts at the 1.8 microvolt level is seen to be 2 for the ADD-15 ØLFM, 3 for the ADD-15 IBFM, and 0 for the FMD-B15. At the 1.6 microvolt level the number of dropouts is 27, 14, 20 in the same order as above. This small variation among the three data outputs is most likely due to an insufficient statistical sampling interval for the particular dropout probability, rather than any significant performance differences among the demodulators.

On the basis of the S/N curves of figure 32, the phase lock demodulator would be expected to provide a measurable improvement in performance. One factor which reduces the expected phase lock improvement is that the threshold of the subcarrier demodulators occurs at approximately 1.6 microvolts which is below the demodulator threshold and where the S/N improvement indicated in figure 32 is only about 1 dB.

5.2.2 PCM/FM SIMULATION

For this test the RF/FM generator was modulated with a PCM format obtained from a PCM Program Simulator, Telemetric Model 513. The video output of the receiver is applied to the

PCM data processing equipment which includes a TDM Diagnostic Unit, Telemetric Models 6022, 6024, and 6715. The TDM Diagnostic Unit effects comparison between the data output of the receiver and the modulating signal from the simulator, and provides a numerical readout of the number of bit errors in a predetermined number of bits.

The bit errors for the different demodulators is measured with step variations in RF input level corresponding to bit error rates from zero to approximately 40 percent.

The numerical readout data and test conditions are shown in tables 13 and 14.

Of all the Phase II and Phase III simulation tests, the PCM bit error measurements provide the most accurate and most objective performance data. The ADD-15 WBFM produces a somewhat better bit error rate than the FMD-C15 at useful signal levels. However, since PCM threshold is very sharp, the RF level change required to equalize the bit errors between the two demodulators is less than 1 dB. Perhaps a more significant difference between the standard and digital wideband demodulators is the fact that the bit error rate is quite sensitive to receiver tuning errors with the FMD-C15, but remains essentially constant for large tuning errors when using the ADD-15 WBFM. This effect is evidently due to the much wider bandwidth of the ADD-15.

The ADD-15 IBFM produces a slightly better bit error rate than the FMD-B15. The ADD-15 ØLFM produces a bit error rate significantly improved with respect to both the ADD-15 IBFM and the FMD-B15. It was first suspected that the improvement might be due to a bandwidth compression in the ADD-15 ØLFM. However, the tests were repeated with a 50 kc receiver video bandwidth with essentially the same performance. The improved performance of the phase lock demodulator is supported by the signal-to-noise ratio data in figure 32.

5.3 PHASE III TEST - PREDETECTION PLAYBACK

The Phase III tests consist of an evaluation of demodulator performance with various PDM and PCM signal formats obtained from predetection tape recordings. In order that these experiments could be conducted with a minimum of interference to the normal operation of the TEL IV complex, the tests were run in accordance with the applicable portions of the standard TEL IV System Operational Acceptance Tests 80-4, test procedure number 1330. This test procedure utilizes standardized pre-recorded tapes as a signal source, and completely defines the test setup and station configuration, the signal formats, and the equipment test conditions.

The pre-recorded predetection tapes were played back on an Ampex Model AMR-FR-1400. The output of the tape recorder was applied to a predetection up converter which provides a 10 mc signal to the predetection input of the TMR-15 playback demodulator group, ADU-15, and VAU-15. The PDM or PCM signal output of the demodulators is applied to the Time Division Multiplex system, Telemetric Models 6703, 6704, and 6717. The digital output of the TDM is fed through a Digital-to-Analog Converter, Monitor Model 2119, to the photo oscillographs, Honeywell Visicorder 1612.

5.3.1 PCM TESTS

The PCM tests were run in accordance with Test Procedure 1330, Mission II. The test setup, and summary of test conditions for Mission II, is shown in figures 1 and 7 respectively of Test Procedure 1330. The oscillographs recorded the unmodulated analog data channels derived from the demultiplexed PCM output of the demodulators.

The RF input level to the receivers used to record the test tapes was varied in known steps over a wide range, with a corresponding variation in recorded S/N. As the recorded signal quality deteriorates the PCM bit synchronizer loses lock which is indicated by an abrupt change in oscillograph deflection (dropout). Since the oscillograph paper was run at a low linear rate, frequent dropouts appear as "noise" on the recorded traces. The number of dropouts

per time or "noise" on the analog channels is a measure of the demodulator performance at any indicated RF level.

The test conditions and corresponding figure numbers for the PCM tests are shown in table 15.

In Run 1 threshold occurs at approximately 2 microvolts and at this level the FMD-B15 produces about one half the number of dropouts as the ADD-15 IBFM. However, as can be seen from figure 36, the bit synchronizer threshold is very abrupt and the differences in dropout rate between the two demodulators corresponds to a small difference in RF level.

In Run 2 there is evidence of operational difficulties in obtaining bit synchronization. In the transition from 2.0 to 3.0 microvolts, the FMD-B15 records indicate a delay in synchronizing at the higher level. (Receiver signal strength records are available on the original oscillographs.) Also the ADD-15 trace shows complete loss of synchronization at intervals during the 2.0 microvolt level. After synchronization is established at the 3.0 microvolt level, the FMD-B15 produces about one half the number of dropouts as the ADD-15 IBFM.

In Run 3 at the threshold level of 5.0 microvolts, the FMD-C15 produces about 5/7 the number of dropouts as the ADD-15 WBFM.

In Run 4 the ADD-15 WBFM demodulator produces somewhat fewer dropouts than the FMD-C15 at the 1.0 microvolt level and produces a somewhat greater number of dropouts than the FMD-C15 at the 20 microvolt level. There is evidence in the ADD-15 WBFM trace that the data S/N is cyclically fluctuating and producing bursts of dropouts. This effect is most likely caused by accumulations on the tape recorder playback head and could easily result in the slight performance differences between the two demodulators.

5.3.2 PDM TESTS

The PDM Tests were run in accordance with Test Procedure 1330 Mission III. The summary of test conditions for Mission III is shown in Table II-6 of Test Procedure 1330.

The PDM tests required essentially the same setup and test procedure as the PCM tests described in 5.3.1, except that the TDM system had to be programmed for the different format.

The test conditions and corresponding figure number for the PDM tests are shown in table 16.

In Run 1 threshold occurs at about 2.0 microvolts. At 1.0 microvolt and below the ADD-15 IBFM records indicate a complete loss of bit synchronization. It was subsequently verified with the operating personnel that this effect was due to a slight misadjustment of the TDM unit. At threshold and above all three demodulators produce essentially the same data quality.

Throughout Run 2, the ADD-15 ØLFM demodulator produced no useful data. No evidence of a malfunction was found in the phase lock demodulator during the two week test program so it might be surmised that the difficulties were in the test setup. Since the ADD-15 ØLFM trace indicates a random output from the bit synchronizer, the problem probably was ahead of the TDM system.

Threshold occurs at about 4.0 microvolts and at this level and above the FMD-B15 and ADD-15 IBFM produce essentially the same quality data. Below threshold the ADD-15 IBFM seem to produce a much more severe loss of synchronization than the FMD-B15, as was the case in Run 1.

SECTION VI

FINAL CONCLUSIONS

The overall program objectives set forth in Section I and the final design objectives summarized in Section II have been fulfilled.

An FM demodulator for telemetry application utilizing a new design approach has been constructed and has been thoroughly evaluated under both laboratory and operational conditions.

A slight change in emphasis from the original proposal was made, in that receiver capture ratio was recognized as a significant area of improved performance over the standard TMR-15 demodulators.

A detailed comparison has been made between the capabilities of the Advanced Digital Demodulator and the standard FMD series of demodulators. The new demodulator performance is significantly improved in the critical areas of deviation bandwidth and capture ratio. Equally important, most of the other measured capabilities of the new unit are essentially the same as the standard unit, particularly those characteristics measured in the Phase II and Phase III experiments which are concerned with performance under realistic operational conditions and signal formats. Somewhat degraded performance is apparent in a few areas which are discussed below.

The digital demodulator provides a peak-to-peak deviation bandwidth of almost 2 mc in the IBFM mode and almost 20 mc in the WBFM mode. Compared to the linearity of the corresponding standard demodulator over this range, the new unit provides a very marked improvement. However, when comparing the two demodulators over the linear range of the FMD units, the corresponding modes of the ADD-15 demodulator in some cases exhibit a somewhat poorer linearity than the standard units. There are two factors contributing to this result. First, the TMR-15 demodulators exhibit an excellent linearity over the originally specified bandwidth. In fact, because of the accumulated non-linearities of other elements of a complete telemetry link (such as transmitter VCO), further improvement in linearity over this range would probably effect a negligible improvement in the overall accuracy of most present telemetry systems. Second, the static linearity plot for the digital demodulator indicates a number of "wiggles" in the response. This distortion is caused by small non-linearities in the presently used delay lines. It must be emphasized however, that these imperfections do not represent any inherent or fundamental limitations in the digital demodulator approach. The particular delay lines used were readily available units which were not originally designed for this application. Furthermore, the delay line linearity was experimentally "trimmed" by adjusting the source and load impedance while observing the swept response on an oscilloscope. However, as is apparent in the illustrations of paragraph 5.1.2, the wideband linearity of presently available sweep generators is less than satisfactory for this purpose. Although quite tedious, the delay lines could be trimmed by adjusting circuit constants while repeatedly plotting static curves. However, inherently more linear delay lines can also be obtained. Thus, it is reasonable to assume that improved "narrow bandwidth" linearity can be provided in the digital demodulator, if and when the design is pursued further. The digital demodulator can also be provided with a narrowband FM mode equivalent in deviation sensitivity to the FMD-A15. This mode would be obtained by incorporating a third delay line with ten times the delay of the IBFM unit, that is, a delay of 5 microseconds. This value of linear delay at a 10 mc center frequency would require some special techniques, but a preliminary investigation indicates that a suitable design is feasible.

As indicated in the Performance Summary table 1 in the Introduction Section, high capture ratio, utilizing the Arguimbau approach, was achieved by virtue of the very wide digital demodulator bandwidth. This characteristic was greatly improved over the standard FMD-B15 demodulator, and since the performance was achieved without restricting other capabilities of the unit, the advantage of this approach is thus indicated.

The signal-to-noise ratio and threshold characteristics of the ADD-15, IBFM mode and the FMD-B15 are nearly equal. The measured threshold levels of both units equal the calculated threshold values, however the measured signal-to-noise ratio of both the ADD-15, IBFM and the FMD-15 is approximately 2 dB below the calculated values. The measured signal-to-noise ratio of the ADD-15, ØLFM mode equals the calculated value but since the measured (1 dB) threshold level of the ADD-15, ØLFM equals the threshold level of the FMD-B15 and the ADD-15, IBFM, the phase lock FM mode did not exhibit the calculated threshold improvement. The phase lock FM mode provided an improved performance in the PCM tests. However no significant improvement was realized in the FM/FM tests for which the circuit had presumably been optimized.

The signal-to-noise ratio of the ADD-15, WBFM mode and the FMD-C15 are essentially the same for video signal-to-noise ratios greater than 10 dB and less than -10 dB. However, the threshold level of the FMD-C15 is approximately 1.5 dB less than the threshold level for the ADD-15, WBFM mode. The measured signal-to-noise ratio of the FMD-C15 and the ADD-15, WBFM are 2.0 dB and 4.0 dB, respectively, below the calculated signal-to-noise ratio corresponding to the calculated RF threshold level of 5.7 microvolts.

The differences between calculated and measured signal-to-noise ratio could be due to a degraded receiver noise figure, an unknown attenuation of the RF signal, or accumulated calibration error in the test setup. The differences in threshold performance between the FMD-C15 and the ADD-15, WBFM are presently unexplained.

As indicated in Section IV, a possible fundamental limitation in the present digital demodulator design was discovered in the AM rejection measurements. The AM rejection is significantly degraded at the low modulating frequencies as compared to the FMD performance. At the higher modulating frequencies, the new demodulator was somewhat improved over the FMD. This limitation can be completely eliminated by preceding the digital demodulator with a limiter, but it is not clear at this time what effect a non-sinusoidal input signal to the delay lines would have on the intermodulation distortion and other performance characteristics.

The remaining demodulator characteristics measured during the test program were essentially the same for the digital and corresponding FMD demodulators.

The phase-lock PM mode was not evaluated during the test program at AFETR. However, tests during the design of this circuit indicate excellent "short-loop" performance which closely agrees with the mathematical predictions of Section IV. The performance characteristics of the PM mode are given in Summary Table 1. One of the important results of this program is the augmentation of the technique for increasing the capture range and decreasing the acquisition time of the digital phase lock loop. The wide bandwidth capabilities of the PM mode, as shown in figure 4, provide the new demodulator package with considerable signal handling flexibility.

The new digital demodulator could be used to considerable advantage in the present TMR-15 receiver group and as part of the TRKI-12 System. For example, a single plug-in package could be supplied which duplicates the functions, and exceeds the performance of the FMD-A15, FMD-B15, and FMD-C15 units, and in addition, provides a phase-lock FM and phase-lock PM mode. All modes would be selected by a single front panel switch. Additional capabilities such as tape speed compensation are also possible. The high capture ratio could provide a significant advantage, particularly in a ship or airborne installation. The solid-state design will provide increased reliability, but this factor is probably less important when the unit is used in conjunction with a vacuum tube system.

Future application could utilize the very wide bandwidth capabilities of the digital demodulator.

Future development of this demodulator should include additional experiments on the performance capabilities of the unit. For example, quantitative data is needed on the effects of high capture ratio on data reliability under conditions of severe multipath. These tests should be

done under laboratory conditions where multipath effects can be simulated. Additional S/N and threshold data in all functional modes is also desirable.

In closing this report, it should be noted that considerable useful information and experience has resulted from this program. These results are applicable to both the present TRKI-12 System and future requirements for telemetry signal acquisition.

APPENDIX I

ILLUSTRATIONS
and
DATA REPRODUCTIONS

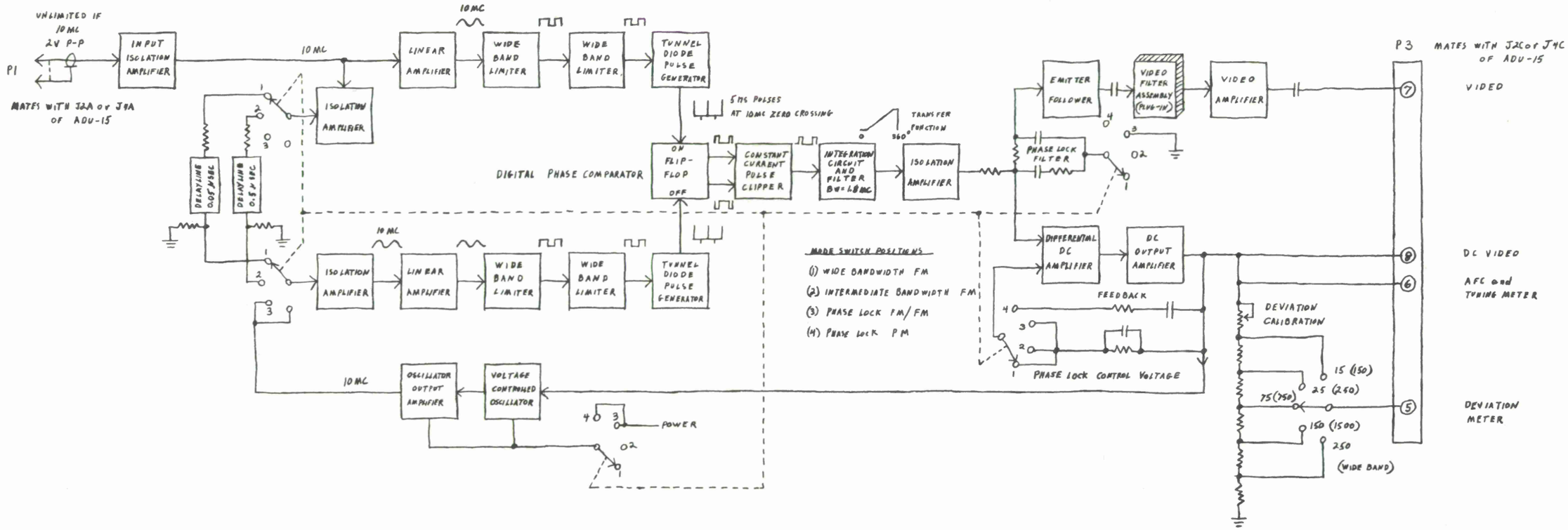

Figure 1. Model ADD-15 Advanced Digital Demodulator, Simplified Functional Block Diagram

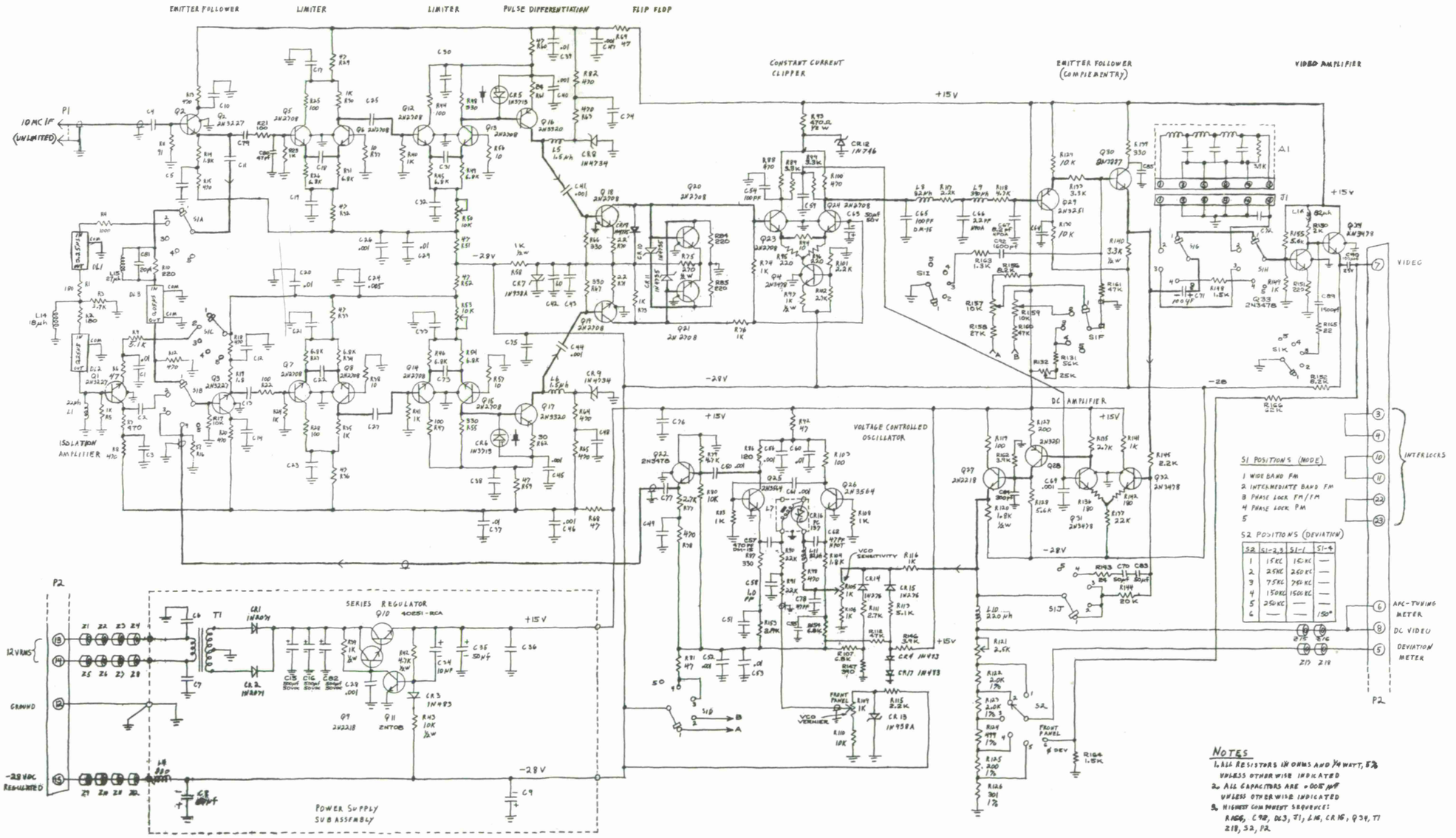

Figure 2. Model ADD-15 Advanced Digital Demodulator, Schematic Diagram

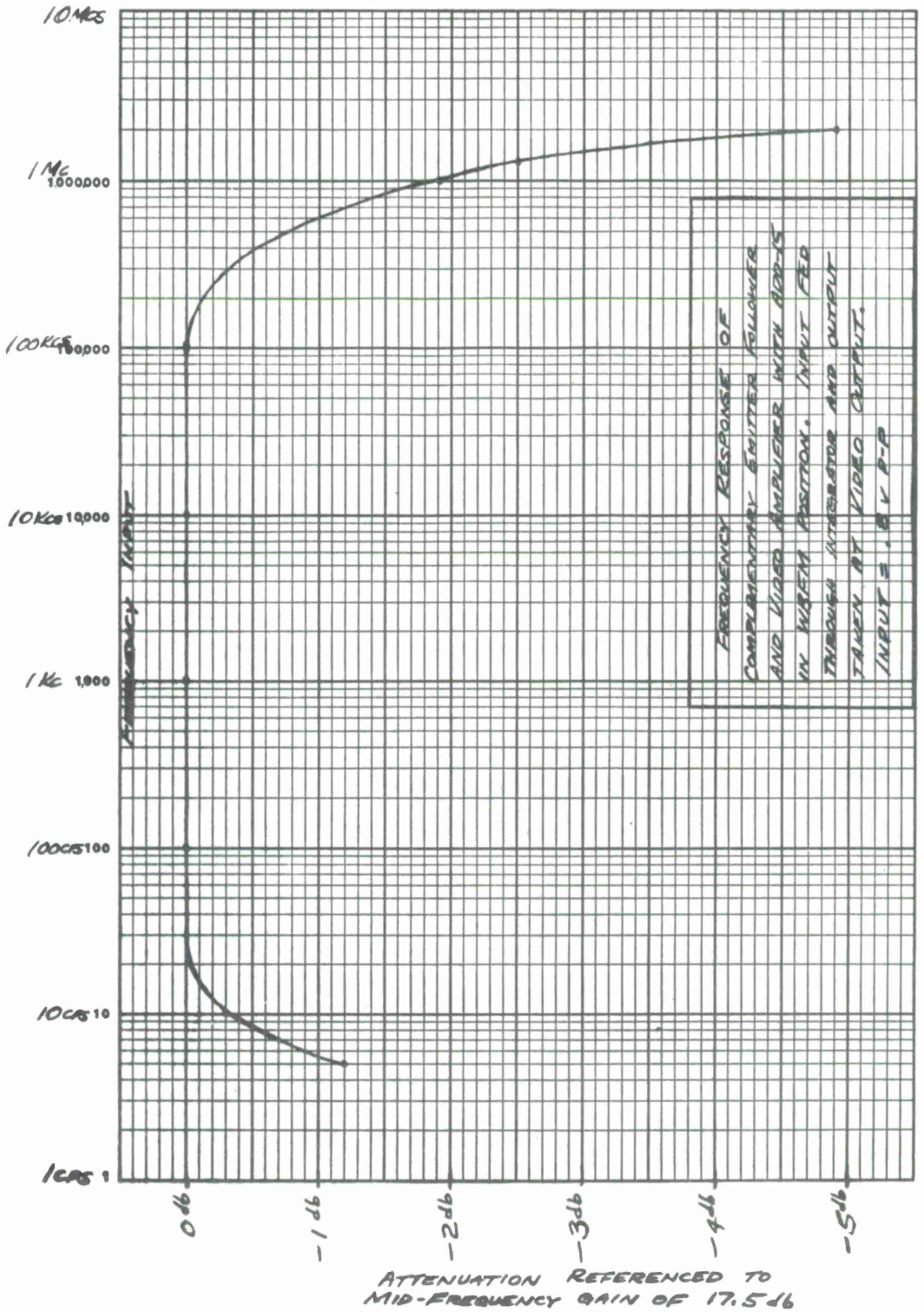
10 MCS
1 MC 1,000,000
100 KCS 100,000
10 KCS 10,000
1 KC 1,000
100 CPS 100
10 CPS 10
1 CPS 1
FREQUENCY INPUT
0 db
-1 db
-2 db
-3 db
-4 db
-5 db
ATTENUATION REFERENCED TO MID-FREQUENCY GAIN OF 17.5 db
FREQUENCY RESPONSE OF COMPLEMENTARY EMITTER FOLLOWER AND MIXER AMPLIFIER WITH MODES IN MIDDLE POSITION. INPUT FED THROUGH ATTENUATOR AND OUTPUT TAKEN AT VIDEO OUTPUT. INPUT = .8 V P-P

Figure 3

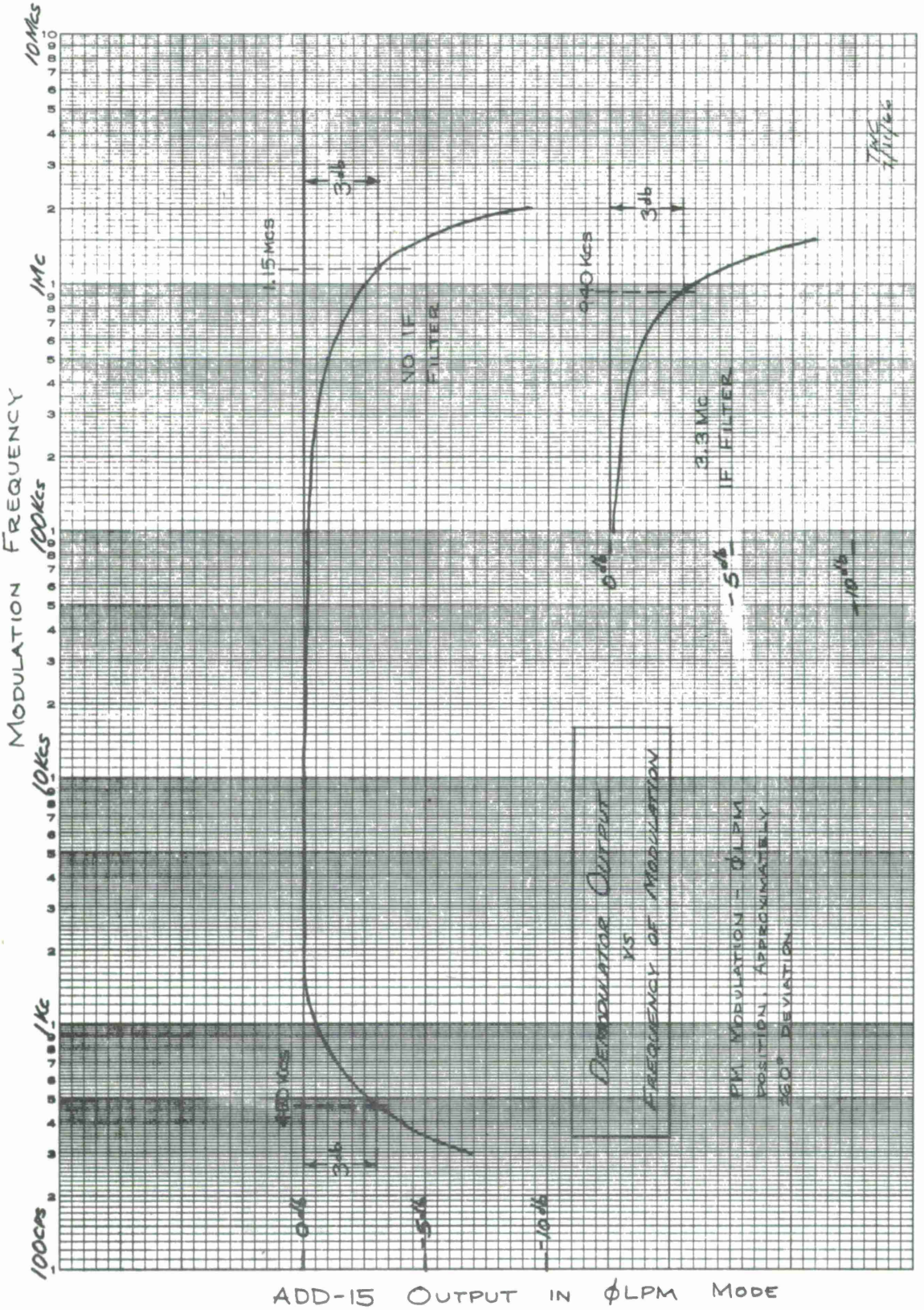
ADD-15 Output in ϕLPM Mode
Modulation Frequency
100cps
1Kc
10Kcs
100Kcs
1Mc
10Mcs
Demodulator Output
vs
Frequency of Modulation
PM Modulation - ϕLPM
Position, Approximately
280° Deviation
1.15Mcs
3db
No IF Filter
440Kcs
3db
3.3 Mc
IF Filter
0db
-5db
-10db

Figure 4

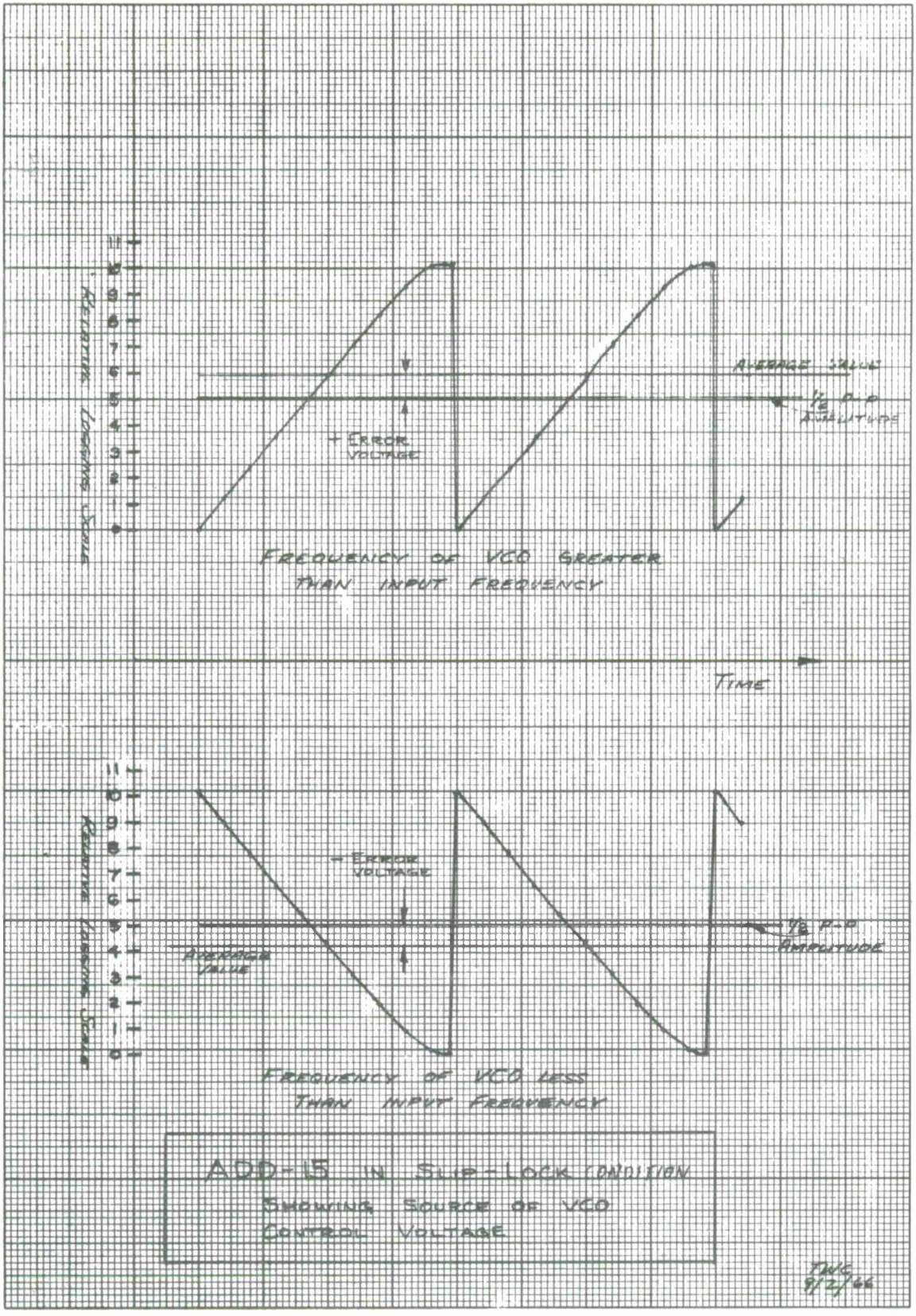
Reading Linear Scale
+ Error Voltage
Average Value
½ P-P Amplitude
Frequency of VCO Greater Than Input Frequency
Time
Reading Linear Scale
- Error Voltage
Average Value
½ P-P Amplitude
Frequency of VCO Less Than Input Frequency
ADD-15 in Slip-Lock condition
Showing Source of VCO Control Voltage
9/2/66

Figure 5

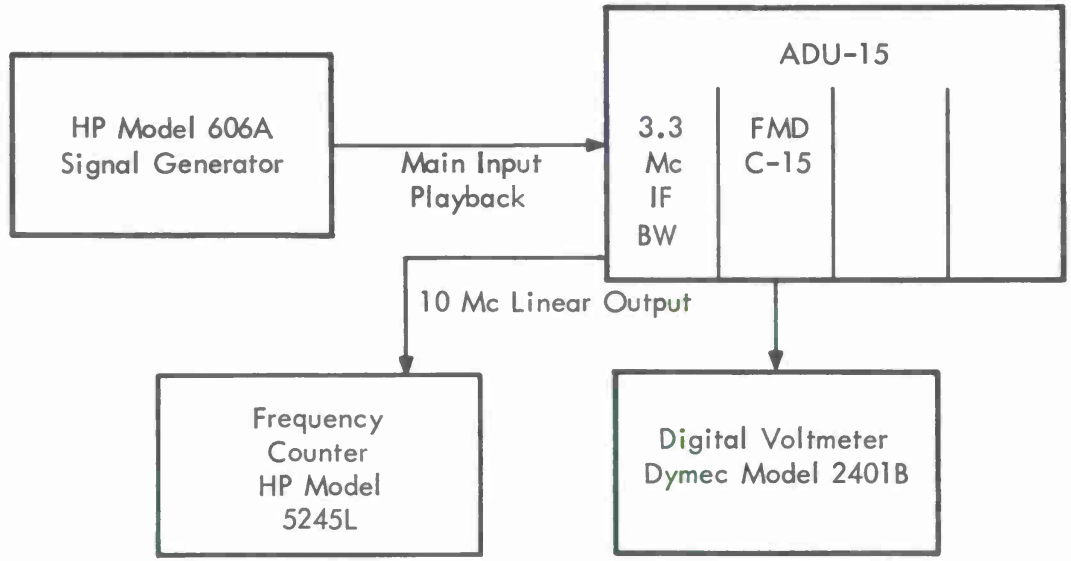

Figure 6a. Static Linearity, FMD-B15, FMD-C15, Test Setup

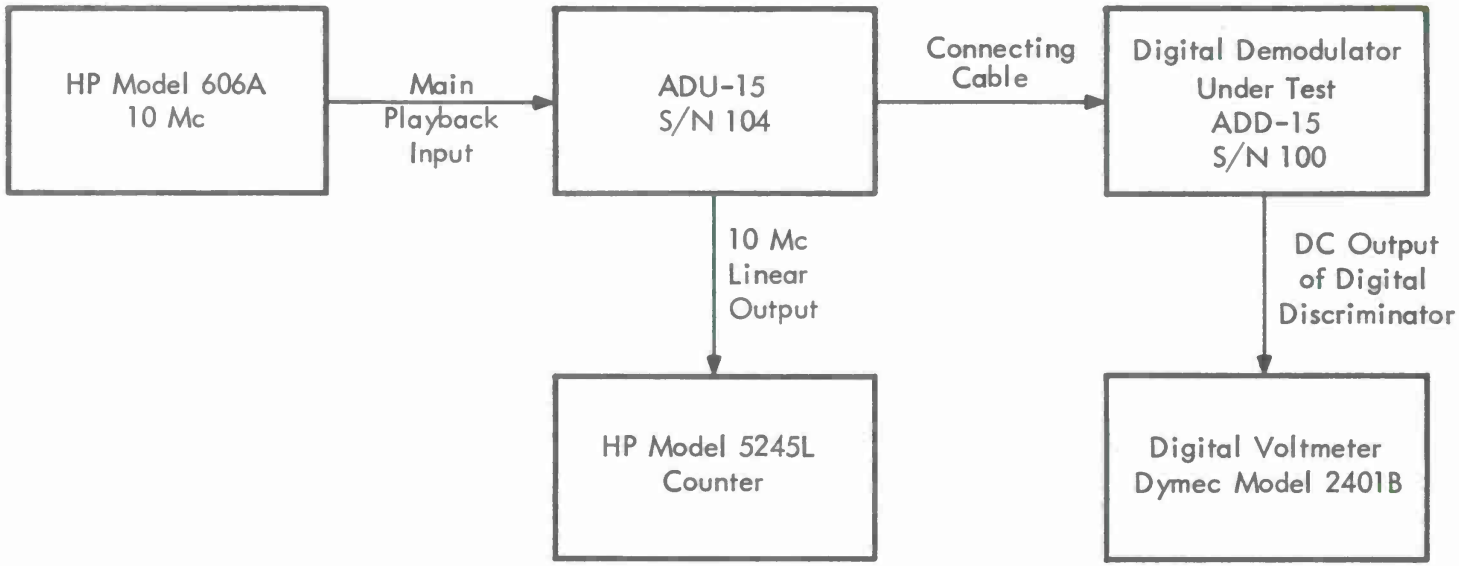

Figure 6b. Static Linearity, ADD-15, Test Setup

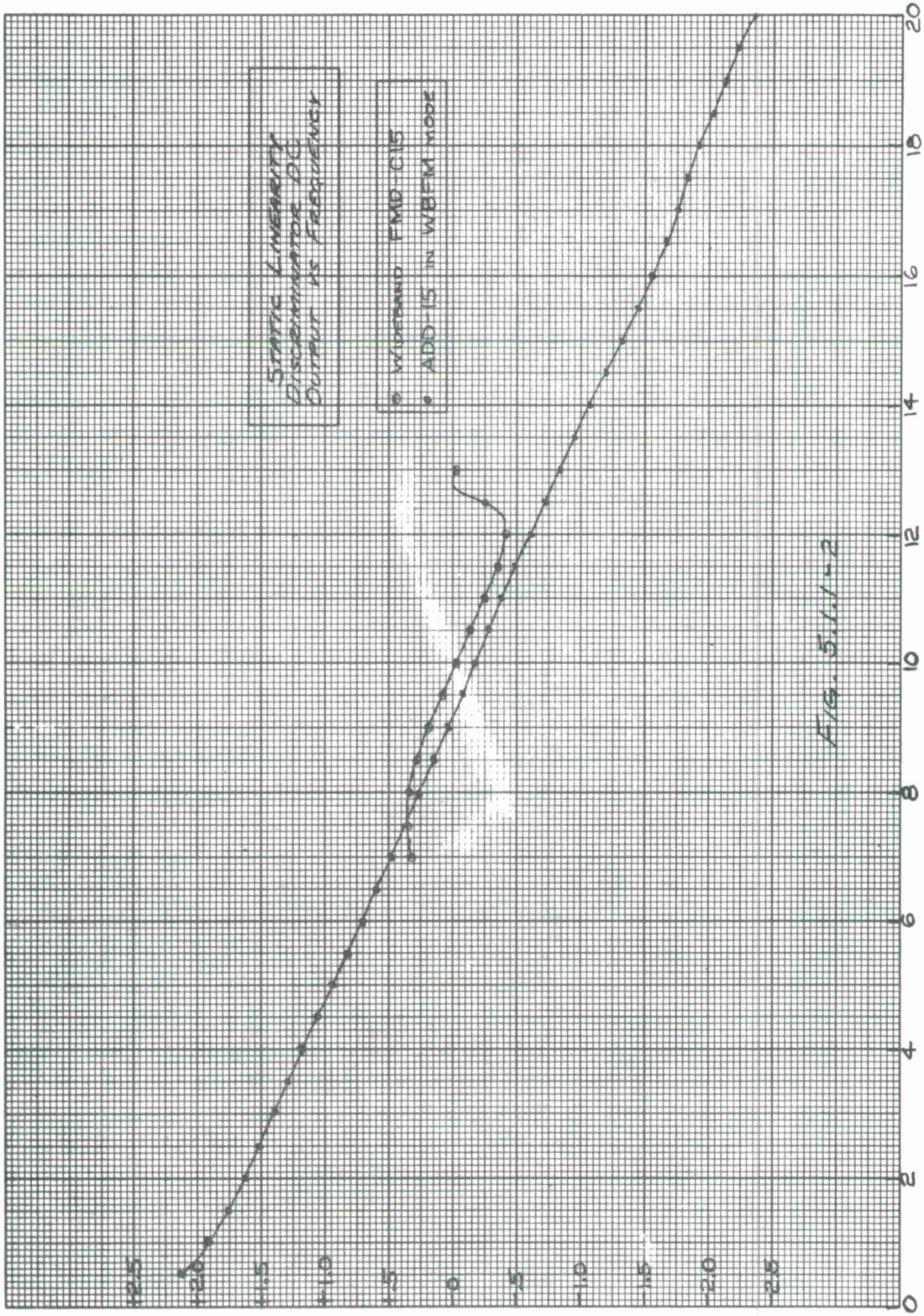
Static Linearity
Discriminator DC
Output vs Frequency
Wideband FMD CIF
ADIS in WBFM Mode
Fig. 5.1.1-2
Frequency - Mc/s
DC Output of Discriminator - Volts

Figure 7

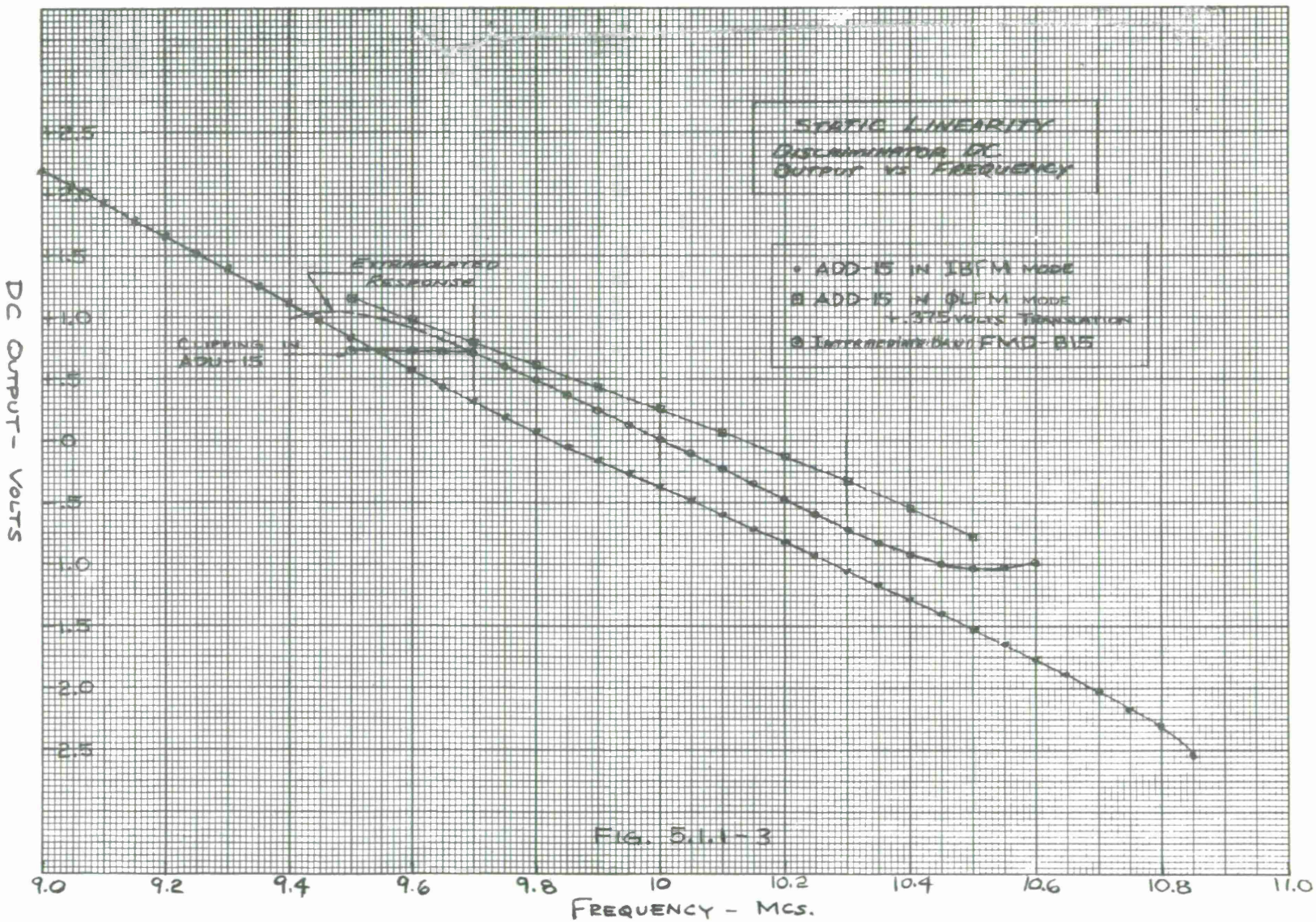

FIG. 5.1.1-3

Figure 8

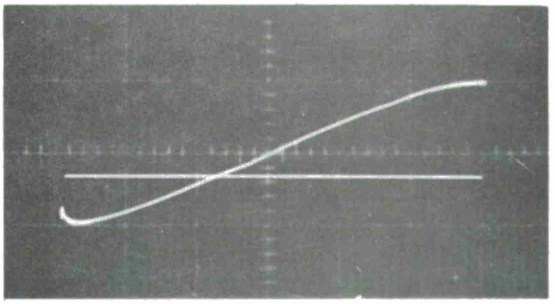

Figure 9

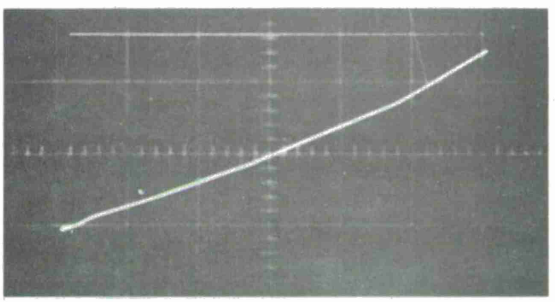

Figure 10

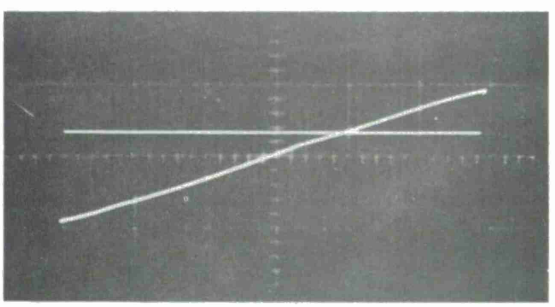

Figure 11

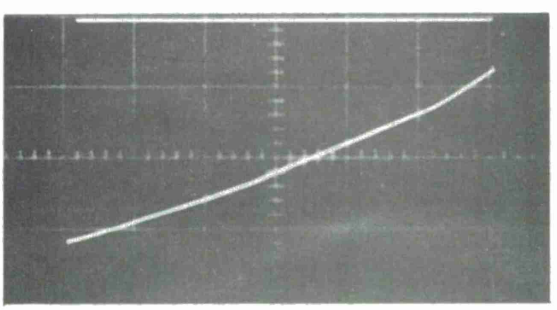

Figure 12

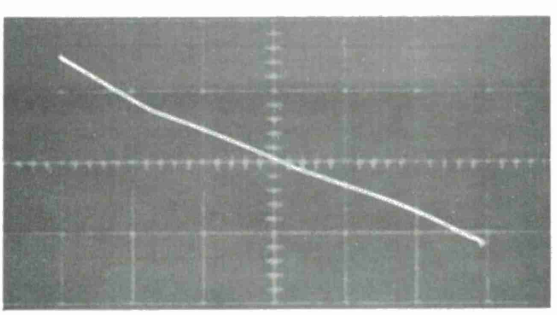

Figure 13

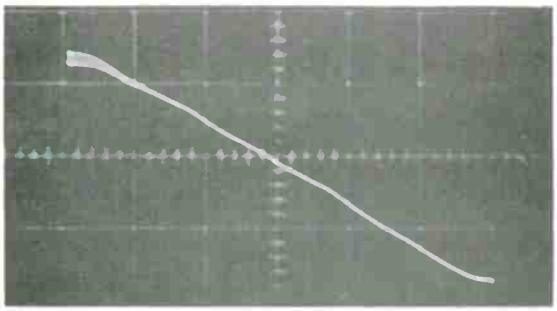

Figure 14

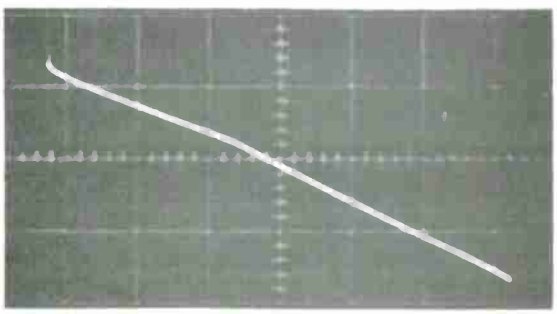

Figure 15

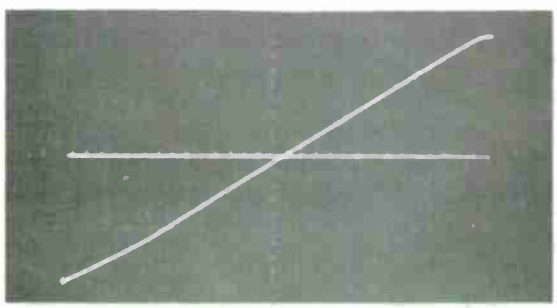

Figure 16

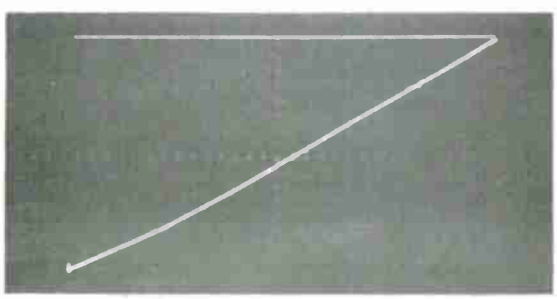

Figure 17

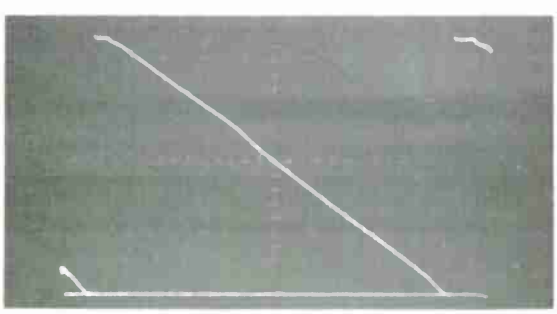

Figure 18

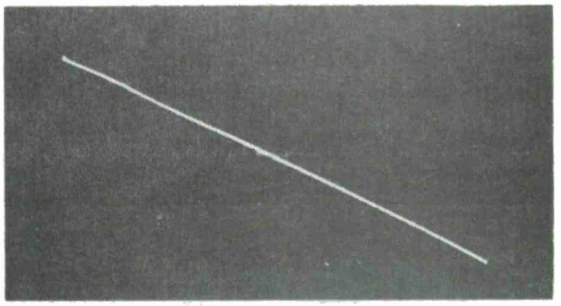

Figure 19

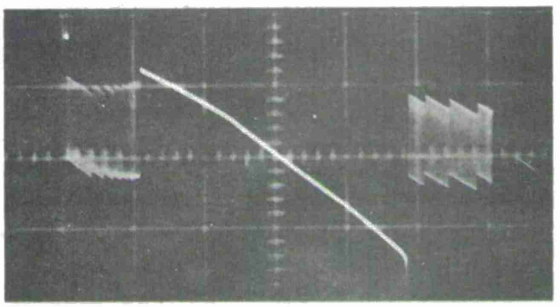

Figure 20

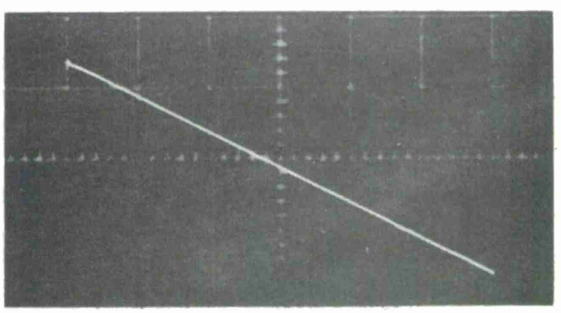

Figure 21

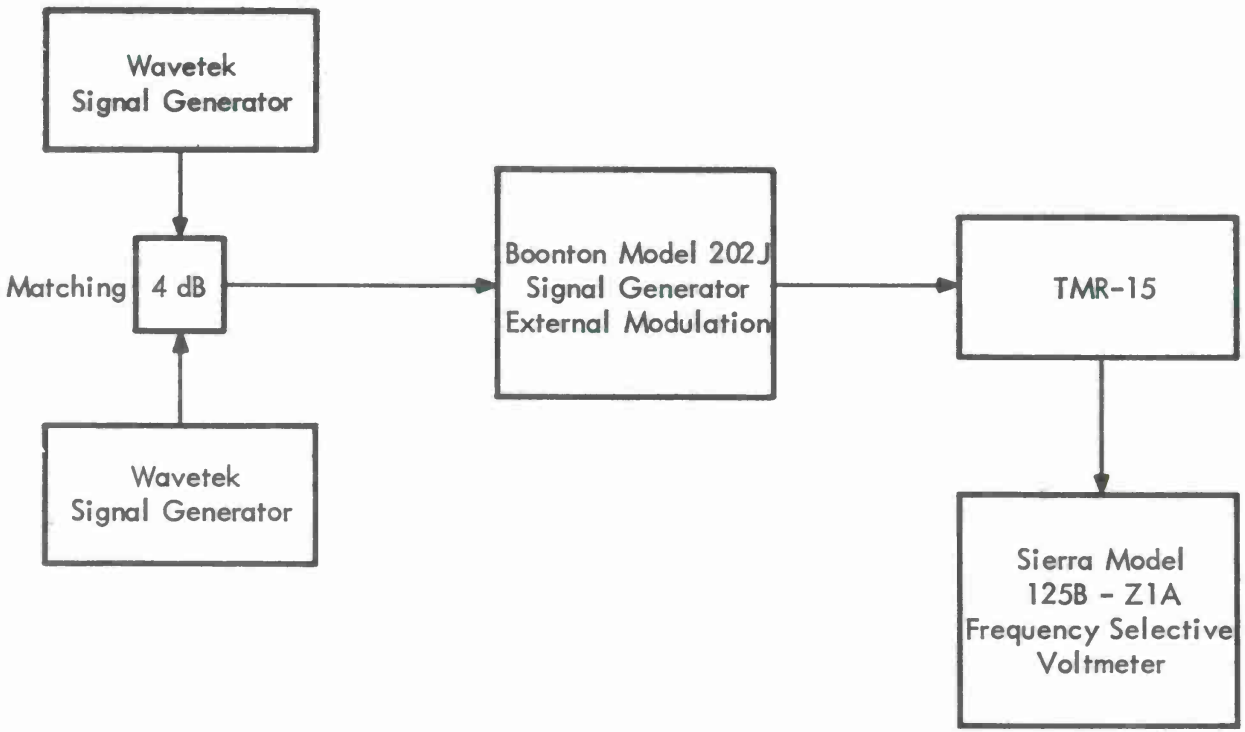

Figure 22. Intermodulation Distortion, Test Setup

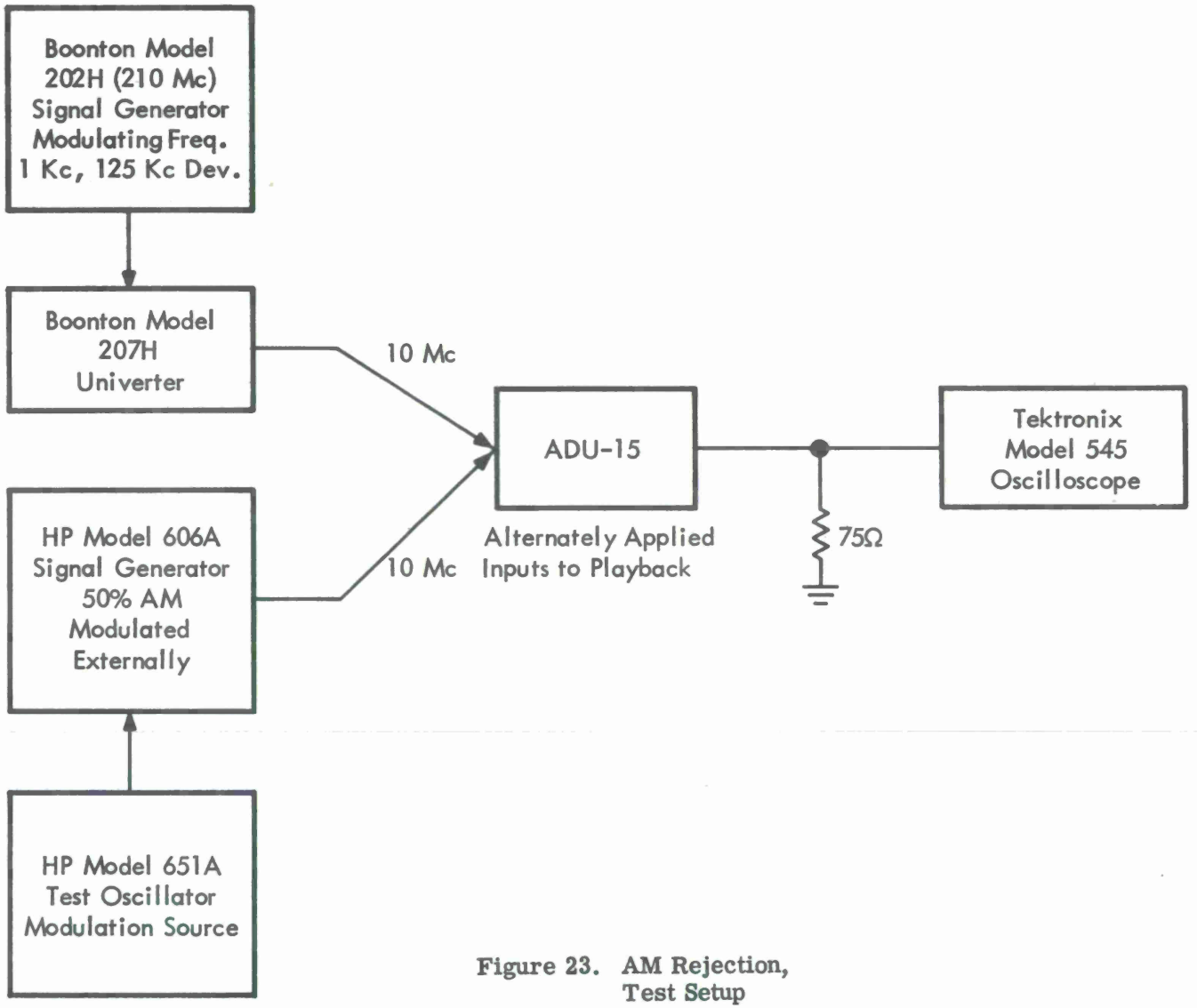

Figure 23. AM Rejection, Test Setup

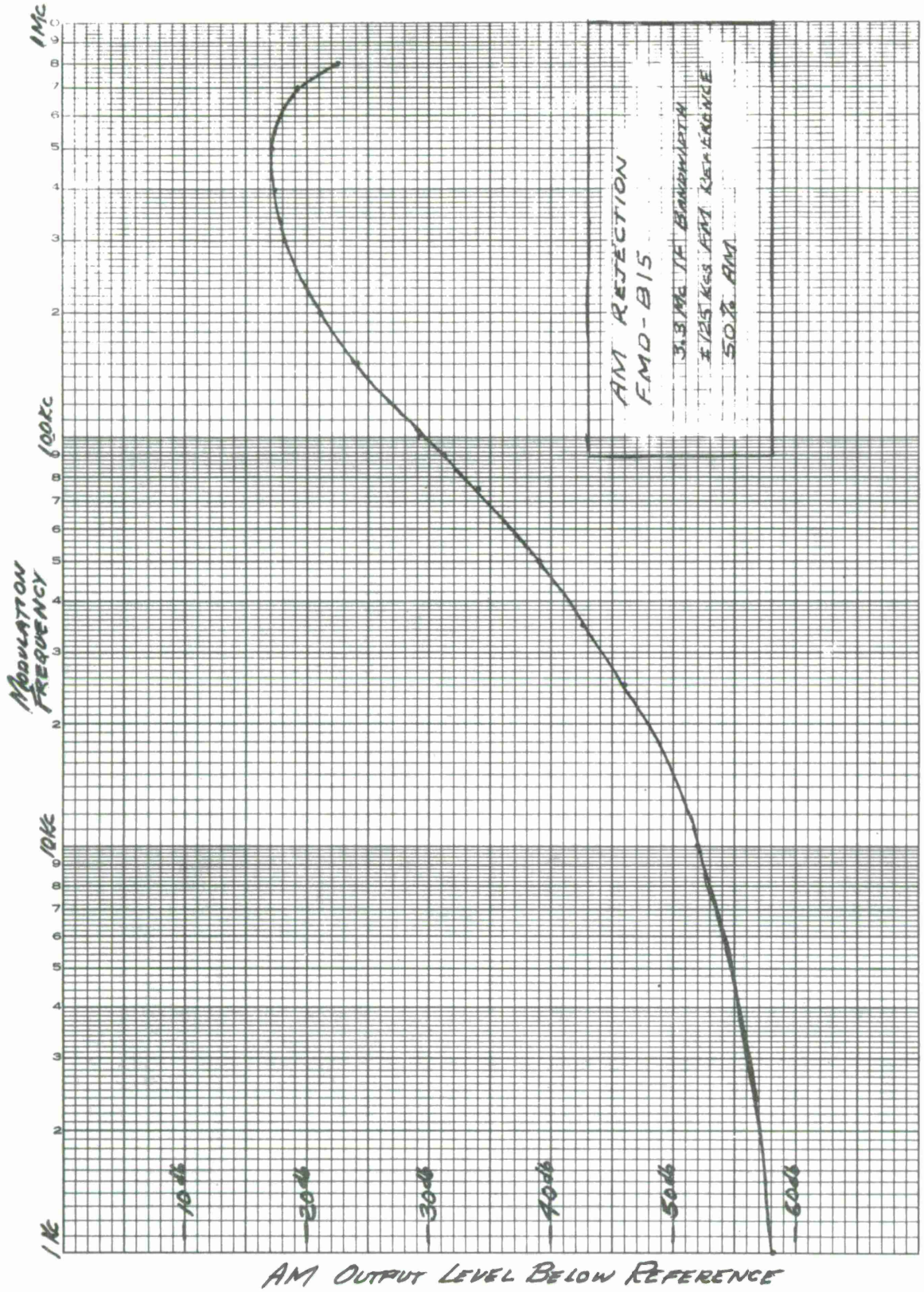
AM REJECTION
FMO-B15
3.3 Mc IF Bandwidth
±125 Kcs AFC Range
50% AM
1Mc
100Kc
10Kc
1Kc
Modulation Frequency
10db
20db
30db
40db
50db
60db
AM Output Level Below Reference

Figure 24

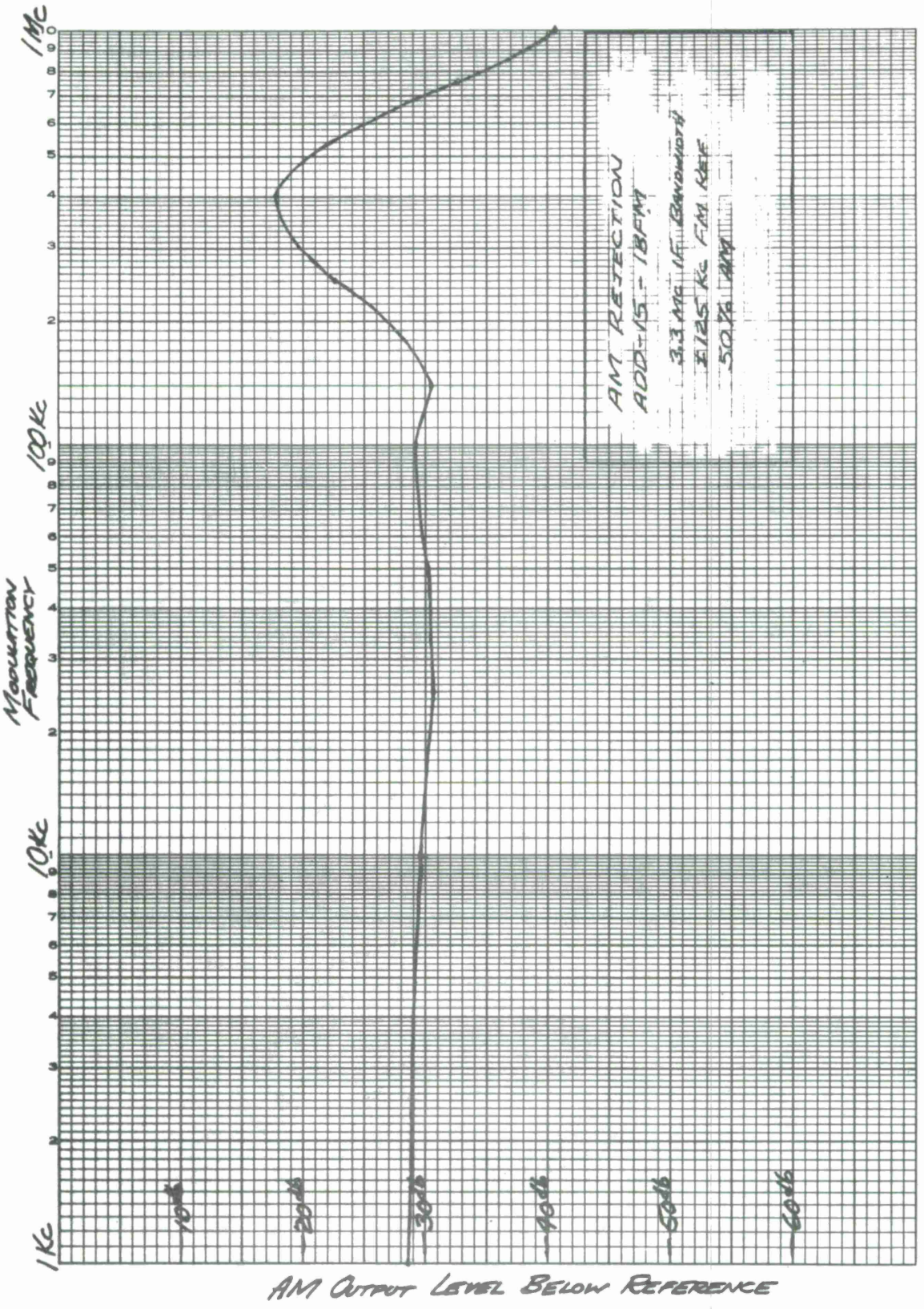
1 Mc
100 Kc
10 Kc
1 Kc
Modulation Frequency
AM Reflection
AOD-15 = 1B/FM
3.3 Mc IF Bandwidth
±125 Kc FM Ref
50% AM
10db
20db
30db
40db
50db
60db
AM Output Level Below Reference

Figure 25

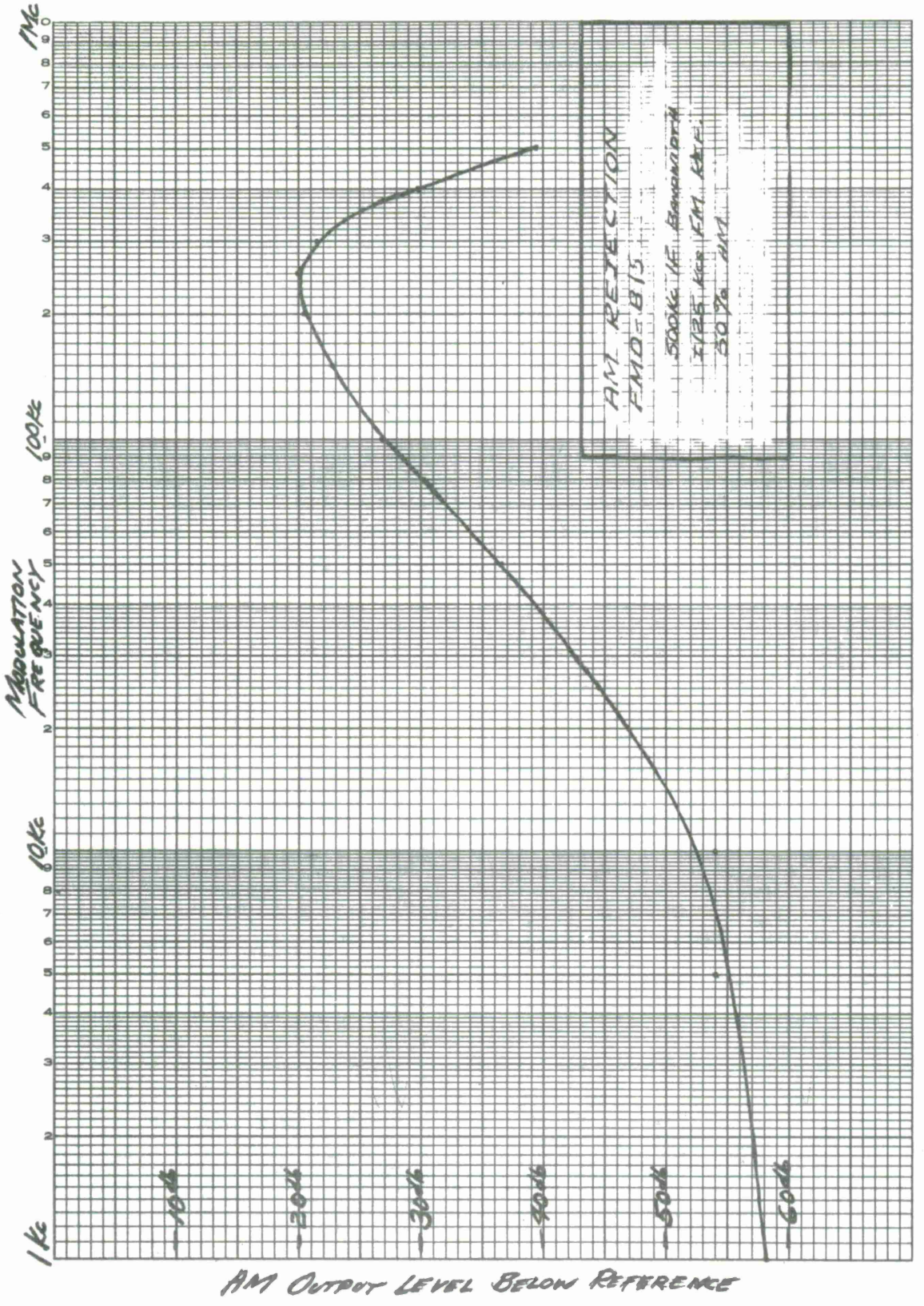
AM REJECTION
FMO-81S
500Kc IF Bandwidth
±125 Kcs FM Dev.
30% AM
1Mc
100Kc
10Kc
1Kc
Modulation Frequency
-10db
-20db
-30db
-40db
-50db
-60db
AM Output Level Below Reference

Figure 26

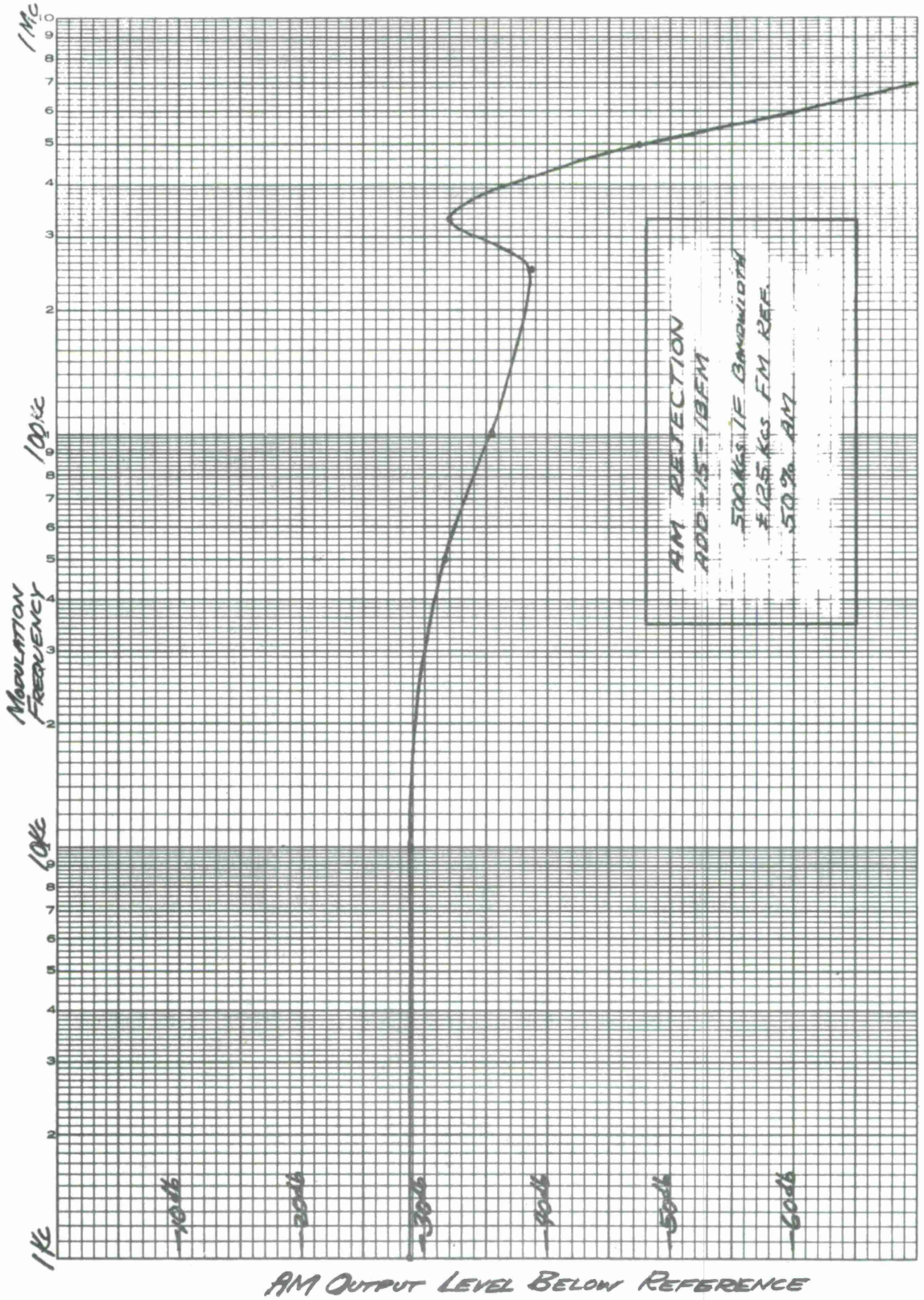
1 Mc
100 Kc
10 Kc
1 Kc
Modulation Frequency
AM Rejection
400 ÷ 15 = 18 FM
500 Kcs IF Bandwidth
±125 Kcs FM Ref.
50% AM
-10 db
-20 db
-30 db
-40 db
-50 db
-60 db
AM Output Level Below Reference

Figure 27

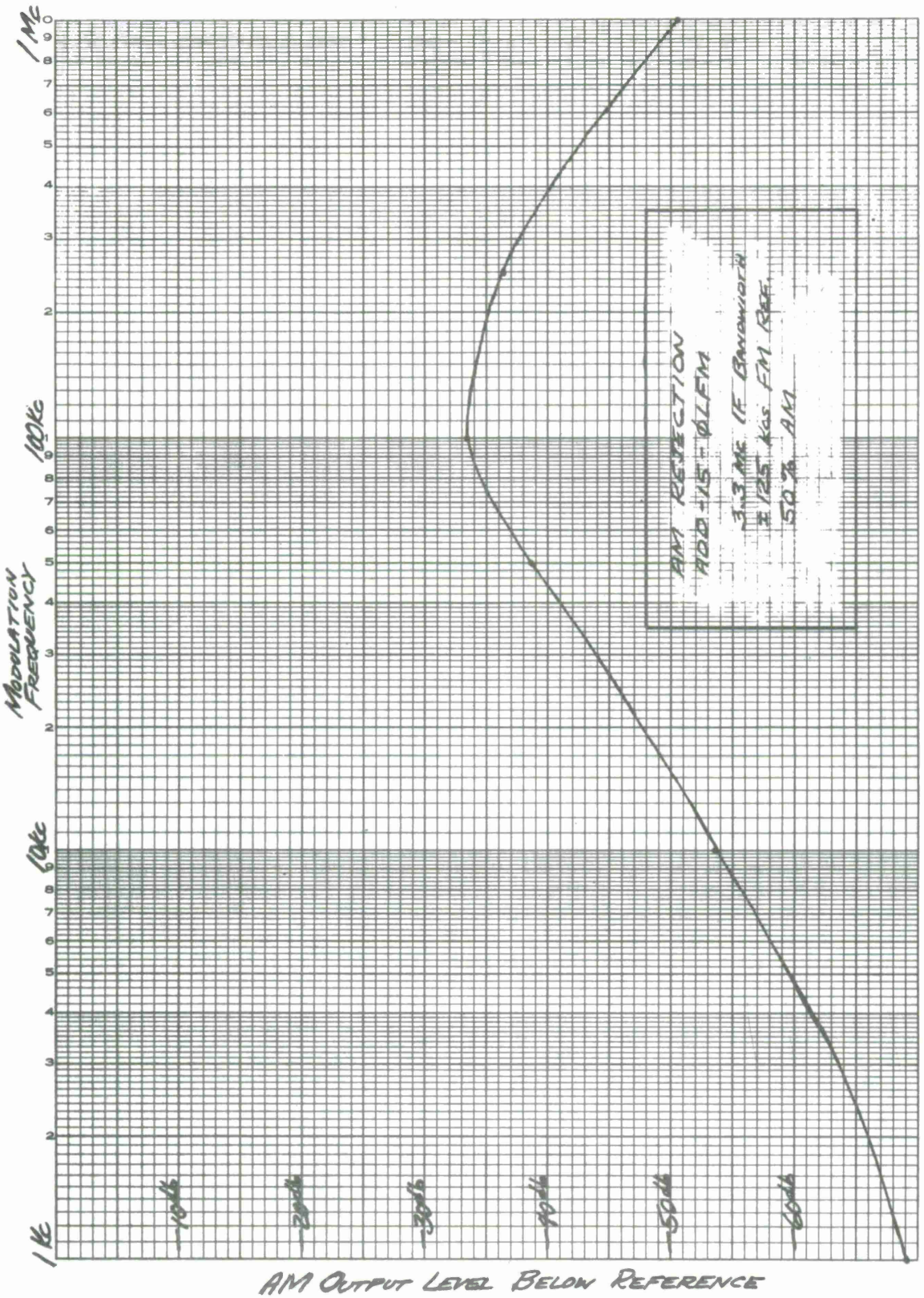
1 Mc
100 Kc
10 Kc
1 Kc
Modulation Frequency
10 db
20 db
30 db
40 db
50 db
60 db
AM Output Level Below Reference
AM Rejection
400 +15 - 0 Cps
3.3 Mc IF Bandwidth
± 125 Kcs FM Ref.
50 % AM

Figure 28

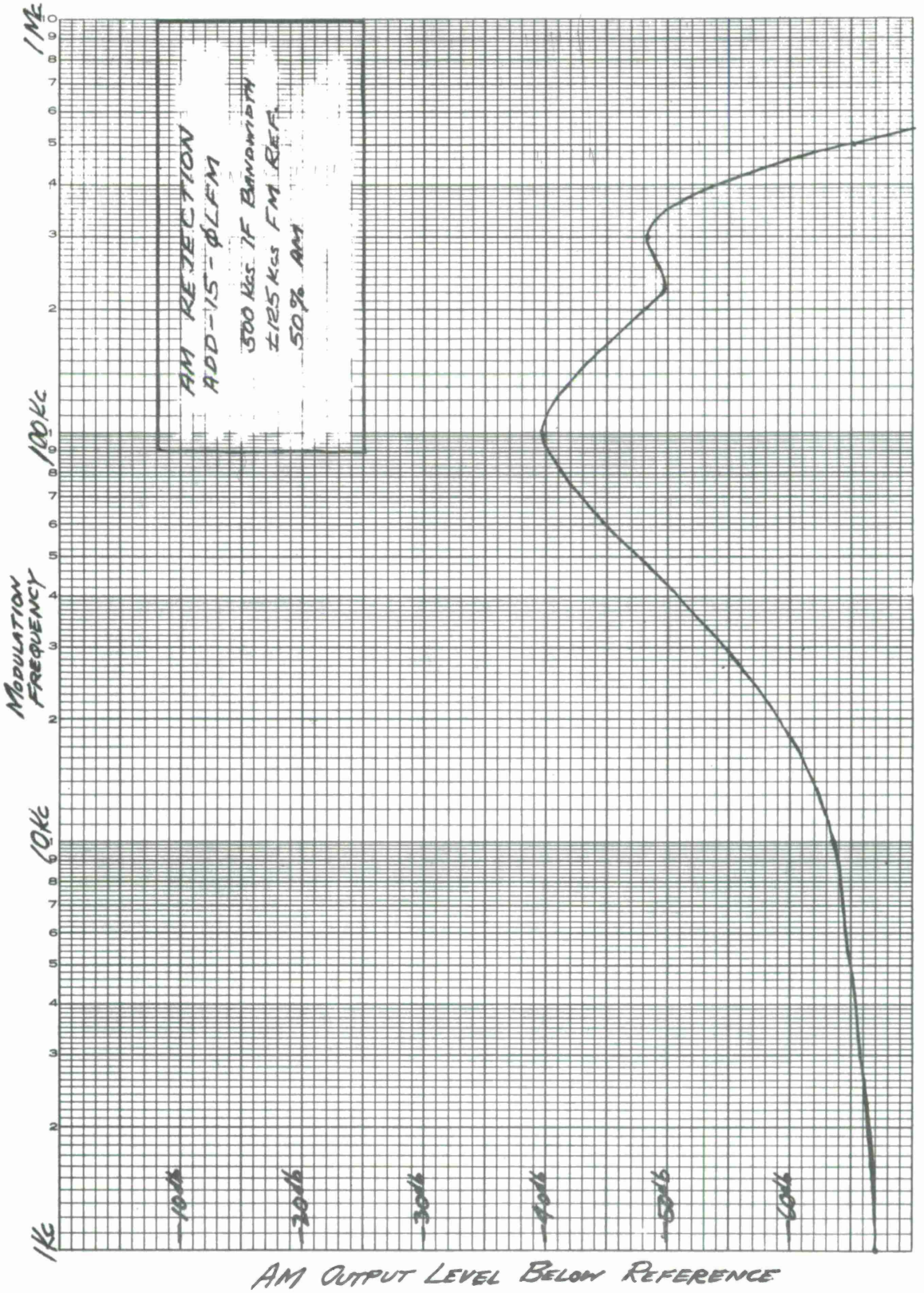
AM REJECTION
ADD -15 - ΦLFM
300 Kcs IF Bandwidth
±125 Kcs FM Ref.
50% AM
1 Mc
100 Kc
10 Kc
1 Kc
Modulation Frequency
-10db
-20db
-30db
-40db
-50db
-60db
AM Output Level Below Reference

Figure 29

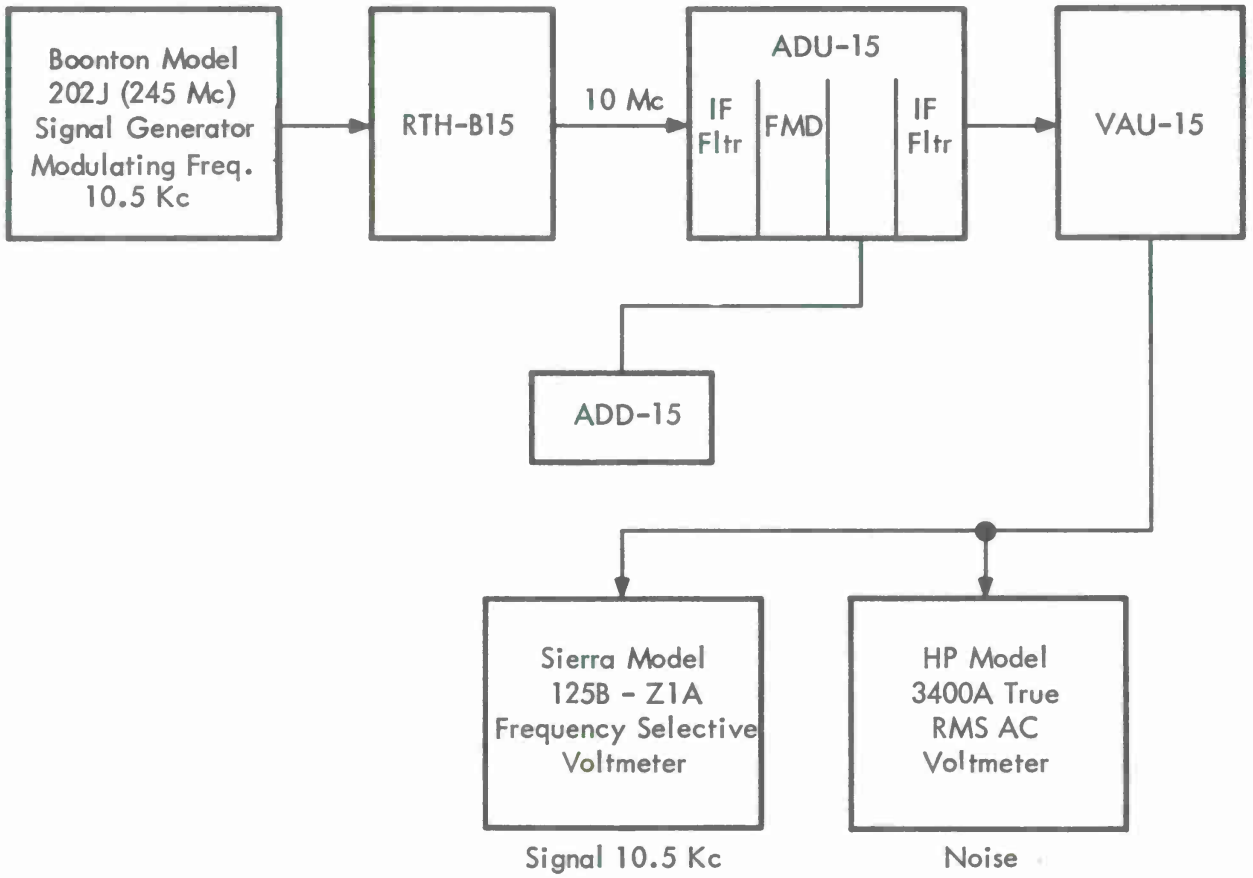

Figure 30. Signal Noise and Threshold, Test Setup

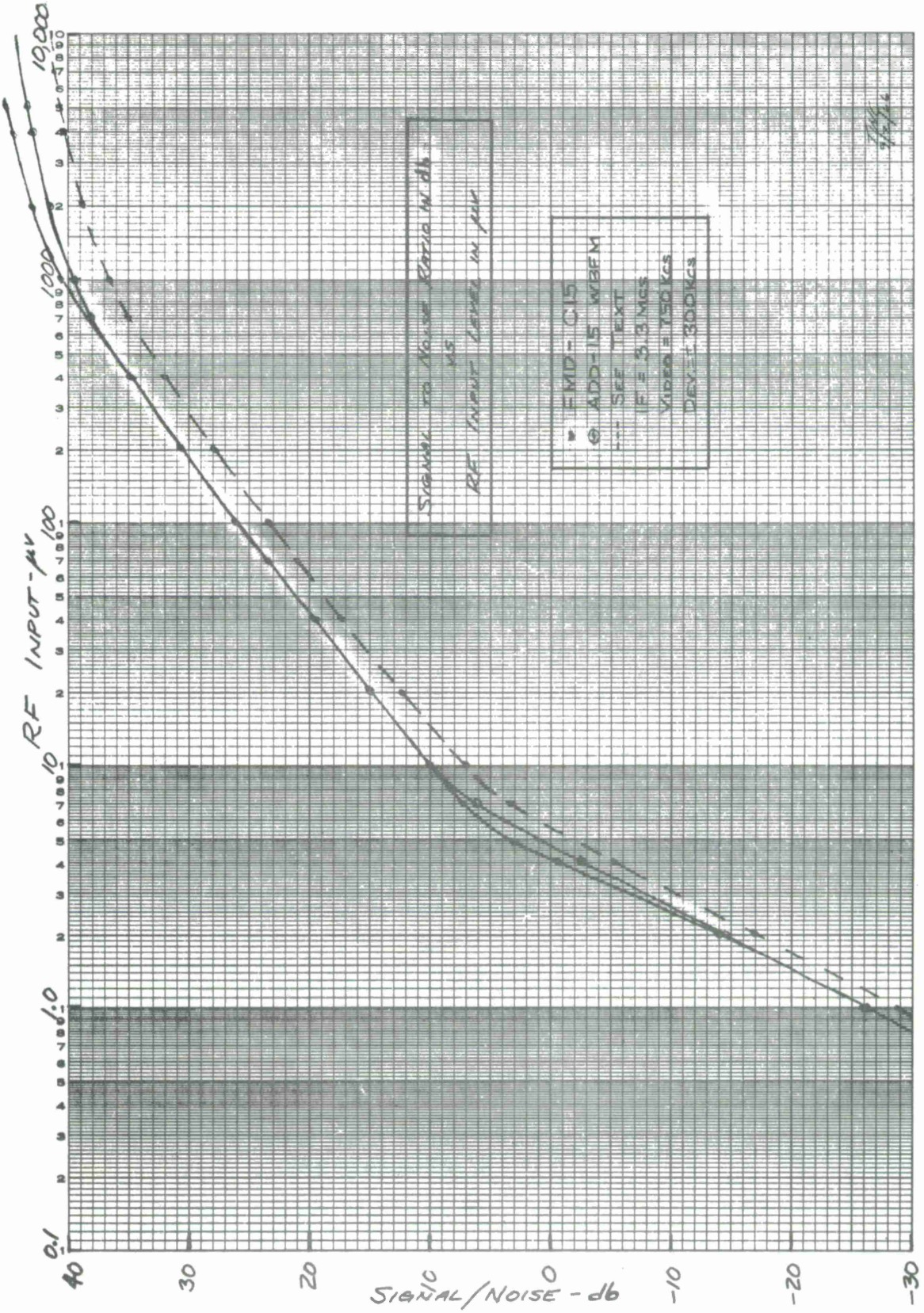
RF INPUT - μV
10,000
1000
100
10
1.0
0.1
40
30
20
10
0
-10
-20
-30
SIGNAL/NOISE - db
Signal to Noise Ratio in db
vs
RF Input Level in μv
EMP-615
ADD-15 W6EPM
SEE TEXT
IF = 3.3 Mcs
Video = 150 Kcs
Dev = ±300 Kcs

Figure 31

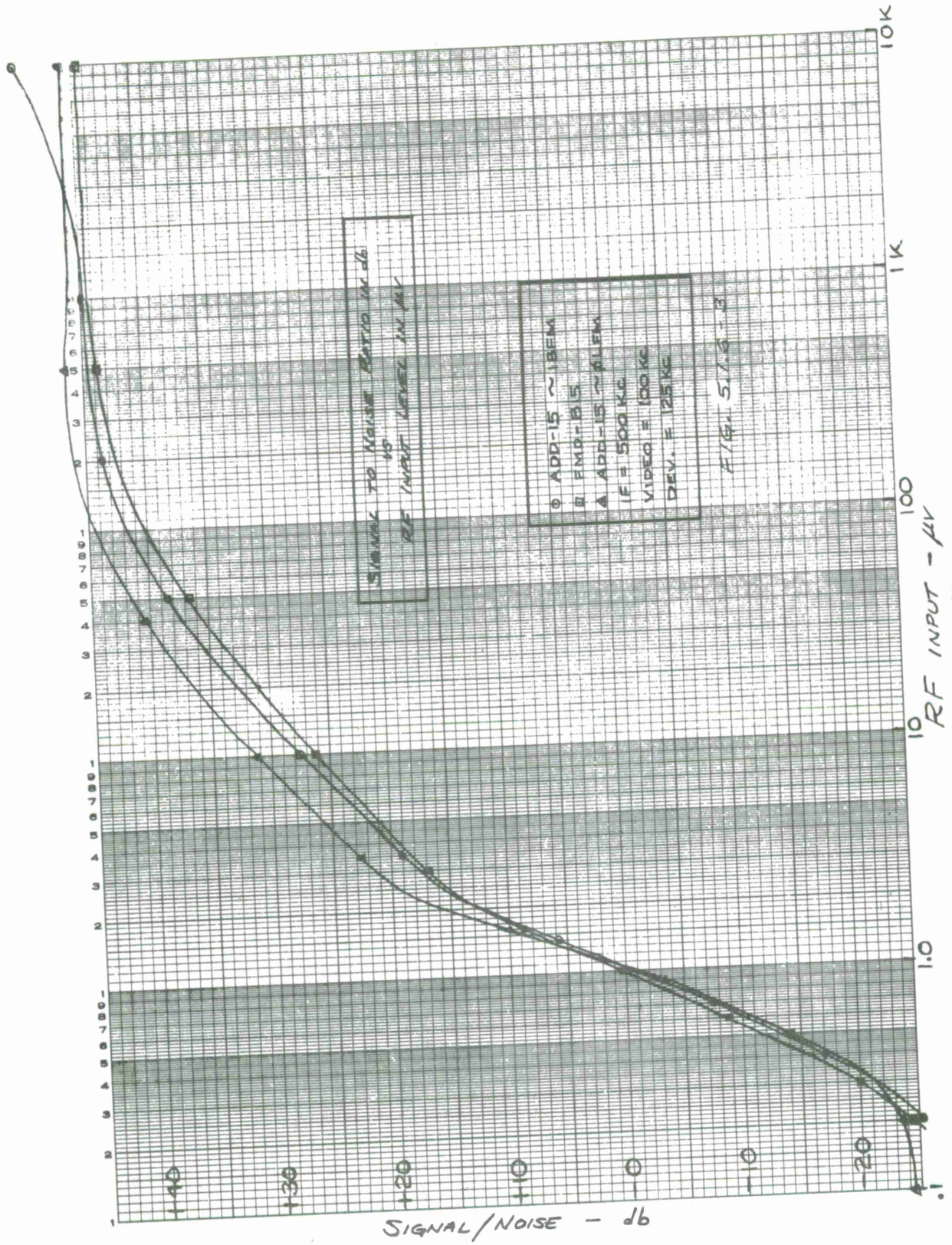
10K
1K
100
10
1.0
.1
RF INPUT - μV
SIGNAL/NOISE - db
+40
+30
+20
+10
0
-10
-20
Signal To Noise Ratio in db
for Limit Level in μV
© ADD-15 ~ 18FM
® FMD-15
A ADD-15-A/FM
IF = 500 KC
VIDEO = 100 KC
DEV. = 125 KC
FIG. 5/16-13

Figure 32

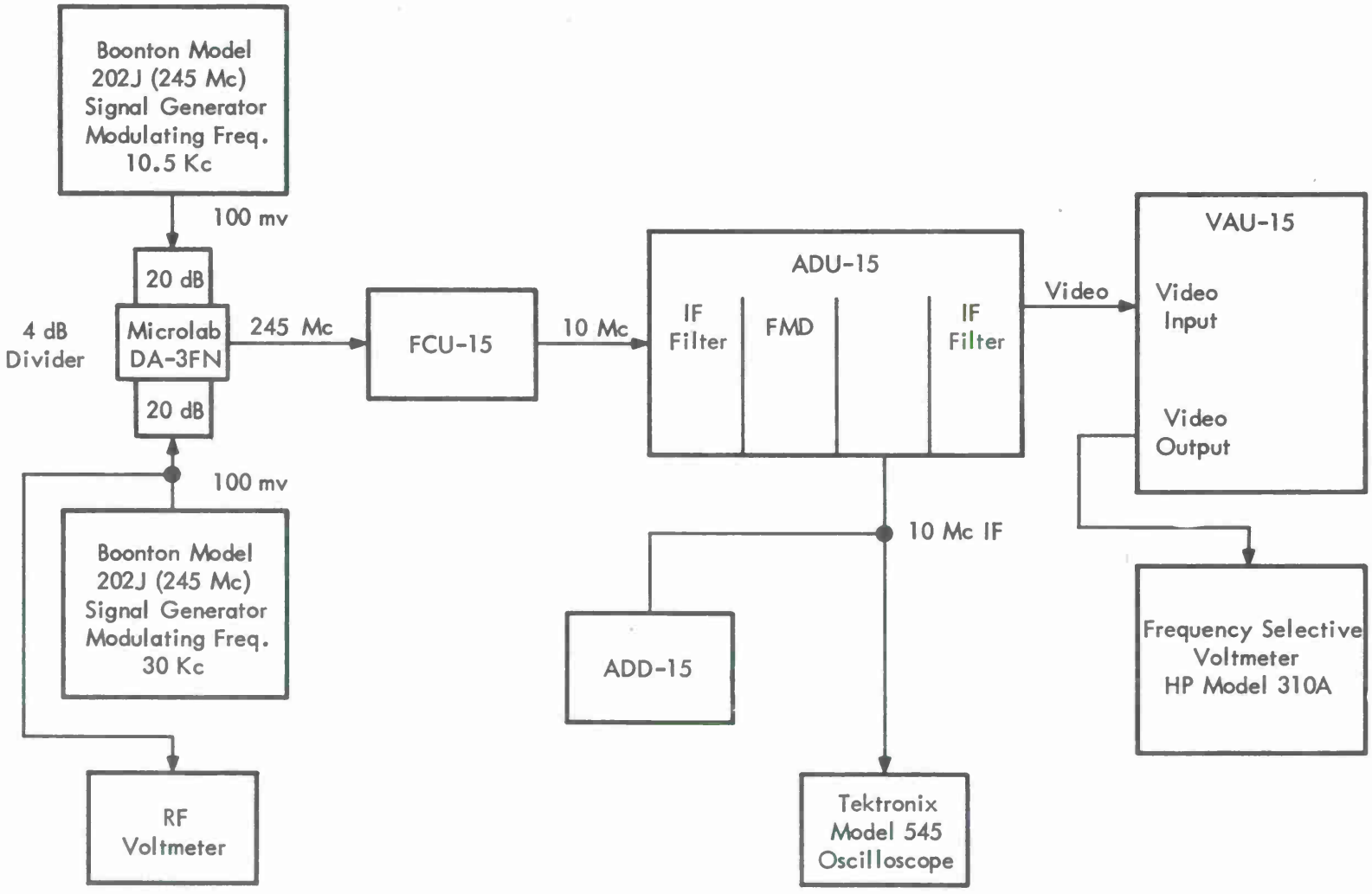

Figure 33. Capture Ratio, Test Setup

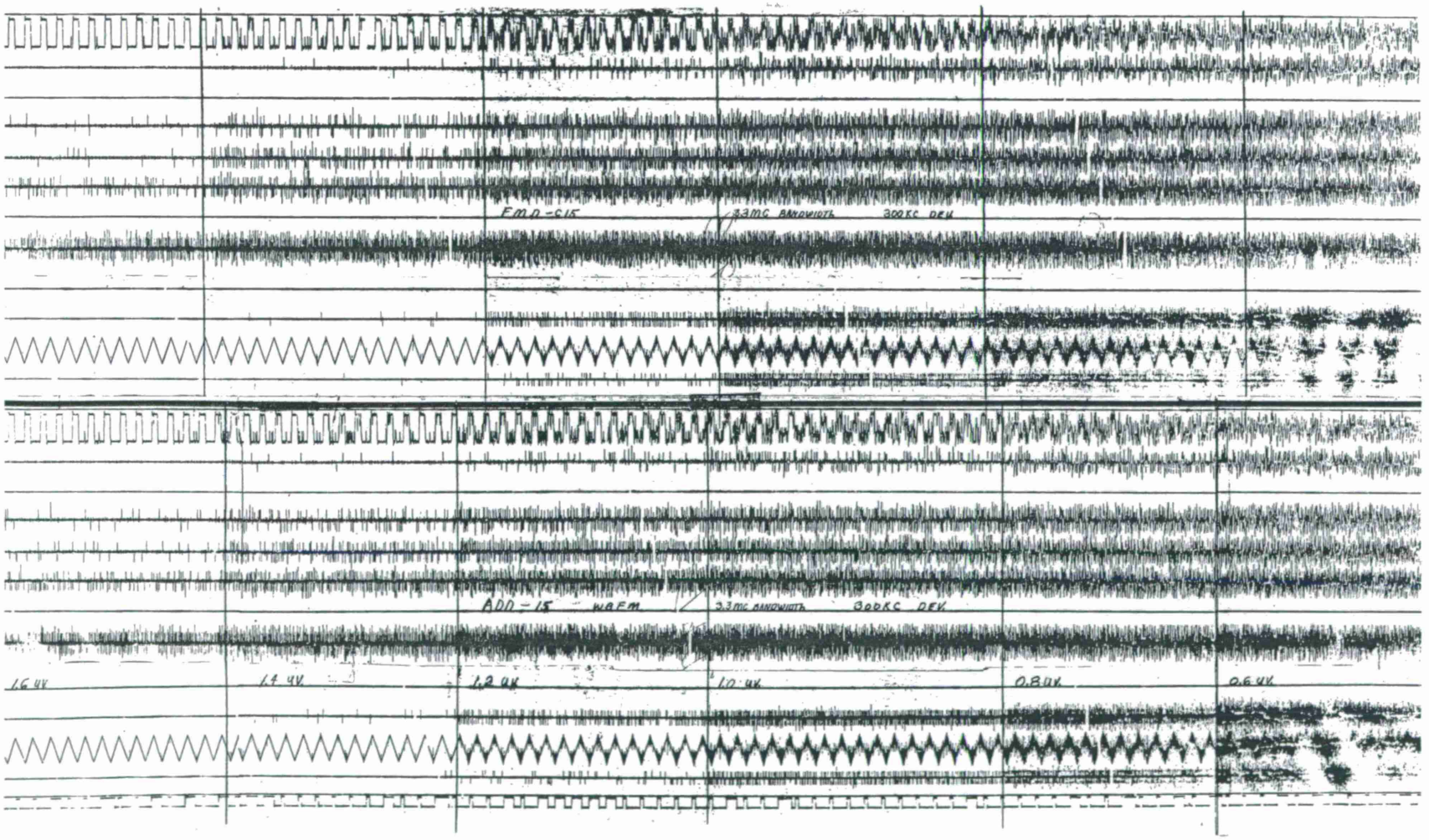
FMO-C15
3.3MC BANDWIDTH
300KC DEV
ADD-15 WBFM
3.3MC BANDWIDTH
300KC DEV
1.6 VK
1.4 VK
1.2 VK
1.0 VK
0.8 VK
0.6 VK

Figure 34

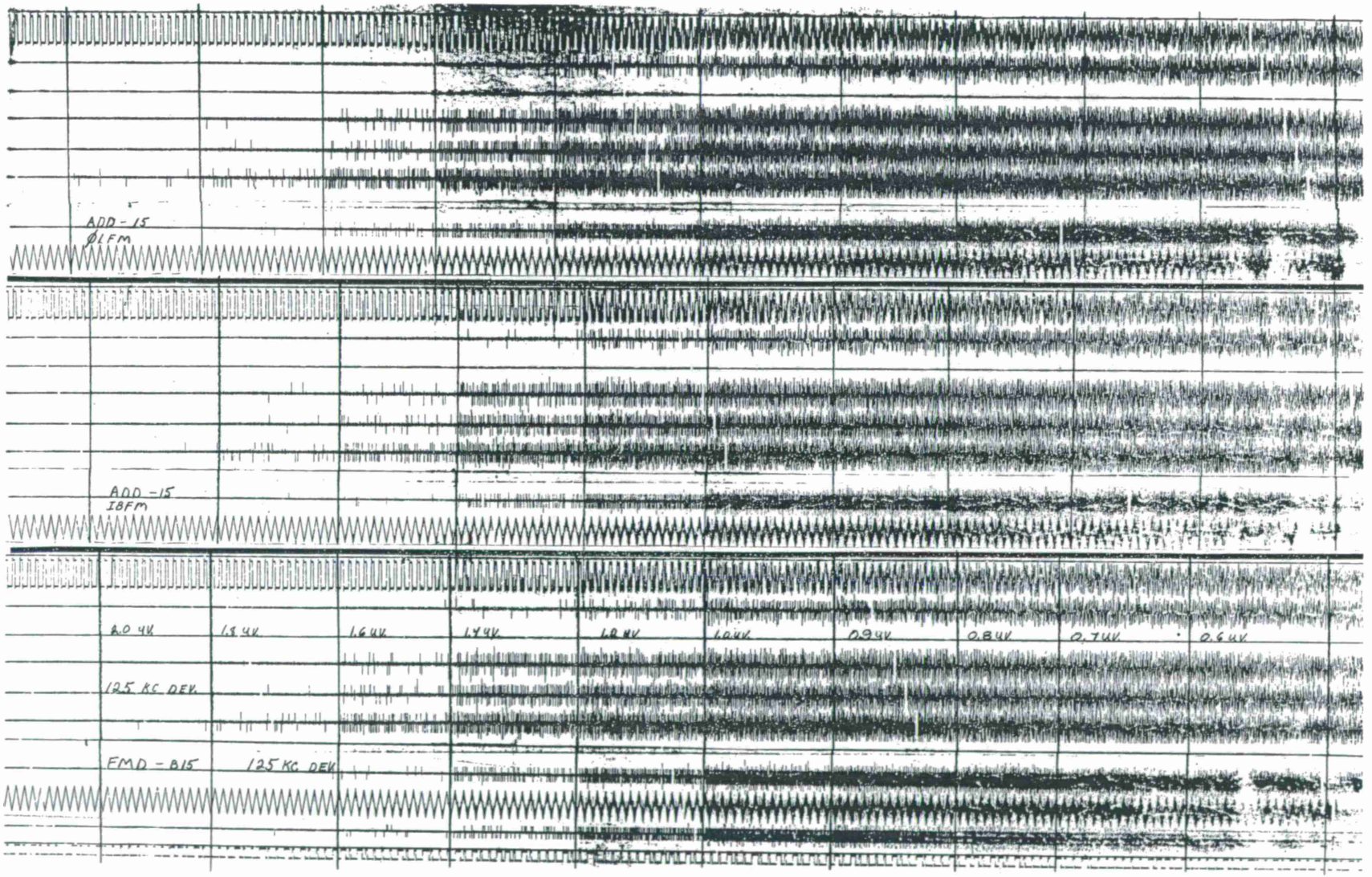
ADD - 15
ØLFM
ADD - 15
IBFM
2.0 μV
1.8 μV
1.6 μV
1.4 μV
1.2 μV
1.0 μV
0.9 μV
0.8 μV
0.7 μV
0.6 μV
125 KC DEV.
FMD - B15
125 KC DEV.

Figure 35

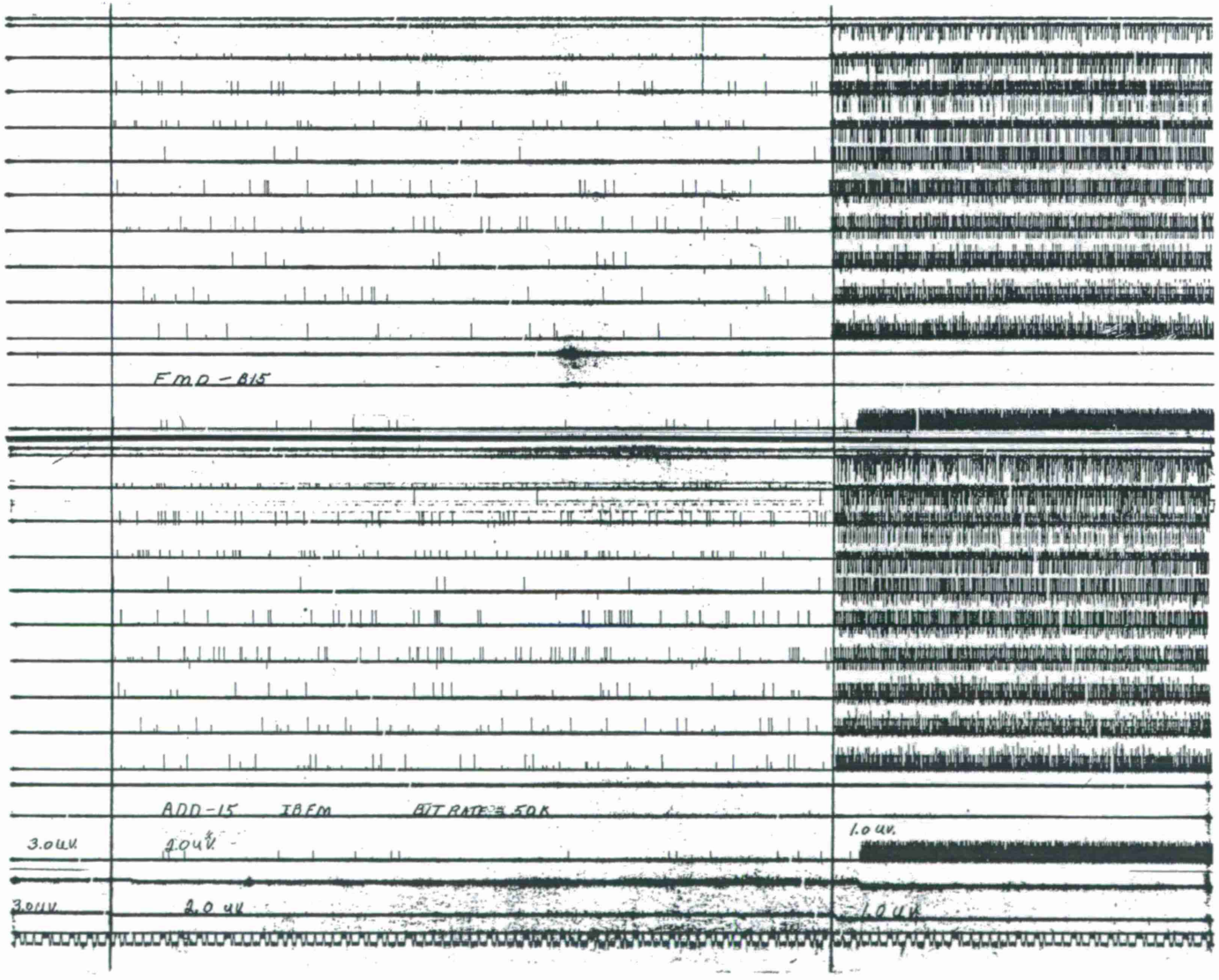

Figure 36

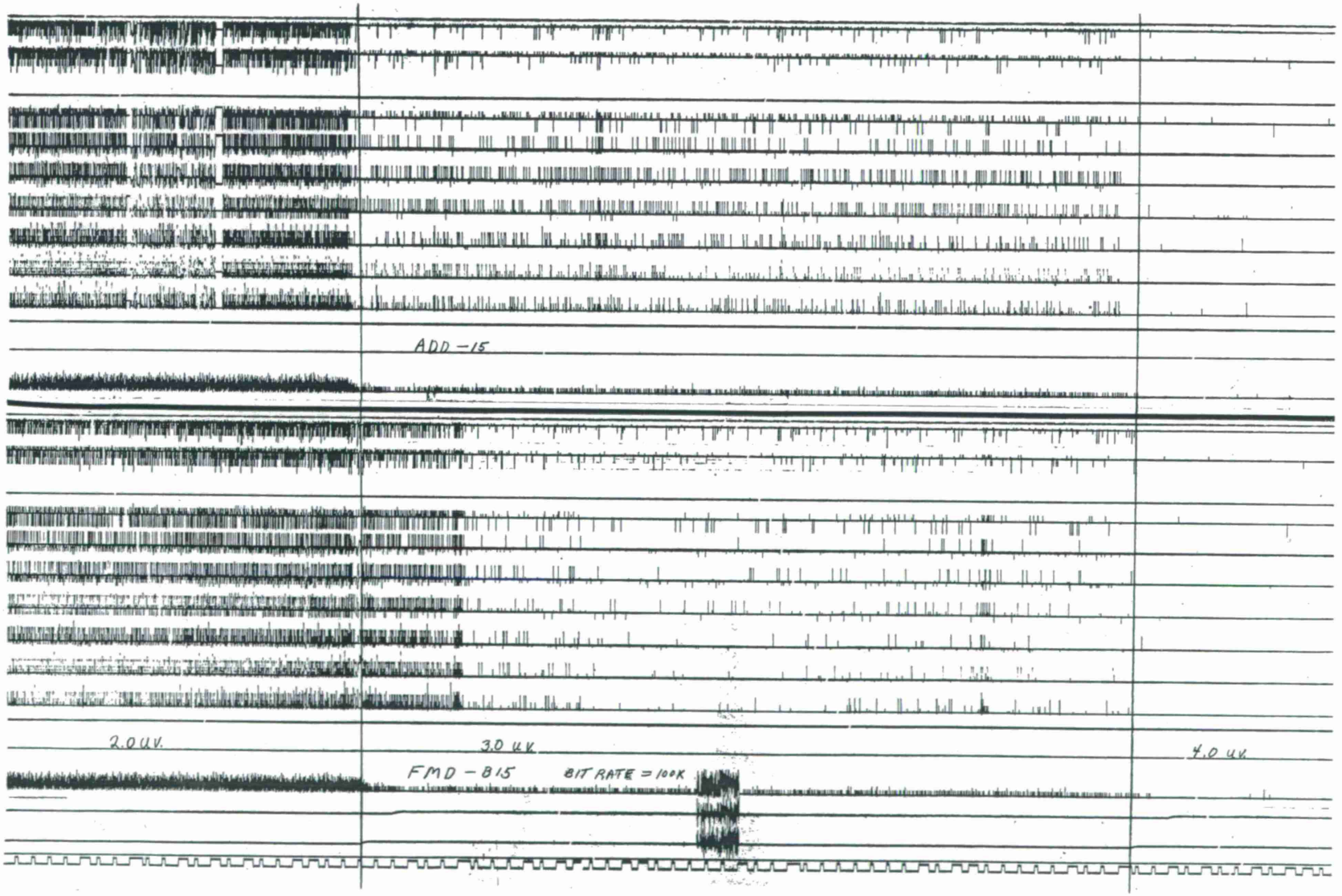

Figure 37

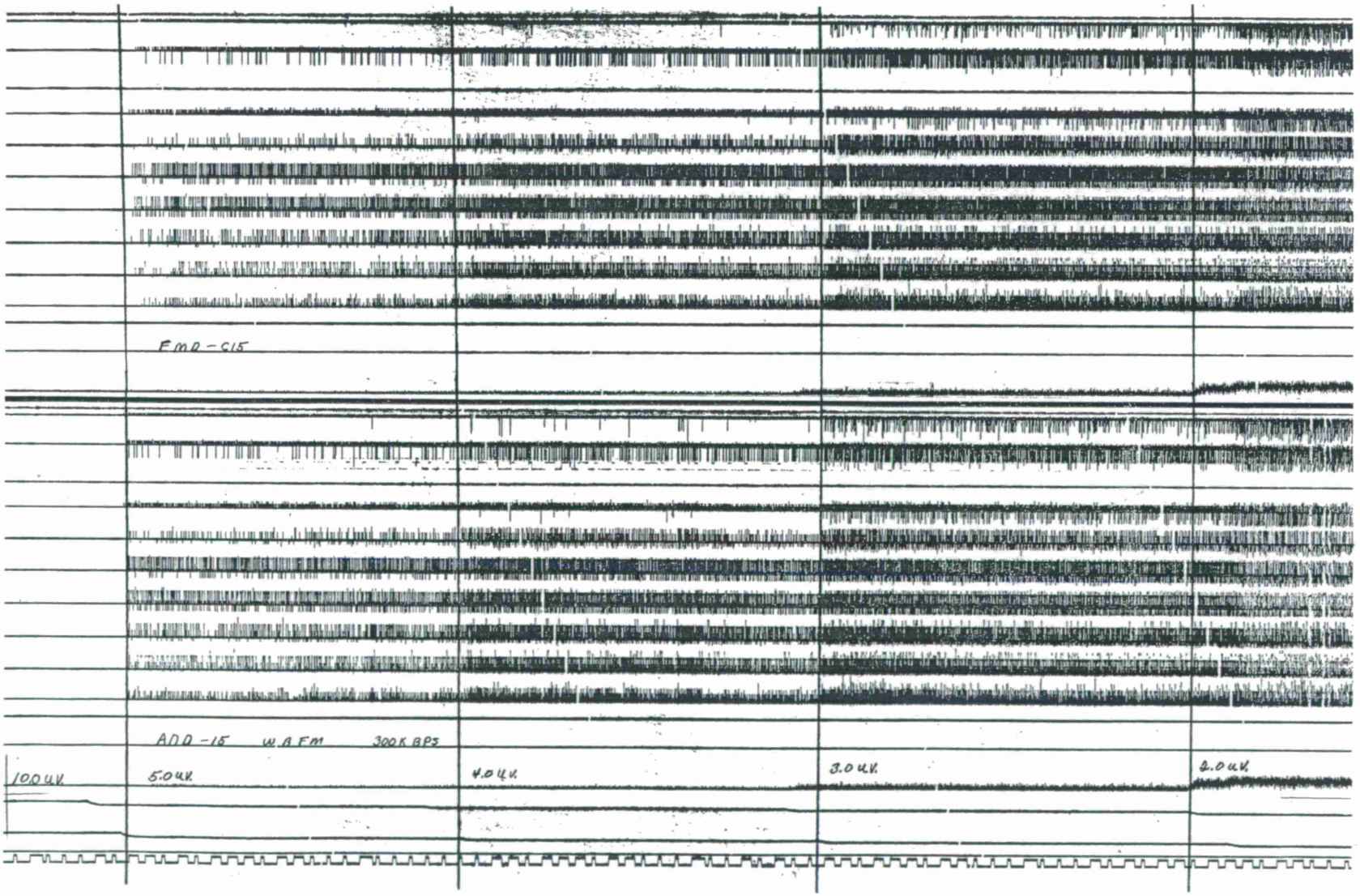

Figure 38

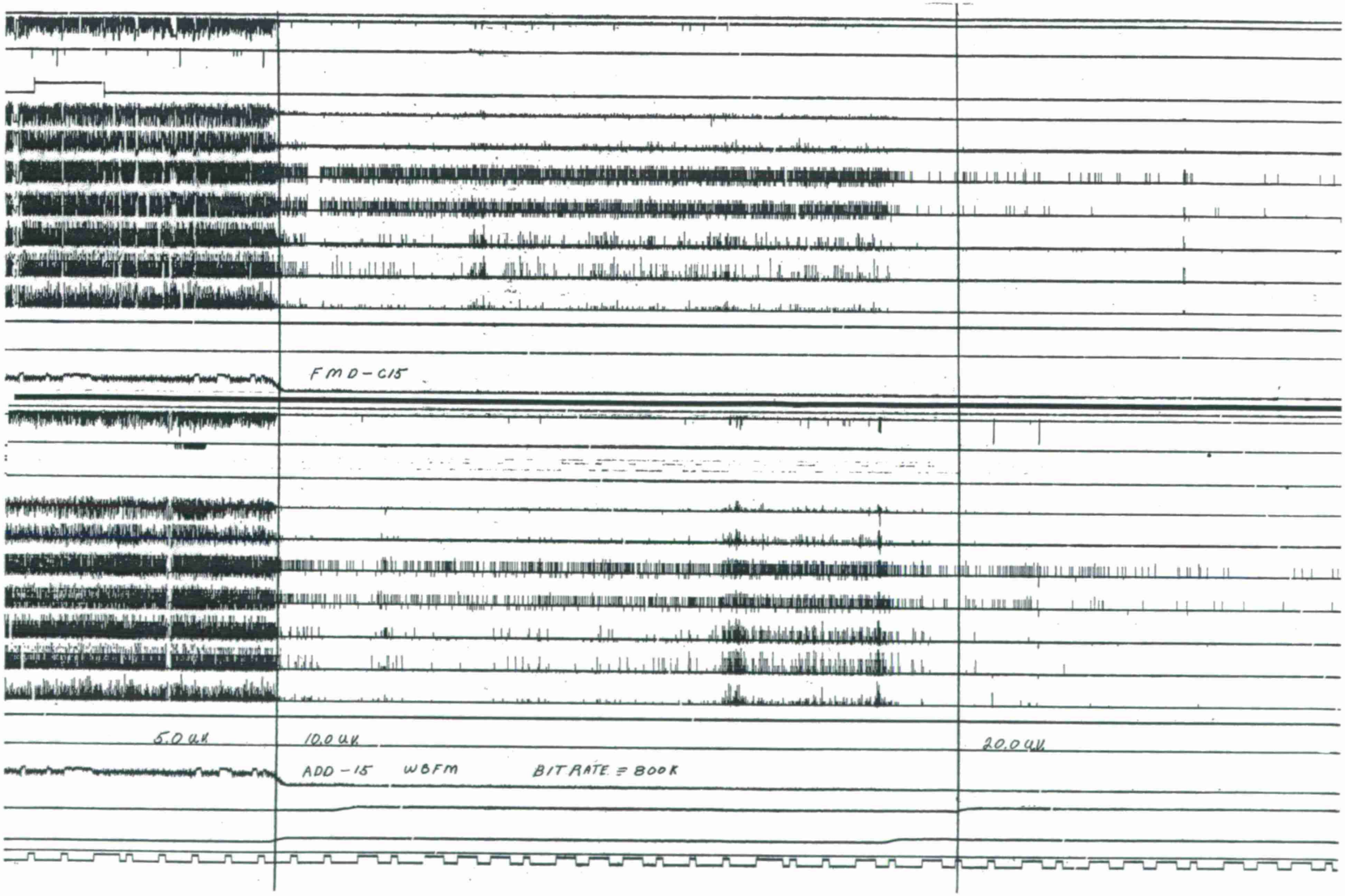

Figure 39

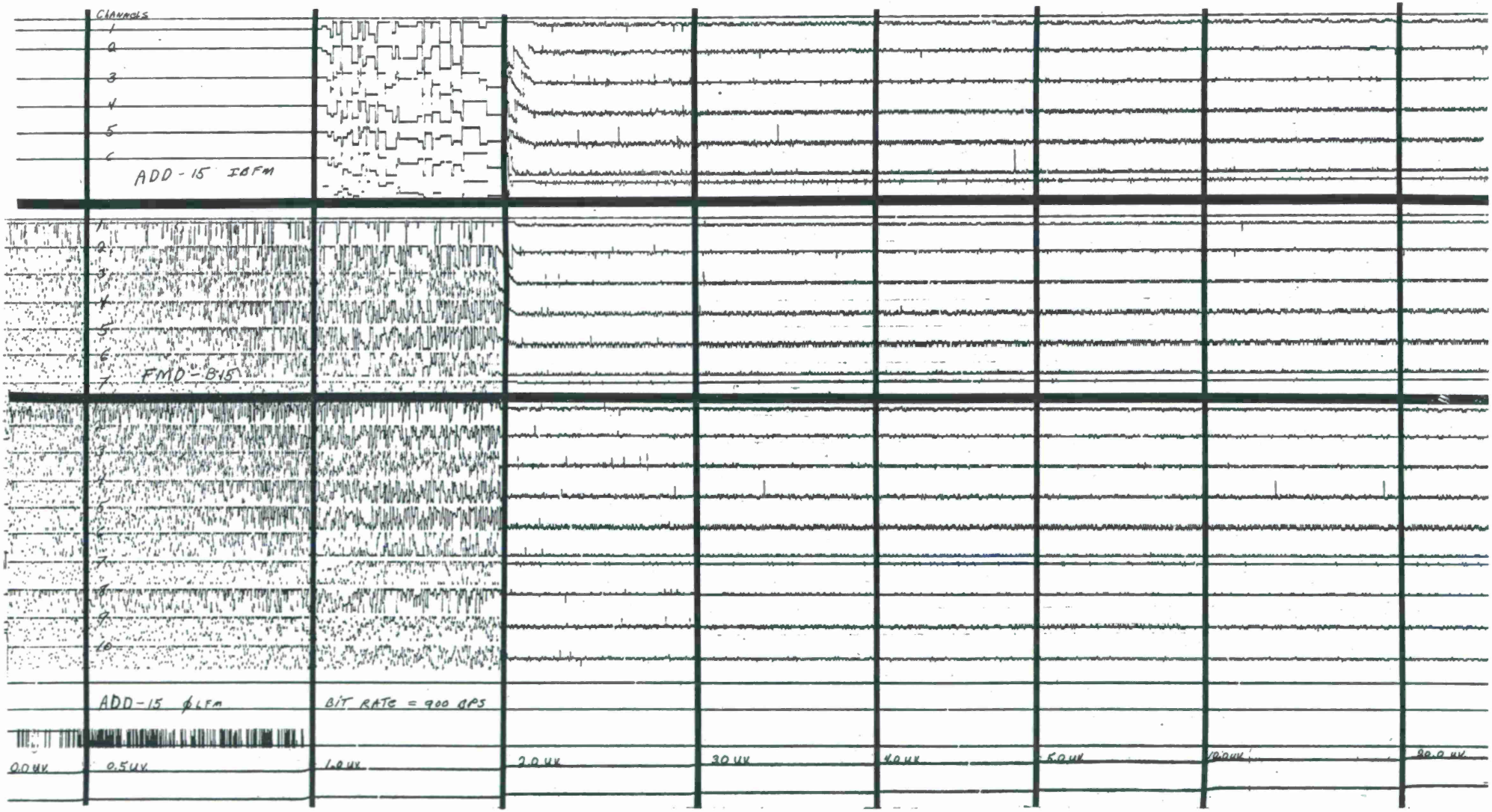
CHANNELS
1
2
3
4
5
6
ADD - 15 IOFM
1
2
3
4
5
6
7
FMD - B45
7
8
9
10
ADD-15 ΦLFM
BIT RATE = 900 BPS
0.0 UV
0.5 UV
1.0 UV
2.0 UV
3.0 UV
4.0 UV
5.0 UV
10.0 UV
20.0 UV

Figure 40

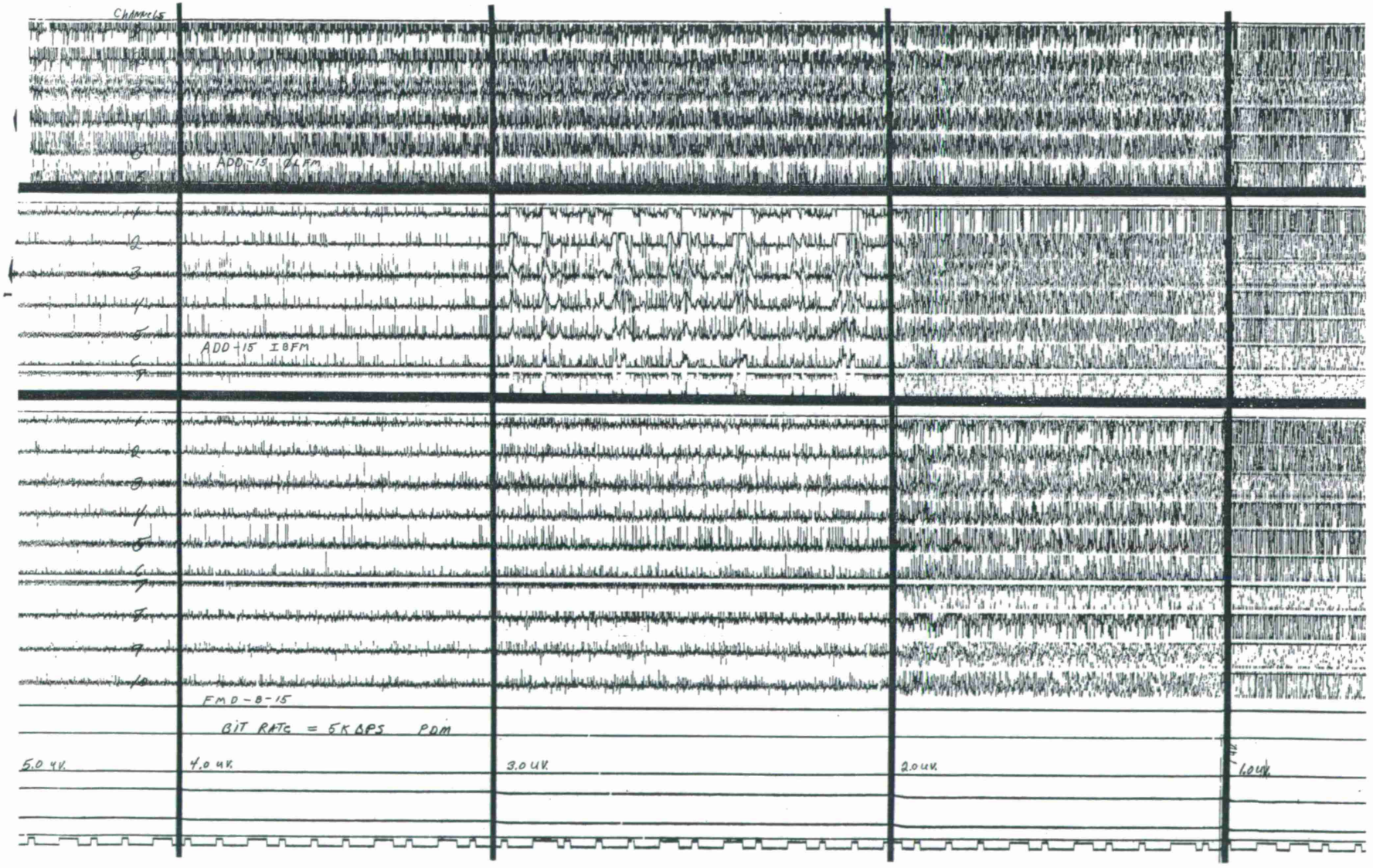
Channels
ADD-15 ØLFM
ADD-15 IBFM
FMD-8-15
BIT RATE = 5K BPS PDM
5.0 UV.
4.0 UV.
3.0 UV.
2.0 UV.
1.0 UV.

Figure 41

TABLE 3. STATIC LINEARITY, FMD-C15

IF Frequency (Mc)	Measured Demodulator Output (Millivolts)	Normalized Frequency (Deviation Reversed Around 10 Mc)	Normalized Demodulator Output Scale Factor +0.163)
10.000	-213	10.000	-34.7
10.250	+127	9.750	+20.6
10.500	+473	9.500	+77
10.750	+821	9.250	+134
11.000	+1162	9.000	+189
11.250	+1476	8.750	+240
11.500	+1748	8.500	+284
11.750	+1952	8.250	+316
12.000	+2080	8.000	+338
12.250	+2141	7.750	+348
12.500	+2147	7.500	+350
12.750	+2118	7.250	+344
13.000	+2054	7.000	+334
10.000	-214	10.000	-34.8
9.750	-550	10.250	-895
9.500	-892	10.500	-145
9.250	-1246	10.750	-203
9.000	-1599	11.000	-260
8.750	-1921	11.250	-312
8.500	-2196	11.500	-357
8.250	-2416	11.750	-393
8.000	-2553	12.000	-416
7.750	-2443	12.250	-398
7.500	-1550	12.500	-252
7.250	-0034	12.750	-5.5
7.000	-221	13.000	-36.0

TABLE 4. STATIC LINEARITY, ADD-15-WBFM

IF Frequency (Mc)	Measured Demodulator Output (Millivolts)	IF Frequency (Mc)	Measured Demodulator Output (Millivolts)
10.00	-189	10.00	-176
10.5	-281	9.5	-080
11.0	-376	9.0	+034
11.5	-494	8.5	+148
12.0	-620	8.0	+271
12.5	-733	7.5	+379
13.0	-836	7.0	+487
13.5	-946	6.5	+594
14.0	-1079	6.0	+711
14.5	-1207	5.5	+828
15.0	-1337	5.0	+944
15.5	-1467	4.5	+1068
16.0	-1570	4.0	+1185
16.5	-1676	3.5	+1299
17.0	-1766	3.0	+1415
17.5	-1841	2.5	+1530
18.0	-1924	2.0	+1650
18.5	-2046	1.5	+1773
19.0	-2133	1.0	+1918
19.5	-2233	.5	+2140
20.0	-2359		
20.5	-2473		
21.0	-2550		

TABLE 5. STATIC LINEARITY, FMD-B15

IF Frequency (Mc)	Measured Demodulator Output (Millivolts)	Normalized Demodulator Output (Scale Factor + 0.141)*	IF Frequency (Mc)	Measured Demodulator Output (Millivolts)	Normalized Demodulator Output (Scale Factor + 0.141)*
10.000	+79	+11.1	10.000	+42	+5.92
10.025	+493	+69.5	9.975	-382	-53.9
10.050	+914	+129	9.950	-802	-113
10.075	+1334	+188	9.925	-1221	-172
10.100	+1756	+247	9.900	-1642	-231
10.125	+2181	+308	9.875	-2067	-292
10.150	+2609	+368	9.850	-2494	-352
10.175	+3036	+428	9.825	-2929	-414
10.200	+3462	+488	9.800	-3355	-473
10.225	+3882	+547	9.775	-3788	-535
10.250	+4295	+605	9.750	-4220	-595
10.275	+4688	+661	9.725	-4652	-656
10.300	+5024	+709	9.700	-5074	-716
10.325	+5113	+721	9.675	-5486	-775
10.350	+5140	+725	9.650	-5877	-829
10.375	+5151	+726	9.625	-6243	-880
10.400	+5156	+727	9.600	-6567	-925
10.425	+5159	+728	9.575	-6849	-967
10.450	+5161	+728	9.550	-7071	-998
10.475	+5160	+728	9.525	-7231	-102
10.500	+5160	+728	9.500	-7318	-103
			9.475	-7337	-103
			9.450	-7289	-103
			9.425	-7180	-101
			9.400	-7020	-990

* Data plotted with frequency deviation reversed around 10 mc, thus reversing slope of curve (see table 1).

TABLE 6. STATIC LINEARITY, ADD-15-IBFM

IF Frequency (Mc)	Measured Demodulator Output (Millivolts)	IF Frequency (Mc)	Measured Demodulator Output (Millivolts)
10.00	-371	10.00	-373
10.05	-484	9.95	-261
10.10	-596	9.90	-152
10.15	-709	9.85	-041
10.20	-822	9.80	+070
10.25	-937	9.75	+185
10.30	-1050	9.70	+314
10.35	-1165	9.65	+444
10.40	-1282	9.60	+573
10.45	-1398	9.55	+702
10.50	-1516	9.50	+837
10.55	-1638	9.45	+972
10.60	-1763	9.40	+1107
10.65	-1891	9.35	+1244
10.70	-2024	9.30	+1381
10.75	-2158	9.25	+1520
10.80	-2317	9.20	+1656
10.85	-2525	9.15	+1793
10.90		9.10	+1930
		9.05	+2065
		9.00	+2173
		8.95	+2269

TABLE 7. STATIC LINEARITY, ADD-15 ØLFM

IF Frequency (Mc)	Measured Demodulator Output (Millivolts)	Normalized Demodulator Output (Translation = +0.375)
10.00	-124	+251
10.05	-219	+156
10.10	-315	+60
10.15	-407	-32
10.20	-504	-129
10.25	-604	-229
10.30	-706	-331
10.35	-812	-437
10.40	-923	-548
10.45	-1038	-663
10.50	-1158	-783
10	-127	+248
9.95	-033	+342
9.90	+058	+433
9.85	+147	+522
9.80	+235	+610
9.75	+329	+704
9.70	+424	+799
9.65	+517	+892
9.60	+607	+982
9.55	+694	+1069
9.50	+778	+1153

TABLE 8. SIGNAL-TO-NOISE RATIO VS RF INPUT LEVEL, FMD-C15

RF Input (Microvolts)	Video (dB)	Noise (dB)	SNR (dB)
0	-26.5	+ 7.8	-34.3
0.2	-26.5	+ 7.7	-34.2
0.5	-25.5	+ 7.6	-33.1
1.0	-19.0	+ 7.1	-36.1
2.0	- 8.9	+ 5.2	-14.1
3.0	- 4.1	+ 2.4	- 6.5
4.0	2	- 1.0	- 1
5.0	- 1	- 3.7	+ 2.7
6.0	-0.5	- 6.1	+ 5.6
7.0	-0.3	- 7.4	+ 7.1
8.0	-0.25	- 8.2	+ 8
9.0	-0.2	- 9.1	+ 8.9
10	-0.1	- 9.9	+ 9.8
12	0	-11.0	+11.0
14	0	-12.1	+12.1
16	0	-13.1	+13.1
18	0	-13.8	+13.8
20	0	-14.6	+14.6
25	0	-16.2	+16.2
30	0	-17.5	+17.5
40	0	-19.7	+19.7
50	0	-21.1	+21.1
60	0	-22.5	+22.5
70	0	-23.4	+23.4
80	0	-24.5	+24.5
90	0	-25.4	+25.4
100	0	-26.1	+26.1
200	0	-30.5	+30.5
300	0	-33.0	+33.0
400	0	-34.8	+34.8
500	0	-36.1	+36.1
1K	0	-40.2	+40.2
5K	0	-48.2	+48.2
10K	0	-50	+50
100K	0	-53.0	+53.0

Test Conditions:

3.3 Mc IF Bandwidth.
750 Kc Video Bandwidth.
±300 Kc Deviation.
10.5 Kc Modulation Frequency.
Noise Figure 9 dB.

TABLE 9. SIGNAL-TO-NOISE RATIO VS RF INPUT LEVEL, ADD-15, WBFM

RF Input (Microvolts)	Video (dB)	Noise (dB)	SNR (dB)	Corrected SNR (Added 2.8 dB)
0	-25.6	+10.6	-36.2	-33.4
.2	-25.6	+10.6	-36.2	-33.4
.5	-25.4	+10.4	-35.8	-33.0
1.0	-19.2	+10.0	-29.2	-26.4
2.0	- 9.2	+ 8.4	-17.6	-14.8
3.0	- 4.7	+ 6.25	-10.95	- 8.15
4.0	- 2.3	+ 3.7	- 6.0	- 3.2
5.0	- 1.1	+ 0.8	- 1.9	+ 0.9
6.0	- .6	- 1.5	+ 0.9	+ 3.7
7.0	- .1	- 3.5	+ 3.4	+ 6.2
8.0	0	- 5.1	+ 5.1	+ 7.9
9.0	0	- 6.4	+ 6.4	+ 9.2
10	0	- 7.1	+ 7.1	+ 9.9
12	0	- 8.6	+ 8.6	+11.4
14	0	- 9.9	+ 9.9	+12.7
16	0	-10.6	+10.6	+13.4
18	0	-11.6	+11.6	+14.4
20	0	-12.5	+12.5	+15.3
25	0	-14.2	+14.2	+17.0
30	0	-15.4	+15.4	+18.2
40	0	-17.3	+17.3	+20.1
50	0	-18.8	+18.8	+21.6
60	0	-20	+20.0	+22.8
70	0	-20.9	+20.9	+23.7
80	0	-21.7	+21.7	+24.5
90	0	-22.5	+22.5	+25.3
100	0	-23.25	+23.25	+26.05
200	0	-27.6	+27.6	+30.40
300	0	-30.1	+30.1	+32.9
400	0	-31.8	+31.8	+34.6
500	0	-33.1	+33.1	+35.9
1K	0	-36.6	+36.6	+39.4
5K	0	-40.7	+40.7	+43.5
10K	0	-41.3	+41.3	+44.1
100K	0	-41.7	+41.7	+44.5

Test Conditions:

3.3 Mc IF Bandwidth.
750 Kc Video Bandwidth.
±300 Kc Deviation.
10.5 Kc Modulation Frequency.
Noise Figure 9 dB.

TABLE 10. SIGNAL-TO-NOISE RATIO VS RF INPUT LEVEL, FMD-B15

RF Input (Microvolts)	Video (dB)	Noise (dB)	SNR (dB)
0	-28	- .25	-27.75
.2	-25	- .5	-24.5
.3	-20.7	- .7	- 2.0
.4	-17.0	- .1	-16
.5	-13.2	- 1.5	-11.7
.6	-10.8	- 2	- 8.8
.7	- 8.8	- 2.6	- 6.2
.8	- 7.2	- 3.3	- 3.9
.9	- 5.8	- 4.2	- 1.6
1.0	- 4.5	- 4.8	+ 0.3
1.2	- 2.9	- 6.6	+ 3.7
1.4	- 1.9	- 8.4	+ 0.5
1.6	- 1.2	-10.0	+ 8.8
1.8	- .8	-11.5	+10.7
2.0	- .5	-13.0	+12.5
2.5	- .2	-15.3	+15.1
3.0	- .1	-17.0	+16.9
3.5	0	-18.2	+17.2
4.0	0	-19.2	+19.2
4.5	0	-20.2	+20.2
5.0	0	-20.8	+20.8
6.0	0	-22.3	+22.3
7.0	0	-23.5	+23.5
8.0	0	-24.5	+24.5
9.0	0	-25.4	+25.4
10.0	0	-26.3	+26.3
15.0	0	-29.0	+29.0
20.0	0	-30.8	+30.8
30.0	0	-33.7	+33.7
40	0	-35.4	+35.4
50	0	-36.7	+36.7
100	0	-40	+40.0
500	0	-43.8	+43.8
1000	0	-44.3	+44.3
10K	0	-44.5	+44.5
100K	0	-44.5	+44.5

Test Conditions:

500 Kc IF Bandwidth.
100 Kc Video Bandwidth.
±125 Kc Deviation.
10.5 Kc Modulation Frequency.
Noise Figure 9 dB.

TABLE 11. SIGNAL-TO-NOISE RATIO VS RF INPUT LEVEL, ADD-15, IBFM

RF Input (Microvolts)	Video (dB)	Noise (dB)	SNR (dB)
0	-26	+ 1.2	-27.2
.2	-24.4	+ .8	-25.2
.3	-20.6	+ .7	-21.3
.4	-16.7	+ .3	-17.0
.5	-13.1	+ .1	-13.0
.6	-10.7	- .7	-10.0
.7	- 8.8	- 1.3	- 7.5
.8	- 6.8	- 1.9	- 4.9
.9	- 5.3	- 2.7	- 2.6
1.0	- 4.1	- 3.7	- 0.4
1.2	- 2.4	- 5.2	+ 2.8
1.4	- 1.5	- 7.2	+ 5.7
1.6	- .8	- 9.1	+ 8.2
1.8	- .4	-10.9	+10.4
2	- .2	-12.7	+12.5
2.5	0	-15.6	+15.6
3	0	-17.4	+17.4
3.5	0	-19	+19
4	0	-19.8	+19.8
4.5	0	-20.8	+20.8
5	0	-21.7	+21.7
6	0	-23.2	+23.2
7	0	-24.6	+24.6
8	0	-25.6	+25.6
9	0	-26.6	+26.6
10	0	-27.5	+27.5
15	0	-30.4	+30.4
20	0	-32.5	+32.5
30	0	-35.3	+35.3
40	0	-37.2	+37.2
50	0	-38.4	+38.4
100	0	-41.7	+41.7
500	0	-44.6	+44.6
1K	0	-44.9	+44.9
10K	0	-50.1	+50.1
100K	0	-44.7	+44.7

Test Conditions:

500 Kc IF Bandwidth.
100 Kc IF Bandwidth.
±125 Kc Deviation.
10.5 Kc Modulation Frequency.
Noise Figure 9 dB.

TABLE 12. SIGNAL-TO-NOISE RATIO VS RF INPUT LEVEL, ADD-15, ØLFM

RF Input (Microvolts)	Video (dB)	Noise (dB)	SNR (dB)
0	-23.8	+ .8	-24.6
.2	-23.0	+ .7	-23.7
.3	-20.7	+ .6	-21.3
.4	-17.3	+ .3	-17.6
.5	-14.2	+ .1	-14.1
.6	-11.5	- .6	-10.9
.7	- 9.3	- 1.2	- 8.1
.8	- 7.5	- 1.9	- 5.6
.9	- 5.8	- 2.7	- 3.1
1.0	- 4.3	- 3.8	- 0.5
1.2	- 2.5	- 5.9	+ 3.4
1.4	- 1.4	- 8.2	+ 6.8
1.6	- .8	-10.8	+10
1.8	- .3	-13.3	+13
2	- .2	-15.5	+15.3
2.5	0	-19.4	+19.4
3	0	-21.3	+21.3
3.5	0	-22.7	+22.7
4	0	-23.8	+23.8
4.5	0	-24.8	+24.8
5	0	-25.6	+25.6
6	0	-27.2	+27.2
7	0	-28.3	+28.3
8	0	-29.4	+29.4
9	0	-30.4	+30.4
10	0	-31.2	+31.2
15	0	-34.2	+34.2
20	0	-36.3	+36.3
30	0	-38.7	+38.7
40	0	-40.5	+40.5
50	0	-41.7	+41.7
100	0	-44.5	+44.5
500	0	-46.5	+46.5
1K	0	-46	+46
10K	0	-46	+46
100K	0	-45.5	+45.5

Test Conditions:

500 Kc IF Bandwidth.
100 Kc Video Bandwidth.
±125 Kc Deviation.
10.5 Kc Modulation Frequency.
Noise Figure 9 dB.

TABLE 13. PCM TEST-WIDEBAND DEMODULATORS

RF Input Level (uv)	Bit Errors per 3 Million Bits ADD-15-WBFM Run 1	FMD-C15 Run 1	ADD-15-WBFM Run 2*	FMD-C15 Run 2*
40	1	4	1	34
20	187	282	203	735
15	902	1,092	1,225	2,578
12.5	1,933	2,422	2,337	4,944
10.0	6,465	7,288	6,997	12,553
9.0	10,239	11,554	11,325	17,467
8.0	18,230	16,760	18,664	26,631
7.0	32,824	28,854	35,292	43,212
6.5	46,915	36,681	48,221	59,034
6.0	67,249	47,792	66,860	74,190
5.5	94,778	86,471	100,666	105,459
5.0	148,602	102,120	153,554	153,951
4.5	216,904	153,646	223,026	216,451
4.0	315,424	256,616	318,077	316,959
3.5	480,024	383,466	476,267	473,736
3.0	688,172	599,254	682,439	709,997

* Run 2 made with receiver detuned approximately 100 kc.

Test Conditions:

3.3 Mc IF Bandwidth.
750 Kc Video Bandwidth.
±300 Kc Deviation.
750 Kilobits per Second.

TABLE 14. PCM TEST-INTERMEDIATE BAND DEMODULATORS

RF Input Level (uv)	Bit Errors per 1 Million Bits ADD-15-IBFM Run 1	FMD-B15 Run 1	ADD-15-ØLFM Run 1	FMD-B15 Run 2*	ADD-15-ØLFM Run 2*
4	0	0	0	-	0
3	16	22	5	11	7
2.5	218	411	84	238	70
2.0	2, 741	3, 940	1, 174	2, 226	1, 041
1.8	6, 648	9, 464	2, 994	5, 685	3, 329
1.6	15, 048	21, 352	7, 344	12, 572	8, 289
1.4	34, 745	39, 203	19, 824	27, 655	19, 180
1.2	66, 133	78, 105	46, 052	56, 283	43, 958
1.0	126, 970	142, 895	88, 056	100, 593	91, 130
.9	169, 112	196, 332	119, 771	136, 777	117, 410
.8	223, 603	241, 264	169, 079	188, 716	161, 171
.7	271, 403	284, 216	224, 433	241, 922	205, 671
.6	314, 502	325, 289	280, 614	326, 398	270, 577
.5	362, 722	372, 374	338, 841	373, 767	340, 072
3.5	0	1	0	-	0
2.75	63	168	12	63	18
2.25	856	1, 641	330	759	446
Threshold RF For 1-5 errors	3.3 uv 3 bit errors	3.4 uv 3 bit errors	3.0 uv 1 bit errors	3.3 uv 4 bit errors	3.0 uv 3 bit errors

Test Conditions:

300 Kc IF Bandwidth.
100 Kc Video Bandwidth*.
±50 Kc Deviation.
100 Kilobits per Second.

* 50 Kc Video Bandwidth.

TABLE 15. PCM PLAYBACK SIMULATIONS

Run 1 Figure 36. FMD-B15 and ADD-15-IBFM:

Bit Rate	50K bps
IF Bandwidth	100 kc
Tape Speed	15 ips
Record Carrier	112.5 kc
Deviation	±25 kc
Video Bandwidth	50 kc

Run 2 Figure 37. FMD-B15 and ADD-15-IBFM:

Bit Rate	100K bps
IF Bandwidth	300 kc
Tape Speed	30 ips
Record Carrier	225 kc
Deviation	±50 kc
Video Bandwidth	100 kc

Run 3 Figure 38. FMD-C15 and ADD-15-WBFM:

Bit Rate	300K bps
IF Bandwidth	500 kc
Tape Speed	60 ips
Record Carrier	450 kc
Deviation	±150 kc
Video Bandwidth	250 kc

Run 4 Figure 39. FMD-C15 and ADD-15-WBFM:

Bit Rate	800K bps
IF Bandwidth	3.3 mc
Tape Speed	120 ips
Record Carrier	900 kc
Deviation	±300 kc
Video Bandwidth	750 kc

TABLE 16. PDM PLAYBACK SIMULATION

Run 1 Figure 40. FMD-B15, ADD-15-IBFM, and ADD-15-ØLFM:

Bit Rate	900 bps
IF Bandwidth	100 kc
Tape Speed	15 ips
Record Carrier	112.5 kc
Deviation	±45 kc
Video Bandwidth	100 kc

Run 2 Figure 41. FMD-B15, ADD-15-IBFM, and ADD-15-ØLFM:

Bit Rate	5K bps
IF Bandwidth	500 kc
Tape Speed	60 ips
Record Carrier	450 kc
Deviation	±250 kc
Video Bandwidth	100 kc

APPENDIX II

ORIGINALLY PROPOSED TEST PROGRAM

Reference Contract AF 19(628)5667

The following is an outline of a test program to evaluate the performance of the advanced digital demodulator designed under Contract AF 19(628)5667.

The tests are divided into three series. The first group of tests consist of laboratory measurements of the more basic demodulator parameters of both the new digital demodulator and the original FMD series demodulator, included as part of the TMR-15 Telemetry Receiving System. A direct performance comparison between the two demodulators will be made for each test.

The second series of tests consists of a simultaneous comparison of two TMR-15 receiving systems under conditions of complex modulating signals. One receiving system will include the new digital demodulator, the other will utilize the standard FMD series demodulator. Modulation formats will be obtained from laboratory simulators and will include FM/FM, PAM, PDM and PCM. Various precisely controlled modulation signals and RF signal levels will be applied to the system to evaluate performance under a wide range of operating conditions. All functional modes of the new demodulator will be compared with the most closely corresponding FMD demodulator, with equal IF bandwidth being used.

The final series of tests will consist of a simultaneous comparison of the two receiving systems as above, but in this case, under simulated "real-time" reception conditions. The test signals will be obtained from predetection magnetic tape recordings taken during actual space-craft shot. Tapes will be selected which demonstrate marginal signal conditions in all the various modulation formats indicated above. In particular, the tapes should contain typical signal degradation due to multipath conditions, including both the effects of small carrier delay (multipath fading) and large carrier delay (data delay distortion). Of special interest will be the effect of the greatly improved capture ratio of the new demodulator on suppressing the delayed reflected carriers, and the resulting reduction in data degradation. The advanced digital demodulator is referred to as ADD-WB, IB, PL corresponding to the wide bandwidth, intermediate bandwidth and phase lock mode respectively. Standard TMR-15 module designations are also referenced.

Test Series I

Demodulator Tests and Comparison

	Tests	Data	Test Equipment (Refer to Equipment List)
1	Static (DC) Linearity	Linearity (% of straight line) ADD-WB ADD-IB ADD-PL FMD-C15 FMD-B15	(1) (26) (2) (3)
2	Swept Linearity and Demodulator peak-to-peak bandwidth	Bandwidth (KC P-P) ADD-WB ADD-IB ADD-PL FMD-C15 FMD-B15	(4) (26) (5) (6)

continued

	Tests	Data	Test Equipment
			(Refer to Equipment List)
3	Video Frequency and Pulse Response	Video Bandwidth - low (3 dB) - high (3 dB), pulse rise time - decay time Square wave tilt (± % of peak) ADD-WB ADD-IB ADD-PL FMD-C15 FMD-B15 VAU - 15 BW = "DIRECT"	(6) (26) (7) (8) (2) (4)
4	Total Harmonic Distortion	% at 1 kc; % at 1/10 IF BW Peak deviation 1/5 IF BW or 300 kc maximum ADD-WB IFA-P15 ADD-IB IFA-G15 ADD-PL IFA-G15 FMD-C15 IFA-P15 FMD-B15 IFA-G15	(7) (26)
5	AM Rejection	50% AM ref peak deviation 1/5 IF BW at 1 kc, 10 kc, and 100 kc ADD-IB IFA-G15 FMD-B15 IFA-G15	(2) (26) (9) (7) (4)
6	Signal-to-Noise Ratio and Threshold	RF input level for $\frac{S+N}{N}$ = 30 dB $\frac{S+N}{N}$ = 10 dB at 1 kc, Video BW = 1/2 IF BW ADD-WB IFA-P15 ADD-IB IFA-E15 ADD-IB IFA-G15 ADD-IB IFA-J15 ADD-PL IFA-G15 FMD-C15 IFA-P15 FMD-B15 IFA-E15 FMD-B15 IFA-G15 FMD-B15 IFA-J15	(7) (26)
7	Capture Ratio	30 dB suppression of undesired modulation fd = 10.5 kc fu = 30 kc ADD-WB IFA-P15 ADD-IB IFA-G15 FMD-C15 IFA-P15 FMD-B15 IFA-G15	(4) (26) (10) (6) (27)

Test Series II

Complex Modulation Simulation and System Comparison

	Tests	Test Equipment (Refer to Equipment List)	Data
1	FM/FM Simulation	(5) (12) (26) (4) (13) (14) (27)	System set-up with standard IRIG video and IF BW corresponding to modulation format.
2	PAM/PDM Simulation	(15) (4) (16) (14) (26) (27)	System comparison made by simultaneous chart recording of decommutated data. Measurements made under both strong signal and threshold condition. All applicable functional modes of ADD demodulator will be compared with the most closely corresponding FMD demodulator.
3	PCM Simulation	(17) (4) (18) (19) (26) (14)	

Test Series III

Real-Time Simulation and System Comparison

	Tests	Test Equipment (Refer to Equipment List)	Data
1	FM/FM Tape	(20) (22) (23) (13) (21) (14) (26)	System set-up with standard IRIG video and IF BW corresponding to modulation format.
2	PAM and/or PDM Tape	(26) (14) (20) (21) (22) (16) (24)	Predetection tape playback through receivers utilizing predetection up converters.
3	PCM Tape	(20) (21) (22) (14) (26) (18) (25)	All applicable functional modes of ADD demodulator will be compared with most closely corresponding FMD demodulator.

TEST EQUIPMENT

REFERENCE CONTRACT AF 19(628)5667

The following is a summary list of standard test instruments and special equipment required to perform all proposed tests and comparisons on the digital FM demodulator. Available test instruments with equivalent pertinent specifications can be substituted for indicated models. Numeric designations correspond to references in test program.

1. Digital DC Voltmeter	HP 3439A w/3441A Plug-In
2. RF - IF/AM Generator	HP 606A
3. Frequency Counter	HP 5245L
4. Two each RF/FM Generators	Boonton 202J
5. Function Generator	HP 202
6. Oscilloscope	Tektronix 651A w/1A2 Plug-In
7. Audio Generator	HP 200CD
8. Pulse Generator	HP 211A
9. RMS AC Voltmeter	HP 2300A
10. Selective Voltmeter	HP 310A
11. Distortion Analyzer	HP 331A
12. Data Insertion Converter	DEI DIC-1
13. Two each Bandswitching Subcarrier Discriminator	Airpax FDS-25
14. Chart Recorder	Brush MK-200
15. PAM/PDM Simulator	
16. Two each PAM/PDM Decommutator	
17. PCM Simulator	
18. Two each PCM Bit Synchronizer and Conditioner	
19. Bit Error Monitor	DEI BA-101 or BA-102
20. Magnetic Tape Recorder	
21. Video Distribution Amplifier	DEI VDA-1
22. Two each Predetection Playback Units	DEI PRU-2 w/PM-20 Plug-In
23. FM/FM Test Tape	
24. PAM/PPM Test Tape	
25. PCM Test Tape	

NOTE

Predetection Test Tapes recorded under real-time operational conditions such as data distortion, weak signals, multipath fading and phase shift, spacecraft tumbling, etc..

26. Two each DEI TMR-15 Telemetry Receivers, each including the following subunits:
    - 26.1 Frequency Converter Unit, FCU-15 with RTH-B15 Tuning Unit, 216 to 260 mc.
    - 26.2 IF Amplifier/Demodulator Unit with the following plug-in units:
        - 26.2.1 FMD-B15 FM Demodulator
        - 26.2.2 FMD-C15 FM Demodulator
        - 26.2.3 IFA-E15 IF Amplifier, 100 KC BW
        - 26.2.4 IFA-G15 IF Amplifier, 300 KC BW
        - 26.2.5 IFA-J15 IF Amplifier, 750 KC BW
        - 26.2.6 IFA-P15 IF Amplifier, 3300 KC BW*
27. RF Power Divider — Microlab DA-3FN
28. Ten Coaxial cables, 50 ohm impedance, BNC connectors, approximately 5 feet long.

* Only one unit required.

APPENDIX III

ELECTRICAL PARTS LIST

ITEM	PART NUMBER	VENDOR	NOMENCLATURE/DESCRIPTION	REF. DES.	QTY. PER ASSEMBLY -1	-2	-3	-4	-5	-6
	CK63/103Z	ERIE	CAPACITOR, CERAMIC, DISC, .01uf ±100-20%	C1						
	DDM-502	CENTRALAB	" " " .005uf 150VDC	C2						
	DDM-502	"	" " " .005uf "	C3						
	DDM-502	"	" " " .005uf "	C4						
	DDM-502	"	" " " .005uf "	C5						
	DDM-502	"	" " " .005uf "	C6						
	DDM-502	"	" " " .005uf "	C7						
	NLW	C-D	" ELECTROLYTIC 50uf 50VDC	C8						
	DDM-502	CENTRALAB	" CERAMIC, DISC, .005uf 150VDC	C9						
	DDM-502	"	" " " .005uf "	C10						
	DDM-502	"	" " " .005uf "	C11						
	DDM-502	"	" " " .005uf "	C12						
	DDM-502	"	" " " .005uf "	C13						
	DDM-502	"	" " " .005uf "	C14						
	TVA 1315	SPRAGUE	" ELECTROLYTIC 500uf 50VDC	C15						
	TVA-1215	"	" " 500uf 50VDC	C16						
	DDM-502	CENTRALAB	" CERAMIC, DISC, .005uf 150VDC	C17						
	DDM-502	"	" " " .005uf "	C18						
	DDM-502	"	" " " .005uf "	C19						

REVISED:	CODE IDENT. NO.	SIZE	ADVANCED DIGITAL FM/PM DEMODULATOR TYPE ADD-15
	13639	A	LM
	SCALE		SHEET 1 OF 21

Form: DS-25C 2-65

ITEM	PART NUMBER	VENDOR	NOMENCLATURE/DESCRIPTION	REF. DES.	QTY. PER ASSEMBLY					
					-1	-2	-3	-4	-5	-6
	CK63Y103Z	ERIE	CAPACITOR, CERAMIC, DISC, .01uf +100-20%	C20						
	DDM-502	CENTRALAB	" " " .005uf 150VDC	C21						
	DDM-502	"	" " " .005uf "	C22						
	DDM-502	"	" " " .005uf "	C23						
	DDM-502	"	" " " .005uf "	C24						
	DDM-502	"	" " " .005uf "	C25						
	HR809-X5T	ERIE	" " " .001uf ±10%	C26						
	DDM-502	CENTRALAB	" " " .005uf 150VDC	C27						
	HR809-X5T	ERIE	" " " .001uf ±10%	C28						
	CK63Y103Z	"	" " " .01uf +100-20%	C29						
	DDM-502	CENTRALAB	" " " .005uf 150VDC	C30						
	DDM-502	"	" " " .005uf "	C31						
	DDM-502	"	" " " .005uf "	C32						
	DDM-502	"	" " " .005uf "	C33						
	150D106X9025	SPRAGUE	" TANTALUM 10uf 35VDC	C34						
	NLW	C-D	" ELECTROLYTIC 50uf 50VDC	C35						
	DDM-502	CENTRALAB	" CERAMIC, DISC, .005uf 150VDC	C36						
	CK63Y103Z	ERIE	" " " .01uf +100-20%	C37						
	DDM-502	CENTRALAB	" " " .005uf 150VDC	C38						

REVISED:	CODE IDENT. NO.	SIZE		
	13639	A	LM	ADD-15
	SCALE			SHEET 2 OF 21

Form: DS-25C 2-65

Defense Electronics, Inc.

ITEM	PART NUMBER	VENDOR	NOMENCLATURE/DESCRIPTION	REF. DES.	QTY. PER ASSEMBLY					
					-1	-2	-3	-4	-5	-6
	CK63Y103Z	ERIE	Capacitor, Ceramic, Disc, .01uf +100-20%	C39						
	HR809-X5T	"	" " " .001uf ±10%	C40						
	HR809-X5T	"	" " " .001uf "	C41						
	NP0-A-301-000	"	" " Tubular 1.0 pf ± 0.1pf	C42						
	DDM-502	CENTRALAB	" " Disc, .005uf 150VDC	C43						
	HR809-X5T	ERIE	" " " .001uf ±10%	C44						
	HR809-X5T	"	" " " .001uf "	C45						
	HR809X5T	"	" " " .001uf "	C46						
	HR809X5T	"	" " " .001uf "	C47						
	DDM-502	CENTRALAB	" " " .005uf 150VDC	C48						
	DDM-502	"	" " " .005uf "	C49						
	HR809X5T	ERIE	" " " .001uf ±10%	C50						
	DDM-502	CENTRALAB	" " " .005uf 150VDC	C51						
	HR809X5T	ERIE	" " " .001uf ±10%	C52						
	CK63Y103Z	"	" " " .01uf +100-20%	C53						
	HR839-X5F	"	" " " 100pf ±10%	C54						
	DDM502	CENTRALAB	" " " .005uf 150VDC	C55						
	HR809X5T	ERIE	" " " .001uf ±10%	C56						
	DM15-F471J	ELMENCO	" Mica 470pf ±5%	C57						

REVISED:	CODE IDENT. NO.	SIZE		
	13639	A	LM	A01-15
	SCALE			SHEET 30F21

Form: DS-25C 2-65

ITEM	PART NUMBER	VENDOR	NOMENCLATURE/DESCRIPTION	REF. DES.	QTY. PER ASSEMBLY					
					-1	-2	-3	-4	-5	-6
	NPO-A-301-000	ERIC	CAPACITOR, CERAMIC, TUBULAR 1.0μf ± 0.1 pf	C58						
	DDM-502	CENTRALAB	" " DISC, .005μf 150 VDC	C59						
	C1C63Y103Z	ERIE	" " " .01μf +100 -20%	C60						
	HR809-X5T	"	" " " .001μf ± 10%	C61						
	NPO-T-308-000	"	" " TUBULAR 47pf ± 5%	C62						
	NLW	C-D	" ELECTROLYTIC 50μf 50VDC	C63						
	DDM502	CENTRALAB	" CERAMIC .005 μf 150VDC	C64						
	DM15F101J	ELMENCO	CAPACITOR, MICA 100pf ± 5%	C65						
	NPO-A-301-000	ERIE	" CERAMIC, TUBULAR, 22pf ± 5%	C66						
	NPO-A-301-000	"	" " " 8.2pf ± 0.25pf	C67						
	NOT USED			C68						
	HR809-X5T	ERIE	CAPACITOR, CERAMIC, DISC, .001μf ± 10%	C69						
	NLW	C-D	" ELECTROLYTIC 50μf 50VDC	C70						
	150D107X9020S2	SPRAGUE	" " 100μF 20VDC	C71						
	DDM502	CENTRALAB	" " " .005 150VDC	C72						
	DDM502	CENTRALAB	" CERAMIC, DISC, .005μf 150VDC	C73						
	DDM502	"	" " " .005μF 150VDC	C74						
	DDM502		" .005μf	C75						
	DDM502		" .005μf	C76						

REVISED:	CODE IDENT. NO.	SIZE		
	13639	A	LM	ADD-15
	SCALE			SHEET 4 of 21

Form: DS-25C 2-65

ITEM	PART NUMBER	VENDOR	NOMENCLATURE/DESCRIPTION	REF. DES.	QTY. PER ASSEMBLY -1	-2	-3	-4	-5	-6
	DDM502	CENTRALAB	CAPACITOR, CERAMIC, DISC, .005 uf 150VDC	C77						
	NPO-T-308-000	ERIE	" " Tubular 47pf ±5%	C78						
	DDM502	CENTRALAB	" " Disc .005uf 150VDC	C79						
	NPO-T-308-000	ERIE	" " Tubular 47pf ±5%	C80						
	NPO-A-301-000	"	" " " 30pf ±5%	C81						
	TVA1315	SPRAGUE	" ELECTROLYTIC 300uf 50VDC	C82						
	NLW	C-D	" ELECTROLYTIC 50uf 50VDC	C83						
	DM10F301J	ELMENCO	" MICA 300pf ±5%	C84						
	DDM-502	CENTRALAB	" CERAMIC, DISC, .005uf 150VDC	C85						
	NOT USED			C86						
	NOT USED			C87						
	NOT USED			C88						
	DM19F152J	ELMENCO	" MICA 1500pf ±5%	C89						
	ME-7G-100	ARCO	" ELECTROLYTIC 100uf 25VDC	C90						
	DDM502		" CERAMIC DISC .005uf 150VDC	C91						
	DM19F162J	ELMENCO	" MICA 1600pf ±5%	C92						

REVISED:	CODE IDENT. NO.	SIZE		
	13639	A	LM	ADD-15
	SCALE			SHEET 5 OF 31

Form: DS-25C 2-65

ITEM	PART NUMBER	VENDOR	NOMENCLATURE/DESCRIPTION	REF. DES.	QTY. PER ASSEMBLY -1	-2	-3	-4	-5	-6
	IN2071		Diode, Silicon	CR1						
	IN2071		" "	CR2						
	IN483		"	CR3						
	IN483		" "	CR4						
	IN3713		"	CR5						
	IN3713		"	CR6						
	IN938A		" , Zener	CR7						
	IN4734		" "	CR8						
	IN4734		" "	CR9						
	IN4735		" "	CR10						
	IN4735		" "	CR11						
	IN746		" "	CR12						
	IN938-A		" "	CR13						
	IN276		"	CR14						
	IN276		"	CR15						
	PC137		" Varicap	CR16						

REVISED:	CODE IDENT. NO.	SIZE		
	13639	A	LM	ADD-15
	SCALE			SHEET 6 OF 21

Form: DS-25C 2-65

ITEM	PART NUMBER	VENDOR	NOMENCLATURE/DESCRIPTION	REF. DES.	QTY. PER ASSEMBLY -1	-2	-3	-4	-5	-6
	IN483		DIODE SILICON	CR17						
	IN4735		" "	CR18						
	WEE22	Nytronics	INDUCTOR 22uh	L1						
			"	L2						
			"	L3						
	wee 220		" 220uh	L4						
			" 1.5uh	L5						
			" 1.5uh	L6						
			"	L7						
	WEE 82	Nytronics	" 82uh	L8						
	WEE 390	"	" 390uh	L9						
	WEE220		220uh	L10						
	Wee 82		82 uh	L11						
	NOT USED			L12						
	NOT USED			L13						
	WEE18		18uh	L14						
	WEE 27		27uh	L15						
	WEE 82		82uh	L16						

REVISED:	CODE IDENT. NO.	SIZE	
	13639	A	LM ADD-15
	SCALE		SHEET 7 OF 21

Form: DS-25C 2-65

ITEM	PART NUMBER	VENDOR	NOMENCLATURE/DESCRIPTION	REF. DES.	QTY. PER ASSEMBLY					
					-1	-2	-3	-4	-5	-6
	2N3227	MOTOROLA	TRANSISTOR, SILICON, NPN	Q1						
	2N3227	"	" " "	Q2						
	2N3227	"	" " "	Q3						
	2N3478	RCA	" " "	Q4						
	2N2708	RCA	" " "	Q5						
	2N2708	"	" " "	Q6						
	2N2708	"	" " "	Q7						
	2N2708	"	" " "	Q8						
	2N2218	MOTOROLA	" " "	Q9						
	40251	RCA	" " "	Q10						
	2N708	"	" " "	Q11						
	2N2708	"	" " "	Q12						
	2N2708	"	" " "	Q13						
	2N2708	"	" " "	Q14						
	2N2708	"	" " "	Q15						
	2N3320		"	Q16						
	2N3320		"	Q17						

REVISED:	CODE IDENT. NO.	SIZE	
	13639	A	LM ADD-15
	SCALE		SHEET 8 OF 21

Form: DS-25C 2-65

ITEM	PART NUMBER	VENDOR	NOMENCLATURE/DESCRIPTION	REF. DES.	QTY. PER ASSEMBLY -1	-2	-3	-4	-5	-6
	2N2708	RCA	TRANSISTOR, SILICON, NPN	Q18						
	2N2708	"	" " "	Q19						
	2N2708	"	" " "	Q20						
	2N2708	"	" " "	Q21						
	2N3478	RCA	" " "	Q22						
	2N2708	"	" " "	Q23						
	2N2708	"	" " "	Q24						
	2N3564	FAIRCHILD	" " "	Q25						
	2N3564	"	" " "	Q26						
	2N2218	MOTOROLA	" " "	Q27						
	2N3251	"	" " PNP	Q28						
	2N3251	"	" " "	Q29						
	2N3227	MOTOROLA	" " NPN	Q30						
	2N3478	RCA	" " "	Q31						
	2N3478	"	" " "	Q32						
	2N3478	"	" " "	Q33						
	2N3478	"	" " "	Q34						

REVISED:	CODE IDENT. NO.	SIZE	
	13639	A	LM ADD-15
	SCALE		SHEET 9 OF 31

Form: DS-25C 2-65

ITEM	PART NUMBER	VENDOR	NOMENCLATURE/DESCRIPTION	REF. DES.	QTY. PER ASSEMBLY					
					-1	-2	-3	-4	-5	-6
	CB1815	AB	RESISTOR, Composition, Fixed, 180Ω ±5% ½WATT	R1						
	CB1815	"	" " " 180Ω " "	R2						
	CB2725	"	" " " 2.7K " "	R3						
	CB1025	"	" " " 1K " "	R4						
	CB1025	"	" " " 1K " "	R5						
	CB4705	"	" " " 47Ω " "	R6						
	CB4715	"	" " " 470Ω " "	R7						
	CB4715	"	" " " 470Ω " "	R8						
	CB5125	"	" " " 5.1K " "	R9						
	CB2215	"	" " " 220Ω " "	R10						
	CB9105	"	" " " 91Ω " "	R11						
	CB4715	"	" " " 470Ω " "	R12						
	CB4715	"	" " " 470Ω " "	R13						
	CB1825	"	" " " 1.8K " "	R14						
	CB4715	"	" " " 470Ω " "	R15						
	CB5105	"	" " " 51Ω " "	R16						
	CB1035	"	" " " 10K " "	R17						
	CB4715	"	" " " 470Ω " "	R18						
	CB1825	"	" " " 1.8K " "	R19						

REVISED:

CODE IDENT. NO. 13639 | SIZE A | LM ADD-15

SCALE

SHEET 10 OF 21

Form: DS-25C 2-65

Defense Electronics, Inc.

ITEM	PART NUMBER	VENDOR	NOMENCLATURE/DESCRIPTION	REF. DES.	QTY. PER ASSEMBLY -1	-2	-3	-4	-5	-6
	CB4715	AB	RESISTOR, COMPOSITION, FIXED, 470Ω ±5% ¼WATT	R20						
	CB1015	"	" " " 100Ω " "	R21						
	CB1015	"	" " " 100Ω " "	R22						
	CB1025	"	" " " 1K " "	R23						
	CB1025	"	" " " 1K " "	R24						
	CB1015	"	" " " 100Ω " "	R25						
	CB6825	"	" " " 6.8K " "	R26						
	CB6825	"	" " " 6.8K " "	R27						
	CB1015	"	" " " 100Ω " "	R28						
	CB4705	"	" " " 47Ω " "	R29						
	CB1025	"	" " " 1K " "	R30						
	CB6825	"	" " " 6.8K " "	R31						
	CB4705	"	" " " 47Ω " "	R32						
	CB4705	"	" " " 47Ω " "	R33						
	CB6825	"	" " " 6.8K " "	R34						
	CB1025	"	" " " 1K " "	R35						
	CB4705	"	" " " 47Ω " "	R36						
	CB1005	"	" " " 10Ω " "	R37						
	CB1005	"	" " " 10Ω " "	R38						

REVISED:

CODE IDENT. NO.	SIZE	
13639	A	LM ADD-15
SCALE		SHEET 11 of 31

Form: DS-25C 2-65

ITEM	PART NUMBER	VENDOR	NOMENCLATURE/DESCRIPTION	REF. DES.	QTY. PER ASSEMBLY -1	-2	-3	-4	-5	-6
	CB1025	AB	Resistor, Composition, Fixed, 1K ±5% 1/2 watt	R39						
	CB1025	"	" " " 1K ±5% 1/4 watt	R40						
	CB1025	"	" " " 1K " "	R41						
	CB4725	"	" " " 4.7K " 1/2 watt	R42						
	CB1035	"	" " " 10K " "	R43						
	CB1015	"	" " " 100Ω " "	R44						
	CB6825	"	" " " 6.8K " "	R45						
	CB6825	"	" " " 6.8K " "	R46						
	CB1015	"	" " " 100Ω " "	R47						
	CB3315	"	" " " 330Ω " "	R48						
	CB6825	"	" " " 6.8K " "	R49						
	62PR10K	HELITRIM	" Variable 10K	R50						
	CB4705	AB	" Composition, Fixed 47Ω ±5% 1/4 watt	R51						
	CB4705	"	" " " 47Ω " "	R52						
	62PR10K	HELITRIM	" Variable 10K	R53						
	CB6825	AB	" Composition, Fixed 6.8K ±5% 1/4 watt	R54						
	CB3315	"	" " " 330Ω " "	R55						
	CB1005	"	" " " 10Ω " "	R56						
	CB1005	"	" " " 10Ω " "	R57						

REVISED:	CODE IDENT. NO.	SIZE		
	13639	A	LM	ADD-15
	SCALE			SHEET 12 OF 21

Form: DS-250 2-65

ITEM	PART NUMBER	VENDOR	NOMENCLATURE/DESCRIPTION	REF. DES.	QTY. PER ASSEMBLY -1	-2	-3	-4	-5	-6
	EB1025	AB	Resistor, Composition, Fixed, 1K ±5% 1/2 watt	R58						
	CB4705	"	" " " 47Ω " 1/4 watt	R59						
	CB4705	"	" " " 47Ω " "	R60						
	CB2405	"	" " " 24Ω " "	R61						
	CB3005	"	" " " 30Ω " "	R62						
	CB4715	"	" " " 470Ω " "	R63						
	CB4715	"	" " " 470Ω " "	R64						
	CB4715	"	" " " 470Ω " "	R65						
	CB3315	"	" " " 330Ω " "	R66						
	CB3315	"	" " " 330Ω " "	R67						
	CB4705	"	" " " 47Ω " "	R68						
	CB4705	"	" " " 47Ω " "	R69						
	CB2205	"	" " " 22Ω " "	R70						
	CB2205	"	" " " 22Ω " "	R71						
	NOT USED			R72						
	CB1025	"	" " " 1K " "	R73						
	CB1025	"	" " " 1K " "	R74						
	EB2715	"	" " " 270Ω " 1/2 watt	R75						
	CB1025	"	" " " 1K " 1/4 watt	R76						

REVISED:	CODE IDENT. NO.	SIZE		
	13639	A	LM	ADD-15
	SCALE			SHEET 13 OF 21

Form: DS-25C 2-65

ITEM	PART NUMBER	VENDOR	NOMENCLATURE/DESCRIPTION	REF. DES.	QTY. PER ASSEMBLY					
					-1	-2	-3	-4	-5	-6
	CB2725	AB	RESISTOR, COMPOSITION, FIXED, 2.7K ±5% 1/4 WATT	R77						
	CB4715	"	" " " 470Ω " "	R78						
	CB4725	"	" " " 4.7K " "	R79						
	CB1035	"	" " " 10K " "	R80						
	CB4705	"	" " " 47Ω " "	R81						
	CB4715	"	" " " 470Ω " "	R82						
	CB1025	"	" " " 1K " "	R83						
	CB2215	"	" " " 220Ω " "	R84						
	CB2215	"	" " " 220Ω " "	R85						
	CB1215	AB	" " " 120Ω ±5% 1/4 WATT	R86						
	CB3315	"	" " " 330Ω " "	R87						
	CB4715	"	" " " 470Ω " "	R88						
	CB3325	"	" " " 3.3K " "	R89						
	CB2235	"	" " " 22K " "	R90						
	CB2235	"	" " " 22K " "	R91						
	CB4705	"	" " " 47Ω " "	R92						
	CB4715	"	" " " 470Ω " 1/2 WATT	R93						
	CB1005	"	" " " 10Ω " 1/4 WATT	R94						
	CB2215	"	" " " 220Ω " "	R95						

REVISED:	CODE IDENT. NO.	SIZE	
	13639	A	LM ADD-15
	SCALE		SHEET 14 of 31

Form: DS-25C 2-65

ITEM	PART NUMBER	VENDOR	NOMENCLATURE/DESCRIPTION	REF. DES.	QTY. PER ASSEMBLY -1	-2	-3	-4	-5	-6
	CB2215	AB	RESISTOR, COMPOSITION, FIXED, 220Ω ±5% 1/4 WATT	R96						
	EB1025	"	" " " 1K ±5% 1/2 WATT	R97						
	CB4715	"	" " " 470Ω " 1/4 WATT	R98						
	CB3325	"	" " " 3.3K " "	R99						
	CB4715	"	" " " 470Ω " "	R100						
	CB2225	"	" " " 2.2K " "	R101						
	CB2725	"	" " " 2.7K " "	R102						
	CB1015	"	" " " 100Ω " "	R103						
	CB1825	"	" " " 1.8K " "	R104						
	62PR1K	HELITRIM	" VARIABLE 1K	R105						
	CB1025	AB	" COMPOSITION, FIXED 1K ±5% 1/4 WATT	R106						
	CB6825	"	" " " 6.8K " "	R107						
	CB1025	"	" " " 1K " "	R108						
	62PR1K	HELITRIM	" VARIABLE 1K	R109						
	CB1035	AB	" COMPOSITION, FIXED, 10K ±5% 1/4 WATT	R110						
	CB2725	"	" " " 2.7K " "	R111						
	CB4735	"	" " " 47K " "	R112						
	CB5625	"	" " " 5.6K " "	R113						
	NOT USED			R114						

REVISED:

CODE IDENT. NO. 13639 | SIZE A | LM | ADD-15

SCALE | SHEET 15 OF 21

Form: DS-25C 2-65

ITEM	PART NUMBER	VENDOR	NOMENCLATURE/DESCRIPTION	REF. DES.	QTY. PER ASSEMBLY -1	-2	-3	-4	-5	-6
	CB2225	AB	Resistor, Composition, Fixed 2.2K ±5% 1/4 watt	R115						
	CB1025	"	" " " 1K " "	R116						
	CB2225	"	" " " 2.2K " "	R117						
	CB4725	"	" " " 4.7K " "	R118						
	CB1015	"	" " " 100Ω " "	R119						
	CB1825	"	" " " 1.8K " 1/2 watt	R120						
	62PR2.5K	helitrim	" Variable 2.5K	R121						
	RN60B2001F		" Metal-film 2K ±1%	R122						
	RN60B2001F		" " " 2K ±1%	R123						
	RN60B4990F		" " " 499Ω ±1%	R124						
	RN60B2000F		" " " 200Ω ±1%	R125						
	RN60B3010F		" " " 301Ω ±1%	R126						
	CB2015	AB	" Composition, Fixed 200Ω ±5% 1/4 watt	R127						
	CB5625	"	" " " 5.6K " "	R128						
	CB1035	"	" " " 10K " "	R129						
	CB1035	"	" " " 10K " "	R130						
	CB5635	"	" " " 56K " "	R131						
	6A2No1P253BA	"	" Variable 25K	R132						
	CB3325	"	Resistor, Composition, Fixed 3.3K ±5% 1/4 watt	R133						

REVISED:	CODE IDENT. NO.	SIZE		
	13639	A	LM	AOD-15
	SCALE			SHEET 16 OF 21

Form: DS-25C 2-65

ITEM	PART NUMBER	VENDOR	NOMENCLATURE/DESCRIPTION	REF. DES.	QTY. PER ASSEMBLY -1	-2	-3	-4	-5	-6
	NOT USED			R134						
	CB2725	AB	RESISTOR, COMPOSITION, FIXED 2.7K ±5% 1/4 WATT	R135						
	CB1815	"	" " " " 180Ω " "	R136						
	CB2235	"	" " " " 22K " "	R137						
	NOT USED			R138						
	CB3315	AB	" " " " 330Ω " "	R139						
	CB3325	"	" " " " 3.3K " 1/2 WATT	R140						
	CB1025	"	" " " " 1K " 1/4 WATT	R141						
	CB1815	"	" " " " 180Ω " "	R142						
	CB2405	"	" " " " 24Ω " "	R143						
	CB2035	"	" " " " 20K " "	R144						
	CB2225	"	" " " " 2.2K " "	R145						
	CB3925	"	" " " " 3.9K " "	R146						
	CB3915	"	" " " " 390Ω " "	R147						
	CB1525	"	" " " " 1.5K " "	R148						
	CB1025	"	" " " " 1K " "	R149						
	CB2025	"	" " " " 2K " "	R150						
	CB2215	"	" " " " 220Ω " "	R151						
	CB8225	"	" " " " 8.2K " "	R152						

REVISED:

CODE IDENT. NO.	SIZE	
13639	A	LM ADD-15
SCALE		SHEET 17 OF 21

Form: DS-25C 2-65

ITEM	PART NUMBER	VENDOR	NOMENCLATURE/DESCRIPTION	REF. DES.	QTY. PER ASSEMBLY -1	-2	-3	-4	-5	-6
				R153						
				R154						
	CB5625	AB	RESISTOR, Composition, FIXED 5.6K ±5% 1/4 WATT	R155						
	CB8225	"	" " " 8.2K " "	R156						
	RV6LAYSA103A	CLAROSTAT	" VARIABLE 10K	R157						
	CB2735	A3	" Composition, FIXED 27K ±5% 1/4 WATT	R158						
	RV6LAYSA103A	CLAROSTAT	" VARIABLE 10K	R159						
	CB4735	AB	" Composition, FIXED, 47K ±5% 1/4 WATT	R160						
	CB4735	"	" " " 47K " "	R161						
	CB3925	"	" " " 3.9K " "	R162						
	CB1325	"	" " " 1.3K " "	R163						
	CB1525	"	" " " 1.5K " "	R164						
	CB2205	"	" " " 22Ω " "	R165						
	CB6235	"	" " " 62K " "	R166						

REVISED:	CODE IDENT. NO.	SIZE		
	13639	A	LM	ADD-15
	SCALE			SHEET 18 OF 21

Form: DS-25C 2-65

Defense Electronics, Inc.

ITEM	PART NUMBER	VENDOR	NOMENCLATURE/DESCRIPTION	REF. DES.	QTY. PER ASSEMBLY					
					-1	-2	-3	-4	-5	-6
			SWITCH	S1						
			SWITCH	S2						
	C13-794	DEI	TRANSFORMER	T1						

REVISED:	CODE IDENT. NO.	SIZE	
	13639	A	LM
	SCALE		SHEET 19 OF 21

ADD-15

Form: DS-25C 2-65

ITEM	PART NUMBER	VENDOR	NOMENCLATURE/DESCRIPTION	REF. DES.	QTY. PER ASSEMBLY -1	-2	-3	-4	-5	-6
			FERRITE BEAD	Z1						
			"	Z2						
			"	Z3						
			"	Z4						
				Z5						
				Z6						
				Z7						
				Z8						
				Z9						
				Z10						
				Z11						
				Z12						
	NOT USED			Z13						
	NOT USED			Z14						
			FERRITE BEAD	Z15						
			"	Z16						
			"	Z17						
			"	Z18						

REVISED:	CODE IDENT. NO.	SIZE	
	13639	A	LM
	SCALE		SHEET 2 of 21

ADD 15

Form: DS-25C 2-65

Defense Electronics, Inc.

ITEM	PART NUMBER	VENDOR	NOMENCLATURE/DESCRIPTION	REF. DES.	QTY. PER ASSEMBLY					
					-1	-2	-3	-4	-5	-6
				DL1						
				DL2						
				DL3						

REVISED:	CODE IDENT. NO.	SIZE	
	13639	A	LM ADD-15
	SCALE		SHEET 21 of 21

Form: DS-25C 2-65

Security Classification

DOCUMENT CONTROL DATA - R&D

(Security classification of title, body of abstract and indexing annotation must be entered when the overall report is classified)

1. ORIGINATING ACTIVITY (Corporate author) Defense Electronics, Inc. Rockville, Maryland	2a. REPORT SECURITY CLASSIFICATION Unclassified 2b. GROUP N/A

3. REPORT TITLE

ADVANCED DIGITAL FM-PM DEMODULATOR ADD-15

4. DESCRIPTIVE NOTES (Type of report and inclusive dates)

Final Report

5. AUTHOR(S) (Last name, first name, initial)

N/A

6. REPORT DATE	7a. TOTAL NO. OF PAGES	7b. NO. OF REFS
September 1966	118	8

8a. CONTRACT OR GRANT NO.	9a. ORIGINATOR'S REPORT NUMBER(S)
AF 19(628)-5667 b. PROJECT NO.	ESD-TR-66-516
c. d.	9b. OTHER REPORT NO(S) (Any other numbers that may be assigned this report)

10. AVAILABILITY/LIMITATION NOTICES

Distribution of this document is unlimited.

11. SUPPLEMENTARY NOTES	12. SPONSORING MILITARY ACTIVITY
None	Director of Aerospace Instrumentation, Electronic Systems Division, AFSC, USAF, L. G. Hanscom Field, Bedford, Mass. 01730

13. ABSTRACT

The objective of this program is to design, fabricate, and evaluate an advanced FM-PM demodulator for telemetry applications. This unit will utilize new circuit techniques which show definite promise of providing improved performance, particularly in the areas of threshold and linearity. The compromises and limitations involved in the new techniques will be thoroughly investigated and the program includes a comprehensive series of tests.

DD FORM 1 JAN 64 1473

Security Classification

14. KEY WORDS	LINK A		LINK B		LINK C	
	ROLE	WT	ROLE	WT	ROLE	WT
1. Telemetry Systems - TRKI-12						
2. Telemetry Receivers - TMR-15						
3. Digital Wideband FM Demodulator						
4. Delay Lines						
5. Phase Lock Techniques						
6. Phase Lock Acquisition Range						
7. Test Program and Procedures						
8. Discriminator Bandwidth						
9. Linearity						
10. FM Threshold						
11. FM Capture Ratio						
12. AM Rejection						
13. Telemetry Data Formats, simulation of and testing with FM/FM, PDM/FM, PCM/FM						

INSTRUCTIONS

1. ORIGINATING ACTIVITY: Enter the name and address of the contractor, subcontractor, grantee, Department of Defense activity or other organization *(corporate author)* issuing the report.

2a. REPORT SECURITY CLASSIFICATION: Enter the overall security classification of the report. Indicate whether "Restricted Data" is included. Marking is to be in accordance with appropriate security regulations.

2b. GROUP: Automatic downgrading is specified in DoD Directive 5200.10 and Armed Forces Industrial Manual. Enter the group number. Also, when applicable, show that optional markings have been used for Group 3 and Group 4 as authorized.

3. REPORT TITLE: Enter the complete report title in all capital letters. Titles in all cases should be unclassified. If a meaningful title cannot be selected without classification, show title classification in all capitals in parenthesis immediately following the title.

4. DESCRIPTIVE NOTES: If appropriate, enter the type of report, e.g., interim, progress, summary, annual, or final. Give the inclusive dates when a specific reporting period is covered.

5. AUTHOR(S): Enter the name(s) of author(s) as shown on or in the report. Enter last name, first name, middle initial. If military, show rank and branch of service. The name of the principal author is an absolute minimum requirement.

6. REPORT DATE: Enter the date of the report as day, month, year; or month, year. If more than one date appears on the report, use date of publication.

7a. TOTAL NUMBER OF PAGES: The total page count should follow normal pagination procedures, i.e., enter the number of pages containing information.

7b. NUMBER OF REFERENCES: Enter the total number of references cited in the report.

8a. CONTRACT OR GRANT NUMBER: If appropriate, enter the applicable number of the contract or grant under which the report was written.

8b, 8c, & 8d. PROJECT NUMBER: Enter the appropriate military department identification, such as project number, subproject number, system numbers, task number, etc.

9a. ORIGINATOR'S REPORT NUMBER(S): Enter the official report number by which the document will be identified and controlled by the originating activity. This number must be unique to this report.

9b. OTHER REPORT NUMBER(S): If the report has been assigned any other report numbers *(either by the originator or by the sponsor)*, also enter this number(s).

10. AVAILABILITY/LIMITATION NOTICES: Enter any limitations on further dissemination of the report, other than those imposed by security classification, using standard statements such as:

(1) "Qualified requesters may obtain copies of this report from DDC."

(2) "Foreign announcement and dissemination of this report by DDC is not authorized."

(3) "U. S. Government agencies may obtain copies of this report directly from DDC. Other qualified DDC users shall request through _____."

(4) "U. S. military agencies may obtain copies of this report directly from DDC. Other qualified users shall request through _____."

(5) "All distribution of this report is controlled. Qualified DDC users shall request through _____."

If the report has been furnished to the Office of Technical Services, Department of Commerce, for sale to the public, indicate this fact and enter the price, if known.

11. SUPPLEMENTARY NOTES: Use for additional explanatory notes.

12. SPONSORING MILITARY ACTIVITY: Enter the name of the departmental project office or laboratory sponsoring *(paying for)* the research and development. Include address.

13. ABSTRACT: Enter an abstract giving a brief and factual summary of the document indicative of the report, even though it may also appear elsewhere in the body of the technical report. If additional space is required, a continuation sheet shall be attached.

It is highly desirable that the abstract of classified reports be unclassified. Each paragraph of the abstract shall end with an indication of the military security classification of the information in the paragraph, represented as *(TS), (S), (C), or (U)*.

There is no limitation on the length of the abstract. However, the suggested length is from 150 to 225 words.

14. KEY WORDS: Key words are technically meaningful terms or short phrases that characterize a report and may be used as index entries for cataloging the report. Key words must be selected so that no security classification is required. Identifiers, such as equipment model designation, trade name, military project code name, geographic location, may be used as key words but will be followed by an indication of technical context. The assignment of links, rules, and weights is optional

Printed by
United States Air Force
L. G. Hanscom Field
Bedford, Massachusetts